HEAT TRANSFER IN BUOYANCY INDUCED FLOWS

By

ASTHIGIRI KRISHNAMACHARI CHELLAPPA

DEPARTMENT OF MATHEMATICS

INDIAN INSTITUTE OF TECHNOLOGY KANPUR

JUNE, 1983

HEAT TRANSFER IN BUOYANCY INDUCED FLOWS

A Thesis Submitted
in Partial Fulfilment of the Requirements
for the Degree of
DOCTOR OF PHILOSOPHY

By
ASTHIGIRI KRISHNAMACHARI CHELLAPPA

to the
DEPARTMENT OF MATHEMATICS
INDIAN INSTITUTE OF TECHNOLOGY KANPUR
JUNE, 1983

DEDICATED WITH LOVE AND GRATITUDE TO
MY PARENTS, MY ELDER BROTHER AND
DR. R. JAYAKARAN ISAAC

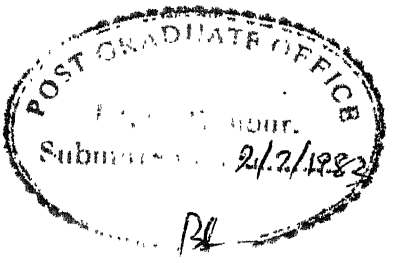

CERTIFICATE

This is to certify that the thesis entitled 'Heat Transfer in Buoyancy Induced Flows' that is being submitted by Shri A.K. Chellappa for the award of the Degree of Doctor of Philosophy to the Indian Institute of Technology, Kanpur is a record of bonafide research work carried out by him under my supervision and guidance. The results embodied in this thesis have not been submitted to any other University or Institute for the award of any degree or diploma.

June - 1983.

(Punyatma Singh)
Professor of Mathematics
Indian Institute of Technology
Kanpur

ACKNOWLEDGEMENTS

I take this opportunity to thank my thesis supervisor Dr. Punyatma Singh, Ph.D., D.Sc., Professor of Mathematics, Indian Institute of Technology, Kanpur for his able guidance, immense patience and constant encouragement throughout the course of this research.

I am indebted to the management of Voorhees College, Vellore for having deputed me to do my research work at I.I.T., Kanpur. Thanks are also due to the University Grants Commission, New Delhi for financial assistance in the form of fellowship under the Faculty Improvement Programme. Also I thank the I.I.T., Kanpur authorities for making available all facilities to do my research work at this Institute. Special words of thanks also go to Dr. J.B. Shukla, Professor and Head of Department of Mathematics, I.I.T., Kanpur, for all his help to me.

To Mr. V. Radhakrishnan, goes a note of thanks for sincerely participating in our discussions on my present research work. I am extremely grateful to the ''Golden King'' who always helped me very generously at times of need. I express my deep sense of gratitude to Mr. G.P. Youvaraj, Mr. S. Athisyaraj, Mr. B.N. Shetty, Mr. G. Arumugam, Mr. R. Venkatesh and Mr. K.S. Raman who have given their

invaluable time for proof-reading and arranging the typed manuscripts. Also I record my thanks to Mr. Winslin Henry Peter Raj, Mr. T. Ram Reddy and Mr. N. Shastry for their act of kindness towards me on various occassions. I appreciate deeply and be always grateful to the same to all of my friends who showered their kindness on me at various occassions all through my period of stay in this I.I.T. campus. Words cannot describe my feelings of gratitude to all those teachers with whom I had opportunities to study and discuss my academic problems. I thank Mr. S.K. Tewari for his immense patience and excellent typing. Also, I thank Mr. A.N. Upadhyaya for cyclostyling the typed manuscript and Mr. D.K. Mishra for drawing figures.

Last, but not the least, I record a note of thanks to my wife, Maya, who has constantly prayed to the Almighty for a successful completion of this course requirements and to my son, Rajesh, who always cheered me with his smiling face on everyday morning so as to start my work happily.

June - 1983.

A. K. CHELLAPPA

CONTENTS

SYNOPSIS

The work presented in this thesis deals with heat transfer in buoyancy induced flows. The flow is a result of interaction between gravitational force and local density differences in the fluid. The density variations are due to temperature differences between a bounding surface and ambient fluid. Chapter II of the thesis is devoted to analyse the flow and heat transfer over a surface which is itself curved or is parallel to the direction of gravity field, while rest of the chapters are concerned with flows arising adjacent to surfaces that are either horizontal or inclined at a small angle to it.

Chapter I is introductory and contains a brief outline of the background that have a direct bearing on our present investigations. A review of the previous work of authors mainly related to present study is also included in this chapter.

In chapter II, the laminar boundary layer description of planar, free convection flow and heat transfer around two-dimensional bodies of arbitrary contour is examined for arbitrarily prescribed surface temperature distributions. The Görtler-type transformation is developed to treat the general wall thermal conditions. Series representations of the

dependent boundary layer variables are developed on the lines of Görtler series method when the wall temperature variations are prescribed as

$$x^{\delta} \sum_{k=0}^{\infty} a_k x^{2k} ,$$

where x is a suitably normalized streamwise distance, a_k are constants with $a_o \neq 0$ and

$\delta = 0$ for round-nosed cylinders

and

$\delta = 1$ for vertical plate.

For round-nosed cylinders, the ordinary differential equations which determine the functional coefficients in the series expansion for the dependent variables are independent of the body contour and wall temperature data. Instead, some of the numerical coefficients in these equations are fixed by the class of body shape (namely, round-nosed here). Hence the solutions can be obtained for this class once and for all for fixed values of Prandtl number. The body contour and wall temperature data enter the problem only when the series are assembled. Only two-terms of the series are found to be sufficient to represent velocity and temperature distributions around the lower-half of the circular cylinder when applied to specific wall-temperature distributions. The results for

the heat-flux density at the surface of the non-isothermal circular cylinder compares well with previous analytical results. The effect of non-isothermal wall condition for the circular cylinder influences significantly the heat transfer variations at the surface. When this method of solution is applied to isothermal circular cylinder, the five-term sum of the series for heat-flux density at the surface yields results accurate upto 87 percent of the angular distance of 150° from the lower stagnation point of the cylinder and in the rest of the portion of it, the results predicted are within an error of $3\frac{1}{2}$ percent from the available exact numerical results. Also, heat transfer at the surface of an isothermal blunt elliptic cylinder of aspect ratio 2:1 is predicted quite accurately by five-term sum of the series for it. In the case of non-isothermal vertical plate problem, 24 functional coefficients associated with the first five-terms in the series expansion for dependent variables are calculated for Prandtl number 1.0 and 0.7. Using these functions which are independent of the prescribed wall temperature data, the boundary layer flow over non-isothermal vertical plate with sinusoidal wall temperature variation is studied. The results obtained for local heat transfer coefficient compares well with available finite difference data.

In chapter III, the boundary layer in free convection flow over the upper surface of a semi-infinite heated horizontal plate inclined at a small angle α with the horizontal is studied analytically for flow and heat transfer by local non-similarity method of solution. The range of α considered here, as obtained from the analysis, is defined by the requirement that Λ, the limit of $Gr^{1/5} \tan \alpha$ as $Gr \to \infty$, be $O(1)$, where Gr is a suitably defined Grashof number. The conservation equations are transformed such that they can lend themselves to local non-similarity solutions. The forms of the local non-similarity method considered here are two and three-equation models, obtained by retaining the transformed conservation equations as such and only selectively neglecting terms in the derived subsidiary equations at the second and third level of the successive approximations. Numerical results for the local surface heat-transfer, wall shear-stress and velocity and temperature distributions are presented for Prandtl number 0.72 and 1.0 when $\Lambda = 1.0, -1.0$. While the two-equation model is found to give boundary layer characteristics sufficiently accurate for engineering purposes, the three-equation model over-corrects these solutions and the results thus obtained compare well with previous analysis. When the angle of inclination is negative, our method of solution predicts the separation of the flow and notably for the case of air, the two-equation model locates the separation

point within an error of $1\frac{1}{2}$ percent from the previous exact value. It is to be noted that there is no evidence of singularity at the point of separation.

In chapter IV, we derive in a systematic way all possible similarity solutions for both steady and unsteady free convection boundary layer flowsover a semi-infinite horizontal plate. The solutions presented are obtained not by assuming specific wall temperature distributions, but rather by deriving the solution forms from similarity conditions. This approach not only results in more general forms than hitherto obtained, but results in all other possible solution forms. Our investigations point out that there are in all four possible cases of similarity for free convection boundary layer flow over a heated semi-infinite horizontal plate. While this analysis has verified that the similarity possibilities for steady cases have essentially been covered in the literature, it also shows that somewhat more general wall thermal conditions could also be taken into account. The other two new possible cases deal with unsteady conditions.

In the last chapter of the thesis, we initiate the study of free convection boundary layer flow over a semi-infinite, non-isothermal horizontal plate. A new Görtler type transformation is introduced to treat the problem of non-isothermal free convection with general wall temperature

distribution. A new parameter characterizing the non-isothermal conditions of the wall is introduced. The transformed non-similar boundary layer equations are solved by the Görtler series expansion and the local non-similarity method. The series expansion is valid for an arbitrary surface temperature variation given by

$$x^n \sum_{k=0}^{\infty} G_k x^{(n+1)pk}$$

where n, p, G_k are constants, $G_o \neq 0$ and x is suitably normalized streamwise coordinate.

Functional coefficients determining the terms in the series expansion for stream function and temperature depend only on n, p and Prandtl number of the fluid. The functions associated with first four-terms of the series expansion for dependent variables are determined for $n = 0$, $Pr = 0.72$ and $p = 1.0, 0.5, 0.25$. The application of the series method is illustrated for a class of wall temperature distributions, $G_o(1 + \varepsilon x^p)$ where ε is some constant. On the other hand, the local non-similarity method at the second level of truncation is applied for the above class of surface temperature variations when $Pr = 0.72, 5.0, 0.1$ and $p = 1.0, 0.5, 0.25$. A comparison of results for local heat transfer at the surface for air indicates that the local non-similarity method gives accurate results for a larger

region in the downstream flow than the four-term sum of the series expansion can give. The effect of non-isothermal wall is significant on heat transfer at the surface and the variation in heat transfer at the surface is greatly influenced by Prandtl number and the shape parameter, p, of wall temperature distribution.

CHAPTER I

INTRODUCTION

1. HEAT TRANSFER PROCESSES

Heat transfer is defined as the transfer of energy across a system boundary caused solely by a temperature difference. The study of heat transfer is but the study of how energy is carried, distributed, and diffused in and by materials. Such a study is of significance in the energy-related applications. For instance, the transfer of heat in power plants from the energy source, be it nuclear, solar or other, to the working fluid is one of the most basic processes in such systems. Similarly, the operation of refrigeration and air-conditioning units depend on the effective transfer of heat in condensers and evaporators. Other applications of particular interest pertaining to environmental control include the minimization of building-heat losses by means of improved insulating techniques and use of supplemental energy sources, such as solar radiation, heat pumps, and fire places.

There are two basically different processes by which heat transfer is accomplished: conduction and radiation. Heat conduction is identified as the process of molecular transport of heat in bodies (or between them), due to temperature variation in the medium. Thermal radiation, on the other hand, depends only on the temperature and on the optical properties of the emitter, with its internal

energy being converted into radiation energy.

The concept of convection embraces the process of heat transfer through the motion of a fluid. Heat is transported simultaneously during the process by convection and conduction. By convection is meant the process of heat transport occurring through the movement of macroparticles of the liquid or gas in space from a region of one temperature to that of another. Convection is possible only in a fluid medium and the transport of heat is directly linked with the transport of the medium itself. Thus a consideration of problems in convective heat transfer involves the science of fluid motion. The practical importance of this mode of heat transfer needs no illustration. The use of moving fluids to transport or remove heat is well-known, ranging from the circulation of coolant through a nuclear reactor to the mounting of a power transistor on a block with cooling fins.

The convective heat transfer process is further divided into two basic processes. If the motion of the fluid arises due to a forcing condition such as an externally-imposed flow of a fluid stream over a heated object, the process is termed as forced convection. If, on the other hand, no such externally-induced flow is provided and the flow is driven simply by the interaction of a difference in density with a body force field, such as the gravitational field, then the process is termed natural convection or free

convection. The agencies which provide the density differences can also be very diverse. For instance, they may be due to temperature and/or composition variations. But in our present investigations, we deal only with temperature caused density differences. Also, our work deals only with free convection flows arising in a very extensive medium due to a given inhomogenity in temperature between a bounding surface and ambient fluid.

As a result of convective processes, local temperature differences exist in the flow field resulting in higher temperature gradients. In most applications, it is of primary interest to know the quantity of heat exchanged between the surface and the stream. For a surface of area A, a heat transfer coefficient, h, is defined by the equation

$$Q = hA\theta_w \,, \tag{1.1}$$

in which Q denotes the heat flux through the area A and θ_w is a characteristic temperature difference between the surface and the fluid. Assuming that the properties on whcih the heat transfer depends can be considered as constants with the exception of the density, the variation of which is expressed by a thermal expansion coefficient (Boussinesq assumption), Nusselt [1] derived the following equation for the heat flow, Q, per unit time

$$Q = kd\ \theta_w\ \varphi\left(\frac{k}{\mu c_p}\,,\ \frac{d^3\rho^2 g\ \beta\ \theta_w}{\mu 2}\right). \tag{1.2}$$

Here, g is the gravitational acceleration, β is the thermal expansion coefficient, d is a characteristic length, c_p is the specific heat of the fluid, k is the thermal conductivity ρ is the density and μ is the viscosity. Again, he extended the thermal analysis to a gas in which the properties depend in the following way on the absolute temperature T

$$\rho = \rho_o \left(\frac{T_o}{T}\right), \quad \mu = \mu_o \left(\frac{T}{T_o}\right)^a,$$

$$k = k_o\left(\frac{T}{T_o}\right)^b, \quad c_p = c_{po} \left(\frac{T}{T_o}\right)^c . \tag{1.3}$$

The index, O, refers to a characteristic fluid temperature. The heat transfer coefficient h, then obtained by him is

$$h = \frac{k}{d} \varphi\left(\frac{d^3\rho^2 g}{\mu^2}, \frac{k}{\mu c_p}, \frac{T_w}{T_o}\right) \tag{1.4}$$

when $a = b = c$.

The names given to the dimensionless parameters appearing in the equations (1.2) and (1.4) are

Nusselt number, $Nu = \frac{hd}{k}$,

Prandtl number, $Pr = \frac{\mu c_p}{k}$,

and

Grashof number, $Gr = \frac{g\beta\rho^2 d^3 \theta_w}{\mu^2}$. (1.5)

The expression used to describe heat transfer in free convection can now be written as

$$Nu = f(Gr, Pr) \tag{1.6}$$

corresponding to (1.2). When a,b,c are all distinct, the relation describing heat transfer is

$$Nu = f(Gr, Pr, \frac{T_w}{T_o}, a, b, c) \ . \tag{1.7}$$

The form of (1.7) is an evidence to the fact that dimensionless relations describing heat transfer become more restricted, the more accurately one tries to describe the fluid properties. On the other hand, the relations of the form (1.6) hold for groups of fluids with the same Prandtl number. They are exact in the limit of small temperature differences. Apart, they describe with fair approximation, conditions at larger temperature differences when average fluid properties are introduced. Sparrow and Gregg [2] developed a reference temperature relation that permits good approximations of variable property results to be obtained quite simply from constant property results.

2. GOVERNING EQUATIONS FOR FREE CONVECTION

The theoretical analysis of free convection requires that the fundamental laws of mass, momentum and energy and the particular laws of viscous shear and conduction be

utilized in the development of mathematical theory for the free convection phenomena. A detailed derivation of the governing equations for the free convection phenomena, based on a Newtonian fluid with Fourier's law governing the molecular flux of heat, is available in [3] and therefore a familiar description will be selected as a starting point in our thesis. The difficulty of analysis in considering the full equations results from the coupling of momentum and energy equations and where important, from the variations in the properties of the fluid ρ, μ and k. An analysis including the full effects of variations in ρ, μ and k is so complicated that some approximations become essential. Consequently the equations governing free convection flow are commonly used in a form obtained with the help of the Boussinesq approximations [3].

In the Boussinesq approximation, variations of density ρ is ignored except in so far as they give rise to gravitational force and the dependence of ρ on temperature T is given by

$$\rho_a - \rho = \rho\beta\,(T - T_a) \qquad (1.8)$$

where suffix 'a' stands for the values of the quantities in the ambient medium. Under this assumption it has been formally justified by Ostrach [4] and Hellums and Churchill [5] that variations of all fluid properties can be ignored completely. Ostrach has also shown that, within the framework

of this approximation, viscous dissipation of energy may be neglected. For very low speeds found in free convection the effects of compression in the energy equation can also be neglected [6].

Under these assumptions, the governing equations for the free convection phenomena without internal heat generation are

$$\nabla \cdot \vec{V} = 0 , \tag{1.9}$$

$$\rho \frac{D\vec{V}}{Dt} = - \nabla p + \mu \nabla^2 \vec{V} + \rho \vec{g} , \tag{1.10}$$

$$\frac{DT}{Dt} + \vec{V} \cdot \nabla T = \bar{\alpha} \nabla^2 T \tag{1.11}$$

where

$\bar{\alpha} = \frac{k}{\rho c_p}$, $\bar{\alpha}$ is known as the thermal diffusivity, p the local pressure, T the local temperature, $\vec{V} = (u,v,w)$ is the local velocity vector and t is the time.

In the force-momentum equation (1.10) the local pressure p may be broken down to two terms, one due to the motion of the fluid, P, known as the viscous pressure and the other due to the hydrostatic pressure p_a. That is, we have

$$p = P + p_a .$$

It can be seen that the hydrostatic pressure with the body force acting on the fluid constitutes the driving mechanism for the free convection flow. The vector

$$\rho \vec{g} - \nabla p$$

in the momentum equation (1.10) can be expressed as

$$\rho \vec{g} - \nabla p = \rho \vec{g} - (\rho_a \vec{g} + \nabla P),$$

where we have used

$$\nabla p_a = \rho_a \vec{g}$$

in the gravitational field.

Using (1.8), finally we get

$$\rho \vec{g} - \nabla p = (\rho - \rho_a) \vec{g} - \nabla P ,$$

$$= - \rho \beta (T - T_a) \vec{g} - \nabla P . \qquad (1.12)$$

Hence the momentum equation (1.10) can now be written as

$$\frac{D\vec{V}}{Dt} = - \frac{1}{\rho} \nabla P + \nu \nabla^2 \vec{V} - \vec{g} \beta (T - T_a) . \qquad (1.13)$$

Here $-\vec{g} \beta (T - T_a)$, to be denoted by $\vec{B}$, is known as the buoyancy force. Equations (1.9), (1.13) and (1.11) constitute the basic equations of free convection in the Boussinesq approximations.

3. BOUNDARY LAYER APPROXIMATION

An understanding of the detailed mechanism and interaction of flow and heat transfer processes was made possible through the application of boundary layer concept, introduced for forced convection flows by Prandtl in 1904.

According to this concept, there exists a thin region near solid objects in which certain quantities describing the flow change very rapidly. The idea is to consider the relative size of certain expressions in the differential equations governing the flow and discard some, due to their relative smallness. This leads to an impressive simplification of the governing equations for the flow. It is to be noted that in forced - flow problems, the validity of this approximation depends on the size of the Reynolds number for the flow and the theory becomes a better approximation as the Reynolds number increases.

However, this important development was brought into free convection phenomena only in 1930. The experiments by E. Schmidt and Beckmann [7] on an isothermal vertical surface in air indicated that boundary layer concepts of Prandtl were also applicable to buoyancy induced flows. However, there exists no unique prescribed characteristic velocity for natural convection flows, Reynolds number, therefore, loses its significance. So a new characteristic velocity must be defined which, as was first explicitly pointed out by Ostrach [4] involves the three prime physical quantities of this phenomenon, namely, β, g, θ_w. Unfortunately, the magnitude of the velocities in natural convection can not be determined from the boundary conditions, so that a characterization of the reference velocity must come from

the differential equations. The explicit form of this velocity depends on the specific problem.

For instance, in order to obtain non-dimensional equations for natural convection over a vertical plate ,

$$U = (g\beta\theta_w d)^{1/2} \tag{1.14}$$

is taken as reference velocity scale and it was shown that Grashof number Gr, plays the role of Reynolds number in this free convection flow and in fact Gr is simply Re^2 based on U as given by (1.14). Also we note that the pressure in the region beyond the boundary layer in natural convection flows is hydrostatic unlike in the case of forced flow where it is being imposed by an external flow. Several other experiments have also upheld the validity of this boundary layer approximation in free convection flows. Boundary layer theory has now been applied with success to a very large number of transport phenomena in buoyancy induced flows.

4. THE BACKGROUND OF PRESENT INVESTIGATIONS

In many interesting and important areas of natural convection, the flow is generated as a consequence of the thermal input from a surface which is itself curved with respect to the direction of gravity field. Surface curvature requires that the boundary layer must continually adjust

to the changing strength of the surface-parallel component of the buoyancy force. Thus an analysis of free convection flow including the effect of surface curvature is more complicated than that for a vertical plate.

One of the earliest theoretical investigations to appear on free convection flow over a curved surface is that of Hermann [8] for cylindrical configuration. By means of a suitable transformation, he was able to solve the boundary layer equations for an isothermal circular cylinder. The agreement between the calculated temperature field and the experimental results of Jodlbauer [9] was good. However, his approximate method of solution is limited to isothermal case and cannot be extended to more general cases. Also, it is not clear how other cylindrical objects are to be treated. Schuh [10] found the natural convection solutions in similarity form for certain curved surface geometries. He considered in detail only the flow over two-dimensional body having everywhere finite curvature and a boundary layer of constant thickness. Later, Merk and Prins [11] made a detailed study of both symmetric two-dimensional and axi-symmetric flows. They showed that the cone is one axially symmetric body having a similarity solution. It was pointed out that neither the horizontal cylinder nor the sphere has a similar solution. They obtained a similarty solution valid near the stagnation point and later

presented an integral solution for horizontal cylinders and spheres. Braun, Ostrach and Heighway [12] generalised the previous two analyses and investigated such flows for similarty for both constant and variable surface temperatures. A group of closed bottom shapes was found for each kind of symmetry. Herring and Grosh [13] and Herring [14] found similar solutions for the vertical cone for power-law surface temperature dependence.

Although horizontal cylinders and spheres do not have similarity solutions for natural-convection flow, their importance has resulted in a number of approximate analyses also based on boundary layer equations. Chiang and Kaye [15] used a Blasius series expansion method to predict the heat transfer coefficients for laminar natural convection from horizontal cylinders and spheres. For forced flow situations, Van Dyke [16] evaluated the Blasius series for a parabolic cylinder of nose radius R and found that the resulting series diverges for $x/R > 0.62$ where x denotes the usual coordinate measured from the nose along the arc. Also Schlichting [6] cautions that even the series for a circular cylinder may become divergent from a certain value of x/R onwards since the coefficients of the series appear to increase after the term of $O(x/R)^9$.

Recognising the need for a procedure to account for the effects of the body shape in a general manner, Saville and

Churchill [17] used a Görtler type series for analysing the two-dimensional, planar and axi-symmetric boundary layer flows over smooth isothermal bodies of fairly arbitrary contours. When applied to horizontal circular cylinders or spheres, the Görtler series converges faster than the corresponding Blasius series [15] . The computed temperature and velocity field at 90° and 150° from the stagnation point showed reasonable agreement with experimental data even if only one term of the series were used. Due to lack of information of the universal functions associated with the higher order terms of the series expansion for flow variables, no definite conclusion can be drawn on the ability of this method to predict heat transfer accurately for other cylindrical configurations. Again, the same problem was treated by Lin and Chao [18] using a series expansion of the form proposed by Merk [19] and corrected by Chao and Fagbenle [20]. Their results agreed well with the previous analyses [15, 17] for horizontal circular cylinders and spheres. The main difficulty in this method of solution is to evaluate the gradients with respect to the configuration parameter of the problem, which necessitates accurate evaluations of Zero-order solutions in the neighbourhood of each value of that parameter and hence calculations are to be performed on a large scale. Finite difference solutions have been obtained by Merkin [21, 22] for horizontal circular and

elliptic cylinders with uniform surface temperature or uniform heat flux. Lin and Chao [23] demonstrated that their series solutions for elliptical configuration agreed satisfactorily with the finite difference data and also pointed out that the various series results are largely dependent on body shape and much less on Prandtl number and coordinate transformations for the variables. Recently, Muntasser and Mulligan [24] applied local non-similarity method of solution [25] to study analytically the free convection over an isothermal horizontal circular cylinder. This method of solution gave results comparable in accuracy with the finite difference data. If the boundary layer characteristics are required only at specific points, the local non-similarity method [25] represents a substantial saving in computer time over full-scale digital methods.

Recently interest is shown in solving the governing equations for free convection over isothermal, horizontal circular cylinder without making boundary layer approximations. Kuehn and Goldstein [26] solved the governing Navier-Stokes and energy equations and obtained solutions over a wide range of Rayleigh number, that is, $10^{\circ} \leq Ra \leq 10^{7}$, where neither asymptotic matching techniques nor boundary layer assumptions are accurate. Their results also include the development of the buoyant plume (the plume begins to form at distance α from the stagnation point, given by $\alpha > 150^{\circ}$) which can not

be obtained using boundary layer methods. Pustovalov and Matveev [27] and Farouk and Güceri [28] have also solved these equations numerically.

For free convection along non-isothermal surfaces, analytical solutions have been found for the situations which yield similarity solutions. However, for laminar free convection exterior to heated surfaces, there are a very few analyses known for arbitrary non-uniform surface temperatures. The free convection over a vertical plate with arbitrarily prescribed non-uniform surface temperature was analysed by Sparrow [29] using the approximate integral method and later by Scherberg [30], utilizing the classical polynomial profiles of Squire [31]. Sparrow has treated a class of special surface-temperature variations [29] for the entire Prandtl number range, while Scherberg considers the non-isothermal surface problem by means of a quasi-uniform-surface temperature scheme, in which the effect of non-zero leading edge boundary-layer thickness is also taken into account. Kuiken [32] obtained an expansion for the case where wall temperature variation is expressed as a power series in terms of the streamwise coordinate. A Görtler-type series expansion has been tried by Kellher and Yang [33] to accommodate more general wall temperature variations. They demonstrated that the integral procedure of Sparrow [29] gave over-estimated values for heat transfer. Recently,

Kao,Domoto and Elrod [34] have developed another approximate method of solution for analysing free convection over non-isothermal vertical plate with arbitrary (though smooth) temperature or heat-flux distributions, while Na [35] obtained finite difference solutions for several wall temperature distributions and he reported that the series solutions of Kao,Domoto and Elrod [34] are in good agreement with his data only in the initial portion of the boundary layer and further downstream they deviate from his computed results.

The free convection over non-isothermal curved surfaces have not received much attention. Koh and Price [36] solved the non-isothermal free convection problem over circular cylinder as formulated by Chiang and Kaye [15]. They eliminated the dependence of polynomial coefficients in the surface condition from the governing equation of the flow by using special transformations. But still the number of terms needed to represent velocity and temperature profiles is directly dependent on the number of terms retained in the wall temperature data. Recently, Lin and Chern [37] extended Merk's type series method of solution to non-isothermal surfaces and presented numerical solutions to horizontal circular cylinder for a specific wall-temperature distribution. Now, this method of solution involves algebraic manipulations also, besides the need to evaluate accurately the gradients with respect to the redefined configuration parameter.

In chapter II of the present thesis, our aim is to study the laminar boundary layer description of planar free convection around two-dimensional isothermal and non-isothermal bodies of arbitrary shapes. The flow is a result of temperature difference between the surface of the object and the fluid. The Görtler-type transformation already proposed for isothermal surface condition [17] is modified to deal with arbitrarily prescribed non-isothermal wall conditions. The resulting transformed boundary layer equations contain two streamwise dependent parameters which characterize both the non-isothermal conditions and the shape of the object. Series representation of the dependent boundary layer variables are developed on the lines of Görtler series method [38], when the wall temperature variations are prescribed as

(i) $\sum_{k=0}^{\infty} a_k x^{2k}$ for round-nosed horizontal cylinders, with $a_o \neq 0$ and x, the distance from stagnation point

and (ii) $x \sum_{k=0}^{\infty} a_k x^{2k}$ for vertical plate, with $a_o \neq 0$ and x, the distance from the leading edge.

For round-nosed cylinders, the ordinary differential equations which determine the functional coefficients in the series expansion for the dependent variables are independent of the body contour and wall temperature data. Instead, some of the numerical coefficients in these equations are

fixed by the class of body shape, namely round-nosed here. Hence solutions can be obtained for this class once and for all the fixed values of the Prandtl number. In the isothermal case, the first five-terms of the series are split into 24 universal functions and the governing equations for them are integrated for Prandtl number 0.7 and 1.0 on a Dec-10 computer with reasonable accuracy. Again, for the non-isothermal case, the first three-terms of the series are split into 16 universal functions and as before the governing equations for those universal functions which account for non-isothermality conditions are integrated for Prandtl numbers 0.7 and 1.0. The body contour and the wall temperature data enter the problem only when the series for flow variables are assembled.

For an isothermal circular cylinder, it is found that a 5-term sum of the series representation for shape parameter accurately represents it over the lower-half of the cylinder while the results obtained for the heat-flux density at the surface with the same number of terms from the corresponding series for it are accurate upto 87 percent of angular distance of 150° from the lower stagnation point of the cylinder and in the rest of the portion the results are predicted within an error of $3\frac{1}{2}$ percent in comparison with the available exact results, thereby showing that this series method is valid as far as 150°. On the other hand,

for blunt elliptic cylinder with aspect ratio 2:1, the shape parameter is well represented by a 5-term sum of its series upto an eccentric angle 45° measured from lower stagnation point and the results for heat-flux density at the surface obtained from sum of the first 5-terms of its series is sufficiently accurate upto 115° on comparison with finite difference data. For non-isothermal circular cylinder, the method of solution is applied to two specific wall temperature distributions. For practical purposes, two terms are found to be just sufficient to represent accurately the velocity and temperature distributions in the vicinity of the lower half of the circular cylinder. Also, it is observed that non-isothermal conditions at the surface has a significant effect on the rate of heat transfer from the surface to the fluid.

For vertical plate problem, we calculated 24 universal functions associated with the first 5-terms in the series expansion for flow variables. These universal functions depend only on Prandtl number and are independent of wall temperature data. These functions are calculated for Prandtl number 0.7 and 1.0 and the boundary layer flow over non-isothermal vertical plate with sinusoidal wall temperature variation is studied. The results obtained for local heat transfer coefficient compares well with available finite difference data [35].

In the study of natural convection phenomena, another area of importance is the flow over flat surfaces which are inclined to the direction of the gravity field. Surface inclination results in a pressure gradient across the boundary layer and leads to an analysis more complicated than that for vertical surface. For small angles of inclination with the vertical, the pressure gradient term in the momentum equation corresponding to the direction along the surface is neglected by an order of magnitude arguments. But retaining of this pressure gradient term becomes very important for boundary layer over surfaces inclined at large angles to the vertical. For surfaces which are horizontal or nearly horizontal, the buoyancy force tangential to the surface is very small. In particular, there is no component of the buoyancy force along a horizontal surface and there is therefore no direct drive of any tangential flow that may result. Rotem and Claassen [39] carried out a flow visualization experiment using a semifocussing Schlieren system which clearly indicated the existence of a boundary layer near the leading edge on the upper side of a heated horizontal surface. Recently, Yousef, Tarrasuk and Mckeen [40] also studied the laminar free convection boundary layer over a heated isothermal surface using Mach-Zehnder interferometer;

Stewartson [41] was the first to give a theoretical description of how a boundary layer is formed over a horizontal surface under the action of buoyancy force. His analysis contains a sign error in the pressure gradient term of the horizontal momentum equation and thus condition for existence of such a boundary layer is that the heated plate is to face downwards. Later, this error in the flow analysis was corrected by Gill, Zeh and del-casal [42] and one finds a horizontal boundary layer above the heated plate driven by an induced pressure, which falls in the direction of flow. This is called ''indirect drive'' and is due to the pressure deficiency in the thermal transport region next to the surface with respect to the ambient medium. It is indirect in that the buoyancy force does not drive the flow. Rather, it produces a pressure field which induces such a flow.

Free convection from nearly horizontal surfaces placed in an extensive body of fluid overlaying it above is vital to meterological and industrial applications. Pera and Gebhart [43] conducted experiments to determine laminar natural convection flow above horizontal and slightly inclined surfaces. For horizontal surfaces, their experimental findings were in close agreement with those of Rotem and Claassen [39]. They observed that for nearly horizontal surfaces with an angle of inclination α to the horizontal, the boundary layer

region is shorter for $\alpha < 4^\circ$ while, at higher inclinations the flow persists further. Also, they studied analytically the effect of a small surface inclination on flow and heat transport as a perturbation of flow over a horizontal surface. They reported that the effect of surface inclination is reflected more strongly in the velocity rather than in the temperature field. For a heated plate inclined at a small angle α to the horizontal, the boundary layer flow over the surface is driven not only by the indirect mechanism but also by a component of the buoyancy force B_t along the surface. Jones [44] studied this flow by considering that except in the neighbourhood of the leading edge, the direct-drive due to B_t dominates induced pressure effects, which can therefore be neglected. The resulting flow far downstream is then, in his analysis, what is described by the classical free convection solution for a heated vertical plate. He developed two series to obtain the solution, one valid near the leading edge and the other at large distances from it. The region where neither series is adequate, a step-by-step numerical procedure was used to obtain solutions of the boundary-layer equations. His numerical method of solution to obtain boundary-layer characteristics of the flow, is the selected points method of Lanczos and hence, necessarily he had to linearize the transformed conservation equations at any downstream location before commencing his numerical procedure. In the initial portion of this patching region,

he solved the set of equations obtained by using variables which account for departures from similarity solution for flow over horizontal surface, while at some downstream location onwards, he switched onto another set of equations using transformations suggested by anology with the classical case of free convection from a heated vertical plate.

In chapter III, the boundary layer in free convection flow over the upper surface of a heated semi-infinite horizontal plate inclined at small angle α with the horizontal is analysed by the local non-similarity method of solution [25]. The range of α considered here, as obtained from the analysis, is defined by the requirement that Λ, the limit of $Gr^{1/5} \tan \alpha$ as $Gr \to \infty$, be $O(1)$, where Gr is a suitably defined Grashof number. The forms of the local non-similarity method considered here are the two and three-equation models obtained by retaining the transformed conservation equations as such and only selectively neglecting terms in the derived subsidiary equations at the second and third level of the successive approximations in this method of solution. The corresponding two-point non-linear boundary value problem for these two models at a streamwise location are solved by the initial value technique as modified by Nachtsheim and Swigert [45]. Particularly, the application of this numerical procedure for the highly non-linear three-equation model was commenced at some downstream location with good

initial estimates of missing wall conditions generated by quasilinearization technique [46] . Numerical results for the local surface heat-transfer, wall shear-stress and velocity and temperature distributions are presented for Prandtl number 0.72 and 1.0 when $\Lambda = 1, -1$.

While the two-equation model is found to give boundary layer characteristics sufficiently accurate for engineering purposes, the three-equation model over-corrects these solutions and the results thus obtained, compare well with that of previous analysis. For small positive angle of inclination of the surface with the horizontal, unlike the previous analysis [44] where a composite non-similar solution was developed, our method of analysis shows solutions for the entire region of flow can be obtained with a single set of transformed boundary layer equations which makes no assumption on the neglect of induced pressure from some distance downstream away from the leading edge of the plate.

When the inclination of the plate to the horizontal is negative, although the pressure gradient associated with the indirect process remains favourable, separation of the boundary layer flow eventually occurs, since B_t now opposes the motion. Our method of solution predicts the point of separation of the flow and notably for the case of air, the two-equation model locates this point within an error of $1\frac{1}{2}$ per cent from the previous exact value [44] . Also, there

is no evidence of singularity at the point of separation of the flow, as also pointed out in [44] .

In the study of free convection boundary layer flow over nearly horizontal isothermal surface, we have seen that the nature of the flow is non-similar, the departure from similarity arising due to the inclination of the surface at an angle α with the horizontal. However, when $\alpha = 0$, the flow is similar and various analyses are available for this situation. Stewartson [41] published solutions for the flow for $Pr = 0.72$, while Gill, Zeh, and del-Casal [42] extended this to $Pr = 1.0$ and 10.0. All these solutions refer to the case in which the temperature of the bounding wall is constant, while Gill [42] also gave the solution for the case in which the boundary layer temperature varies as a power of the distance from the leading edge. Rotem [47] gave similar solution for semi-infinite horizontal plates for a power-law temperature difference between the plate and a uniform ambient fluid. Rotem and Claassen [39] numerically integrated the governing equations of two dimensional steady flow over an isothermal surface and gave the velocity and temperature profiles for various Prandtl numbers. Also they formulated the similarity solution for axi-symmetric flows on infinite surface [48] but no numerical results were given. Blanc and Gebhart [49] obtained some exact solutions to natural convection flows adjacent to horizontal disks,

including the energy effects of pressure and viscous dissipation.

Pera and Gebhart [43] considered both the surface conditions of uniform temperature and uniform heat flux for free convection boundary layer flow over semi-infinite horizontal plate and computed numerical solutions for a wide range of Prandtl numbers. Clarke and Riley [50] considered the prototype problem of Stewartson but allowed for density changes and temperature-dependent viscosity and thermal conductivity. Also they allowed the heated surface to be permeable and considered the effects of blowing upon the flow and thus their analysis can be taken to model the evaporative nature of the fuel surface. Again, they considered the free convective flow induced when a semi-infinite horizontal fuel surface burns in a quiescent oxidizing atmosphere [51]. Recently Mahajan and Gebhart [52] analysed the higher order effects for natural convection flow adjacent to a horizontal surface for a power-law surface temperature variation with leading term in this perturbation problem as the well known Zeroth-order boundary layer similarity solution treated earlier by Rotem and others [39, 43].

Very recently a few analytical studies [53, 54, 55] dealing with unsteady free convection flow over semi-infinite horizontal plate are made and they all deal with

the cases when the plate temperature oscillates in time about a constant non-zero mean temperature. While specific cases of similarity solution are dealt for steady free convection boundary layer flow over horizontal surfaces with different and additional effects, no similarity solution was considered so far for unsteady cases. It is well known that most approximate methods depend to some extent on knowledge of the ''similar'' solutions to the boundary layer equations. As we shall see in the final chapter, it is possible to formulate the boundary layer problem in such a way that the similar solutions form the first, and by far the most significant, term in an exact series solution to the partial differential equations, so that they can be used with considerable success even for non-similar flows.

The first study of a similar boundary layer appears to have been that for flow parallel to a flat surface by Blasius [56] not long after Prandtl [57] first propounded the concept of a boundary layer. The pressure-gradient in the stream direction in the solution by Blasius is zero. The range of similar solutions was then extended by Falkner and Skan [58] who included non-zero values of the pressure-gradient. A major contribution to our understanding of the concept of similarity was made by Mangler [59] who generalized the similarity conditions to include a much wider range of pressure gradients than earlier authors. Yang made a

corresponding study for free convection over a vertical plate and cylinder and gave all possible forms of similarity for both steady and unsteady cases.

In chapter IV we derive in a systematic way all possible similarity solutions for both steady and unsteady free convection boundary layer flow over a semi-infinite horizontal plate. The method consists of defining a new independent variable and three dependent similarity variables in terms of the generalised transformation variables. When these similarity variables are substituted into the boundary layer equations, they are reduced to a set of ordinary differential equations only if the coefficients of the similarity variables and their derivatives can be made constant. These coefficients when made constant are referred to as similarity conditions; they usually contain derivatives of the transformation variables and are thus differential equations themselves. Any solution to the similarity conditions which will result in explicit forms for the transformation variables, will transform the original set of partial differential equations into a set of ordinary differential equations and these are called similarity equations.

We have concluded from our present study that there are in all four possible cases of similarity for free convection over a horizontal surface. This analysis verifies that the similarity possibilities for steady cases have

essentially been covered in the literature, though somewhat more general wall thermal conditions could also be taken into account. The other two new possible cases deal with unsteady flow problems and these situations have not received any attention so far.

In the previous chapter for free convection over a semi-infinite horizontal plate, we have been concerned exclusively with similar boundary layer flows. But the majority of practical engineering problems involve flows for which conditions for similarity are not satisfied. Each problem involving laminar boundary layers has its own particular distribution of surface temperature and to solve the partial differential equations as opposed to the ordinary differential equations derived using similarity arguments, even for one such problem is a major computational task. Only recently, finite difference solutions [35] for non-isothermal vertical plate free convection problem have been obtained and that too, for some specific wall thermal conditions only. The other methods which yield solutions to arbitrary wall temperature variations belong to the series expansion techniques.

Unlike the vertical plate case where the surface characteristics to be determined relate to shear stress and heat flux, the horizontal plate problem includes also of determining the induced pressure at the wall. For vertical plate problem, methods ranging from Karman-Pohlhausen

technique with relatively crude profiles to full scale numerical computation procedures have been developed. On the other hand, to our knowledge, no single study either analytical or experimental is attempted so far for the corresponding case of a horizontal plate.

In the last chapter of the thesis, we initiate the study of free convection boundary layer flow over a semi-infinite non-isothermal horizontal plate for an arbitrarily prescribed surface conditions. A new Gortler-type transformation is introduced to reduce the governing boundary layer equations into non-similar form containing a streamwise dependent parameter which characterizes the non-isothermal conditions at the wall. The resulting equations are solved by the Görtler series expansion and the local non-similarity methods.

Series expansion is valid for an arbitrary surface temperature variations of the form

$$x^n \sum_{k=0}^{\infty} G_k \, x^{n(p+1)k}$$

where n, p, G_k are constants and $G_o \neq 0$ and x is a suitably normalized streamwise coordinate. Universal functions associated with the first 4-terms of the series expansion for flow variables are determined for air when $p = 1.0,\ 0.5,\ 0.25$. Application of the series solution method is illustrated for a class of wall temperature distributions given by

$G_o (1 + \varepsilon x^p)$ for some ε.

Also local non-similarity method at the second level of truncation, namely the two-equation model, is applied for this special case to predict local heat transfer coefficient at the wall for $Pr = 0.1, 0.72, 5.0$ when $p = 1.0, 0.5, 0.25$. A comparison of results for local heat transfer at the surface for air indicates that the local non-similarity method gives accurate results for a larger range of values of $s(= 1+ \varepsilon x^p)$ covered here than the 4-term sum of the series expansion. The effect of Prandtl number on local heat transfer coefficient at the surface for various values of p is studied by the local non-similarity method. It is found that for fixed values of s and p, the percentage increase of non-isothermal heat transfer at the surface over that for an isothermal surface decreases as Prandtl number increases.

REFERENCES

[1] Eckert, E.R.G., ASME, J. Heat Transfer, 103, 409-414 (1981).

[2] Sparrow, E.M., and Gregg, J.L., Recent advances in Heat and Mass Transfer (J.P. Hartnett, editor), Mc-Graw-Hill Book Co., N.Y. (1961).

[3] Jaluria, Y., Natural Convection Heat and Mass Transfer, Pergamon Press, Oxford (1980).

[4] Ostrach, S., NACA TN 2635 (1953).

[5] Hellums, J.D. and Churchill, S.W., Chem. Eng. Progr. Symposium Ser., No. 32, 57, 75 (1961).

[6] Schlichting, H., Boundary layer Theory, McGraw-Hill Book Company, N.Y. (1960).

[7] Schmidt, E., and Bechman, W., Tech. Mech. Thermodyn., 1, 341-391 (1930).

[8] Hermann, R., NACA Tech. Mem. 1366 (1954).

[9] Jodlbauer, K., Forsch. Ing.-Wes. 4, 157-172 (1933).

[10] Schuh, H., Gt. Brit. Ministry of Air Production Volkenrode Repts. and Transls. 1007, Apr. (1948).

[11] Merk, H.J. and Prins, J.A., Appl. Sci. Res. A4, 11-24, 195-206, 207-222 (1953-54).

[12] Braun, W.H., Ostrach, S. and Heighway, J.E., Int. J. Heat Mass Transfer, 2, 121-135 (1961).

[13] Herring, R.G., and Grosh, R.J., ibid 5, 1059 (1962).

[14] Herring, R.C., ibid, 8, 1333-1337 (1965).

[15] Chiang, T., and Kaye, J., Proc. Fourth National Cong. Appl. Mech., University of California, Berkeley, 1213-1219 (1962).

[16] Van Dyke, M., Proc. Ninth International Cong. Appl. Mech., Brussels, 3, 318 (1957).

[17] Saville, D.A. and Churchill, S.W., J. Fluid Mech., 29, 391-399 (1967).

[18] Lin, F.N. and Chao, B.T., ASME, J. Heat Transfer, 96, 435-442 (1974).

[19] Merk, H.J., J. Fluid Mech., 5, 460-480 (1959).

[20] Chao, B.T., and Fagbenle, R.O., Int. J. Heat Mass Transfer, 17, 223-240 (1974).

[21] Merkin, J.H., ASME-AICHE Heat Transfer conference, St. Louis, Mo., August (1976).

[22] _____ , ASME, J. Heat Transfer, 99, 453-457 (1977).

[23] Lin, F.N., and Chao, B.T., ibid, 100, 160-163 (1978).

[24] Muntasser, M.A., and Mulligan, J.C., ibid, 165-167, (1978).

[25] Sparrow, E.M., Quack, H. and Boerner, C.J., AIAA Journal, 8, 1936-1942 (1970).

[26] Kuehn, T.H. and Goldstein, R.J., Int. J. Heat Mass Transfer, 23, 971-979 (1980).

[27] Pustovalov, V.N. and Matveev, yu. ya., Inzhenerno-Fizicheskii Zhurnal, 43, 2 (1982).

[28] Farouk, B. and Güceri, S.I., ASME, J. Heat Transfer, 103, 522-527 (1981).

[29] Sparrow, E.M., NACA TN 3508 (1955).

[30] Scherberg, M.G., Int. J. Heat Mass Transfer, 8, 1319-1331 (1965).

[31] Goldstein, S. Ed. Modern Developments in Fluid Dynamics Clarendon Press, Oxford (1938).

[32] Kuiken, H.K., Appl. Sci. Res., 20, 205-215 (1969).

[33] Kelleher, M., and Yang, K.T., Quart. J. of Mech. and Appl. Math., 25, 445-457 (1972).

[34] Kao, T.T., Domoto, G.A. and Elrod, H.G., ASME J. Heat Transfer, 99, 72-79 (1977).

[35] Na, T.Y., Appl. Sci. Res., 33, 519-543 (1978).

[36] Koh, J.C.Y. and Price, J.F., ASME, J. Heat Transfer, 87, 237-242 (1965).

[37] Lin, F.N., and Chern, S.Y., ibid, 103, 819-821 (1981).

[38] Görtler, H., J. Math. Mech. 6, 1-66 (1957).

[39] Rotem, Z., and Claassen, L., J. Fluid Mech., 39, 173-192 (1969).

[40] Yousef, W.W., Tarasuk, J.D., and Mckeen, W.J., ASME, J. Heat Transfer, 104, 493-500 (1982).

[41] Stewartson, K., Z.A.M.P., 9a, 276-281 (1958).

[42] Gill, W.N., Zeh, D.W., and del-Casel, E., ibid, 16, 539-541 (1965).

[43] Pera, L., and Gebhart, B., Int. J. Heat Mass Transfer, 16, 1147-1163 (1973).

[44] Jones, D.R., Quart. J. of Mech. and Appl. Math., 26, 77-98 (1973).

[45] Nachtsheim, P.R. and Swigert, P., Development of Mechanics, 1, 361-367 (1965).

[46] Roberts, S.M. and Shipmann, J.S., Two-point Boundary Value Problems: Shooting methods American Elsevier NY (1972).

[47] Rotem, Z., Proc. First Canadian Nat'l Congr. Appl. Mech., 2, 309-310 (1967).

[48] Rotem, Z., and Claassen, L., Canadian J. Chem. Eng., 47, 460-467 (1969).

[49] Blanc, P. and Gebhart, B., 5th International Heat Transfer Conference, Tokyo, 3, 20-24 (1974).

[50] Clarke, J.F. and Riley, N., Quart. J. of Mech. and Appl. Math., 28, 373-396 (1975).

[51] _____, J. Fluid Mech., 74, 415-431 (1976).

[52] Mahajan, R.L. and Gebhart, B., ASME, J. Heat Transfer, 102, 368-371 (1980).

[53] Verma , R.L. and Singh, P., Aust. J. Phys., 30, 335-345 (1977).

[54] Singh, P., Sharma, V.P. and Mishra, U.N., Acta Mechanica, 30, 111-128 (1978).

[55] Verma, A.R., Int. J. Engng. Sci., Vol. 21, 35-43 (1983).

[56] Blasius, H., Z. Math. und Phys. 56, 1-37 (1908).

[57] Prandtl, L., Internationalen Mathematiker-Kongresses, Heidelberg, 481-491 (1904).

[58] Falkner, V.M. and Skan, S.W., British Aero. Res. Council, Reports and Memoranda, 1884 (1937).

[59] Mangler, W., Z.A.M.M., 28, 97-103 (1948).

[60] Yang, K.T., Trans. J. Applied Mechanics, 82, 230-236 (1960).

CHAPTER II

LAMINAR FREE CONVECTION OVER TWO-DIMENSIONAL ISOTHERMAL AND NON-ISOTHERMAL BODIES OF ARBITRARY CONTOUR

1 INTRODUCTION

This chapter is primarily concerned with prediction of heat transfer in planar free convection boundary layer flow over smooth bodies of arbitrary shape with uniform and non-uniform surface thermal conditions, placed in an unbounded Boussinesq fluid. There is, at present, adequate information about laminar free convection boundary layers over isothermal bodies of simple shapes such as a vertical plate or cone, for which the flow is similar [1]. However, similarity does not arise in many practical situations in the study of free convection phenomena. Notably, both cylindrical and spherical configurations do not give similarity. Hence, several other methods have been employed for obtaining a solution to the governing equations of such flows.

Hermann [2] has treated analytically the laminar steady state heat transfer from an isothermal cylinder by a modified Pohlhausen's similarity solution for the vertical plate at Prandtl number 0.733. The boundary layer thickness at different angles around the cylinder was obtained by multiplying the flat plate boundary layer thickness by a parameter that is a function only of angle from the stagnation point. Merk and Prins [3] presented analytical results of the heat transfer around horizontal cylinders and spheres using the integral method first introduced by Squire for a flat plate.

Chiang and Kaye [4] used a different scheme for obtaining a solution to the boundary layer equations for free convection over a horizontal cylinder with prescribed surface temperature or surface heat-flux, expressed as polynomials of distances from the stagnation point. The approach was similar to the Blasius series for incompressible viscous flow over arbitrary cylinders. Again, for free convection flow around non-isothermal circular cylinder, Koh and Price [5] devised special transformations to treat the differential equations that arise out of applying Blasius series technique so as to remove their dependence on the polynomial coefficients in the prescribed surface thermal conditions. Later, Chiang, Ossin and Tien [6] also employed the Blasius series method of solution to determine the velocity and temperature profiles for angular positions around a sphere.

Recognizing the need for a procedure to account for the effects of body shape in a general way, Saville and Churchill [7] introduced an analysis closely patterned on Görtler's series for forced flow [8] so as to describe laminar free convection near isothermal horizontal cylinders with fairly arbitrary body contours. When applied to horizontal circular cylinders and spheres, the series converges rapidly than the corresponding Blasius series. Again, Wilks [9] and Lin [10] used the Görtler's series method of solution in studying two-dimensional boundary layers over bodies of uniform

heat-flux. Also this series method has been tried by Kelleher and Yang [11] for treating free convection over a non-isothermal vertical plate with more general wall temperature variations. Kuiken [12] has developed a particular series solution for the free convection over a non-isothermal vertical plate. Lin and Chao [13] used a Merk type series to obtain solutions for various two-dimensional geometries with horizontal circular cylinder as a special case. Later Lin and Chern [14] extended this method of solution for free convection over non-isothermal horizontal circular cylinders. Also, finite difference solutions have been obtained by Merkin [15,16] for horizontal circular and elliptic cylinders of uniform temperature or uniform heat-flux. Na [17] presented finite difference results for heat transfer in laminar free convection over non-isothermal vertical plate.

In the present study, we have developed a Görtler type transformation to study the laminar free convection boundary layers over non-isothermal bodies of arbitrary shape. The resulting transformed boundary layer equations contain two parameters dependent on streamwise locations on the surface. The special data of the problems under our consideration appear only in these parameters. Series representations for the dependent boundary layer variables are developed on the lines of Görtler series method of solution for forced

flows. This method of solution is applied to flow over non-isothermal vertical plate and long horizontal round-nosed non-isothermal cylinders of arbitrary body shapes. Wall temperature variations in these two cases are prescribed as follows:

(i) $\sum_{k=0}^{\infty} a_k x^{2k}$ for round-nosed cylinders, with $a_o \neq 0$, a_k constants and x, a normalized distance from stagnation point and

(ii) $x \sum_{k=0}^{\infty} a_k x^{2k}$ for vertical plate, with $a_o \neq 0$ and x, a normalized distance from the leading edge.

For round-nosed cylinders, the ordinary differential equations which determine the functional coefficients in the series expansion for the dependent variables are independent of the body contour and wall temperature data. Instead, some of the numerical coefficients in these equations are fixed by the class of body shape, namely round-nosed here. Hence, solutions can be obtained for this class once and for all for fixed values of the Prandtl number. In the isothermal case, the first five-terms of the series are split into 24 universal functions and the governing equations for them are integrated for Prandtl number 0.7 and 1.0 on a Dec-10 computer with reasonable accuracy. Again, for the non-isothermal case, the first three-terms of the series are split into 16 universal functions and as before the governing

equations for those universal functions which account for non-isothermality conditions are integrated for Prandtl number 0.7 and 1.0. The body contour and the wall temperature data enter the problem only when the series for flow variables are assembled.

For an isothermal circular cylinder, it is found that a five-term sum of the series representation for shape parameter accurately represents it over the lower-half of the cylinder while the results obtained for the heat-flux density at the surface with the same number of terms from the corresponding series for it are accurate upto 87 per cent of the angular distance 150° from the lower stagnation point of the cylinder and in the rest of the portion the results are predicted within an error of $3\frac{1}{2}$ percent in comparison with the available exact results [15], thereby showing that this series method is valid upto 150°. On the other hand, for blunt elliptic cylinder with aspect ratio 2:1, the shape parameter is well represented upto an eccentric angle of 45° measured from the stagnation point and the results for heat-flux density at the surface is sufficiently accurate upto an eccentric angle of 115° on comparison with finite difference data [16]. For non-isothermal circular cylinder, the method is illustrated for two specific wall temperature distributions. It is found that non-isothermal conditions at the surface have a significant effect on heat transfer. Also the effect of Prandtl number is studied.

For vertical plate problem, proceeding as before we calculated 24 universal functions associated with the first-five terms in the series expansion for flow variables for Prandtl number 0.7 and 1.0. They are dependent only on Prandtl number and are independent of wall temperature data. Using these functions, we investigated the boundary layer flow over non-isothermal vertical plate with sinusoidal wall temperature variation. The result obtained for local heat transfer coefficient compares well with available finite difference data [17].

2. BASIC EQUATIONS

We consider steady laminar flow over two-dimensional bodies of non-uniform surface temperature t_w situated in an ambient fluid of temperature t_∞, where $t_w > t_\infty$. For the steady state free convection phenomena, equations (1.9), (1.13) and (1.11) reduce to:

Continuity equation

$$\nabla \cdot \vec{V} = 0, \tag{2.1}$$

conservation of momentum

$$\vec{V} \cdot \nabla \vec{V} = -\frac{1}{\rho} \nabla P + \nu \nabla^2 \vec{V} - \beta(t-t_\infty)\vec{g}, \tag{2.2}$$

conservation of energy

$$\vec{V} \cdot \nabla t = \alpha \nabla^2 t, \tag{2.3}$$

where t represents the temperature. Using the identity

$$\vec{V}\cdot\nabla\vec{V} = \frac{1}{2}\nabla(\vec{V}\cdot\vec{V}) - \nabla\times\nabla\times\vec{V}$$

in (2.2) and then applying curl operator on both sides, the resulting momentum equation is

$$\vec{V}\cdot\nabla\vec{W} = -\beta\nabla t\times\vec{g} + \nu\nabla^2\vec{W} \qquad (2.4)$$

where $\vec{W} = \nabla\times\vec{V}$.

The momentum equation (2.4) is now free from pressure variable though, of course, we have increased the order of the system.

The boundary conditions of the problem are:

$$\vec{V} = 0, \quad t = t_w \quad \text{on the surface}$$

and

$$\vec{V} = 0, \quad t = t_\infty \quad \text{at infinity}. \qquad (2.5)$$

3. BOUNDARY LAYER MODEL OF FREE CONVECTION IN CURVILINEAR COORDINATES

In order to formulate the governing equations (2.1), (2.3) and (2.4) for a curvilinear system of coordinates, we use the special system of coordinates which is intimately connected with the geometry of the surface namely a horizontal cylinder for our considerations here and also symmetry properties of the problem. For the curves $\bar{x}$ = constant we take the

normals to the wall, and for the curves $\bar{y}$ = constant we take the curves parallel to the wall. The coordinate system is then an orthogonal one based on distances $\bar{x}$ and $\bar{y}$ where $\bar{x}$ is measured along the surface from an intersection of the plane of symmetry parallel to the body, which for flow near horizontal cylinder, is taken as the forward stagnation point while $\bar{y}$ is normal distance from the wall (see figure 1). Tollmien [18] derived expressions for the complete Navier-Stokes equations in this system of coordinates. We shall now derive the boundary layer model of the free convection phenomena on the lines of Goldstein's work [19] for forced flow over a cylinder.

Let φ be the angle measured in the anticlockwise direction between a horizontal plane and the line tangent to the surface at $P(\bar{x},\bar{y})$. The components of $\vec{PQ}$ along $\bar{x}$ and $\bar{y}$ directions are respectively $h_1 d\bar{x}$ and $h_2 d\bar{y}$ where the scale factors h_1 and h_2, are given by $h_1 = 1+\kappa\bar{y}$ and $h_2 = 1$, κ being the local curvature of the wall so that $\kappa = \frac{d\varphi}{d\bar{x}}$, a function of $\bar{x}$. The general expressions for the operators div, curl, grad, etc., in this system of coordinates are

$$\nabla = \frac{1}{1+\kappa\bar{y}}\,\vec{i}\,\frac{\partial}{\partial\bar{x}} + \vec{j}\,\frac{\partial}{\partial\bar{y}},$$

$$\nabla\cdot\vec{V} = \frac{1}{1+\kappa\bar{y}}\left\{\frac{\partial\bar{u}}{\partial\bar{x}} + \frac{\partial}{\partial\bar{y}}(1+\kappa\bar{y})\,\bar{v}\right\},$$

$$\nabla \times \vec{V} = \vec{k}\,\frac{1}{1+\kappa\bar{y}}\left\{\frac{\partial \bar{v}}{\partial \bar{x}} - \frac{\partial}{\partial \bar{y}}(1+\kappa\bar{y})\bar{u}\right\},$$

$$\nabla^2 = \frac{1}{1+\kappa\bar{y}}\left\{\frac{\partial}{\partial \bar{x}}\left(\frac{1}{1+\kappa\bar{y}}\frac{\partial}{\partial \bar{x}}\right) + \frac{\partial}{\partial \bar{y}}(1+\kappa\bar{y})\frac{\partial}{\partial \bar{y}}\right\} \qquad (2.6)$$

where $\bar{u}$ and $\bar{v}$ are respectively the velocities in the $\bar{x}$ and $\bar{y}$ directions, $\vec{i}$, $\vec{j}$, $\vec{k}$ are the unit vectors along $\bar{x}$, $\bar{y}$ and perpendicular to the plane of the flow respectively.

We now introduce the following non-dimensional variables

$$x = \frac{\bar{x}}{L}, \quad y = \frac{\bar{y}}{L}, \quad u = \frac{\bar{u}}{\left(\frac{\nu}{L}\right)},$$

$$v = \frac{\bar{v}}{\left(\frac{\nu}{L}\right)}, \quad \kappa' = \kappa L, \quad \theta = \frac{t-t_\infty}{t_w-t_\infty} \qquad (2.7)$$

where

$t_w - t_\infty = (t_r - t_\infty)\, G(\frac{\bar{x}}{L})$, t_r being some reference temperature. Here L is a characteristic length and $G(x)$ is a prescribed surface temperature variation.

Using (2.6) and (2.7), the governing equations (2.1), (2.4) and (2.3) become

$$\frac{\partial u}{\partial x} + \frac{\partial}{\partial y}(1+\kappa' y)v = 0, \qquad (2.8)$$

$$\left[\frac{u}{(1+\kappa' y)}\frac{\partial}{\partial x} + v\frac{\partial}{\partial y}\right]\frac{1}{(1+\kappa' y)}\left[\frac{\partial v}{\partial x} - \frac{\partial}{\partial y}(1+\kappa' y)u\right]$$

$$= - \frac{g\beta(T_r-T_\infty)L^3 G(x)}{\nu^2} \left[\frac{\cos\varphi}{1+\kappa' y} \frac{\partial\theta}{\partial x} + \sin\varphi \frac{\partial\theta}{\partial y}\right]$$

$$+ \frac{1}{(1+\kappa' y)}\left[\frac{\partial}{\partial x}\left(\frac{1}{1+\kappa' y}\frac{\partial}{\partial x}\right) + \frac{\partial}{\partial y}(1+\kappa' y)\frac{\partial}{\partial y}\right]\frac{1}{(1+\kappa' y)} \times$$

$$\times \left[\frac{\partial v}{\partial x} - \frac{\partial}{\partial y}(1+\kappa' y)u\right], \qquad (2.9)$$

$$\frac{u}{(1+\kappa' y)}\frac{\partial\theta}{\partial x} + v\frac{\partial\theta}{\partial y} + \frac{u\theta}{(1+\kappa' y)}\frac{1}{G}\frac{dG}{dx}$$

$$= \frac{\bar{\alpha}}{\nu(1+\kappa' y)}\left[\frac{\partial}{\partial x}\left(\frac{1}{1+\kappa' y}\frac{\partial\theta}{\partial x}\right) + \frac{\partial}{\partial y}(1+\kappa' y)\frac{\partial\theta}{\partial y}\right]. \qquad (2.10)$$

Here φ is the angle between the surface normal and the body force. The momentum equation (2.9) contains a dimensionless parameter $\frac{g\beta(T_r-T_\infty)L^3}{\nu^2}$, called the Grashof number and to be denoted, hereafter, as Gr. We shall write $\sigma = \frac{\bar{\alpha}}{\nu}$ and σ is a dimensionless parameter of the fluid and this occurs in energy equation (2.10).

We now introduce asymptotically modified variables in equations (2.8) to (2.10)

$$\hat{y} = y\,Gr^{1/4}, \quad \hat{u} = u\,Gr^{1/2}, \quad \hat{v} = v\,Gr^{-1/4}.$$

The introduction of these variables is equivalent to the application of boundary layer approximations. The conservation equations (2.8) to (2.10) now become

$$\frac{\partial\hat{u}}{\partial x} + \frac{\partial}{\partial\hat{y}}(1+\kappa'\hat{y}Gr^{-1/4})\hat{v} = 0, \qquad (2.11)$$

$$\left[\frac{\hat{u}}{(1+\kappa'\hat{y}Gr^{-1/4})}\frac{\partial}{\partial x}+\hat{v}\frac{\partial}{\partial\hat{y}}\right]\frac{1}{(1+\kappa'\hat{y}Gr^{-1/4})}\left[\frac{1}{Gr^{1/2}}\frac{\partial\hat{v}}{\partial x}-\frac{\partial}{\partial\hat{y}}(1+\kappa'\hat{y}Gr^{-1/4})\hat{u}\right]$$

$$=-G(x)\left[\frac{\cos\varphi}{Gr^{1/4}(1+\kappa'\hat{y}Gr^{-1/4})}\frac{\partial\theta}{\partial x}+\sin\varphi\frac{\partial\theta}{\partial\hat{y}}\right]\frac{1}{(1+\kappa'\hat{y}Gr^{-1/4})}$$

$$\left[\frac{1}{Gr^{1/2}}\frac{\partial\hat{v}}{\partial x}-\frac{\partial}{\partial\hat{y}}(1+\kappa'\hat{y}Gr^{-1/4})\hat{u}\right]. \qquad (2.12)$$

$$\frac{\hat{u}}{(1+\kappa'\hat{y}Gr^{-1/4})}\frac{\partial\theta}{\partial x}+\hat{v}\frac{\partial\theta}{\partial\hat{y}}+\frac{\hat{u}\,\theta}{(1+\kappa'\hat{y}Gr^{-1/4})}\frac{1}{G}\frac{dG}{dx}$$

$$=\frac{1}{\sigma}\frac{1}{(1+\kappa'\hat{y}Gr^{-1/4})}\left[\frac{1}{Gr^{1/2}}\frac{\partial}{\partial x}\left\{\frac{1}{(1+\kappa'\hat{y}Gr^{-1/4})}\frac{\partial\theta}{\partial x}\right\}\right.$$

$$\left.+\frac{\partial}{\partial\hat{y}}(1+\kappa'\hat{y}Gr^{-1/4})\frac{\partial\theta}{\partial\hat{y}}\right]. \qquad (2.13)$$

As Gr becomes large and if the curvature of the body, κ, is small in order to insure that $\kappa'Gr^{-1/4}\hat{y}$ remains small, the above system of equations will yield the inner solution valid near the boundary surface and known as the boundary layer solution to the free convection over the surface [19]. Thus, by neglecting the terms which vanish supposedly as $Gr \to \infty$, we arrive at the system

$$\frac{\partial\hat{u}}{\partial x}+\frac{\partial\hat{v}}{\partial\hat{y}}=0, \qquad (2.14)$$

$$(\hat{u}\frac{\partial}{\partial x}+\hat{v}\frac{\partial}{\partial\hat{y}})(-\frac{\partial\hat{u}}{\partial\hat{y}})=-G(x)\sin\varphi\frac{\partial\theta}{\partial\hat{y}}-\frac{\partial^3\hat{u}}{\partial\hat{y}^3}, \qquad (2.15)$$

$$\hat{u}\frac{\partial\theta}{\partial x}+\hat{v}\frac{\partial\theta}{\partial\hat{y}}+\frac{\hat{u}\theta}{G}\frac{dG}{dx}=\frac{1}{\sigma}\frac{\partial^2\theta}{\partial\hat{y}^2} \tag{2.16}$$

with boundary conditions:

$$\hat{y}=0: \quad \hat{u}=0=\hat{v}\ , \ \theta=1\ ,$$

$$\hat{y}\to\infty: \quad \hat{u}\to 0\ , \ \theta\to 0\ . \tag{2.17}$$

The momentum equation (2.15) is integrated once with respect to $\hat{y}$ and then, using boundary conditions, we arrive at the final form of the boundary layer model for the free convection phenomena:

$$\frac{\partial\hat{u}}{\partial x}+\frac{\partial\hat{v}}{\partial\hat{y}}=0\ , \tag{2.18}$$

$$\hat{u}\frac{\partial\hat{u}}{\partial x}+\hat{v}\frac{\partial\hat{u}}{\partial\hat{y}}=G(x)\sin\varphi+\frac{\partial^2\hat{u}}{\partial\hat{y}^2}\ , \tag{2.19}$$

$$\hat{u}\frac{\partial\theta}{\partial x}+\hat{v}\frac{\partial\theta}{\partial\hat{y}}+\hat{u}\theta\frac{1}{G}\frac{dG}{dx}=\frac{1}{\sigma}\frac{\partial^2\theta}{\partial\hat{y}^2}\ , \tag{2.20}$$

with the boundary conditions (2.17).

With the introduction of the stream function Ψ such that

$$\hat{u}=\frac{\partial\Psi}{\partial\hat{y}}\ , \quad \hat{v}=-\frac{\partial\Psi}{\partial x}\ , \tag{2.21}$$

the boundary layer model for two-dimensional surfaces can be written as

$$\Psi_{\hat{y}}\,\Psi_{x\hat{y}} - \Psi_x\,\Psi_{\hat{y}\hat{y}} = G(x)\,S(x)\,\theta + \Psi_{\hat{y}\hat{y}\hat{y}\hat{y}}\,, \tag{2.22}$$

$$\Psi_{\hat{y}}\,\theta_x - \Psi_x\,\theta_{\hat{y}} + \frac{1}{G}\frac{dG}{dx}\Psi_{\hat{y}}\,\theta = \frac{1}{\sigma}\,\theta_{\hat{y}\hat{y}} \tag{2.23}$$

with the boundary conditions:

$$\begin{aligned} &\hat{y} = 0: \quad \Psi = \Psi_{\hat{y}} = 0\,, \quad \theta = 1\,, \\ &\hat{y} \to \infty: \quad \Psi_{\hat{y}} \to 0, \qquad \theta \to 0\,, \end{aligned} \tag{2.24}$$

where the sine of the angle φ between the body force vector and normal to the surface of the object is $S(x)$. It can be seen that for $\varphi = \pi/2$, the above equations with the corresponding conditions are the boundary layer equations to the laminar free convection over a non-isothermal vertical plate.

We now define the important physical characteristics for the boundary layer flow and heat transfer. The Nusselt number, Nu, for the dimensionless heat-flux density at the surface is defined as

$$\mathrm{Nu} = \frac{(\text{heat-flux density})\quad(\text{characteristic length})}{(\text{thermal conductivity})\quad(\text{temperature difference})}\,,$$

$$= -\mathrm{Gr}^{1/4}\left(\frac{\partial\theta}{\partial\hat{y}}\right)_{\hat{y}=0}\,. \tag{2.25}$$

The Nusselt number averaged over a length, L, is

$$\overline{Nu} = \frac{1}{L} \int_0^L Nu(x')dx' \quad . \tag{2.26}$$

The dimensionless shear stress at the surface is

$$\tau_f = \frac{\tau L^2}{\nu \mu} = Gr^{3/4} \left(\frac{\partial^2 \Psi}{\partial \hat{Y}^2}\right)_{\hat{y}=0} \quad , \tag{2.27}$$

and the average shear stress at the wall is

$$\bar{\tau}_f = \frac{1}{L} \int_0^L \tau_f(x')dx' \quad . \tag{2.28}$$

4. TRANSFORMATION OF BOUNDARY LAYER EQUATIONS

We now introduce the following transformation to reduce the laminar boundary layer equations to a system of differential equations containing two streamwise dependent parameters that account for the body shape and non-uniformity in surface thermal conditions:

$$\xi = \int_0^x [G(z)\ S(z)]^{1/3}\ dz \quad , \tag{2.29}$$

$$\eta = \left(\frac{3}{4}\right)^{1/4} \frac{\hat{y}}{\xi^{1/4}} [S(x)G(x)]^{1/3} \quad , \tag{2.30}$$

$$\Psi(x,\hat{y}) = \left(\frac{4}{3}\right)^{3/4} \xi^{3/4}\ F(\xi,\eta) \quad , \tag{2.31}$$

$$T(\xi,\eta) = \theta(x,\hat{y}) \quad . \tag{2.32}$$

It is to be noted that for isothermal bodies, the above transformations reduce to that of Saville and Churchill [7] in their treatment of boundary layer free convection over isothermal bodies of arbitrary contour.

The transformed boundary layer equations are now

$$F_{\eta\eta\eta} + T = \frac{4}{3}\,\xi(F_{\xi\eta}F_{\eta} - F_{\xi}F_{\eta\eta}) - FF_{\eta\eta} + \frac{4}{3}\,K(\xi)\,F_{\eta}^{2}\ , \qquad (2.33)$$

$$\frac{1}{\sigma}\,T_{\eta\eta} = \frac{4}{3}\,\xi(T_{\xi}F_{\eta} - F_{\xi}T_{\eta}) - FT_{\eta} + 4\omega(\xi)\,F_{\eta}T\ , \qquad (2.34)$$

where

$$K(\xi) = \frac{1}{2} + \frac{\xi}{3SG}\,\frac{d(SG)}{d\xi} \qquad (2.35)$$

and

$$\omega(\xi) = \frac{\xi}{3G}\,\frac{dG}{d\xi}\ . \qquad (2.36)$$

The boundary conditions are now

$$\eta = 0 : \quad F(\xi,\eta) = \frac{\partial F(\xi,\eta)}{\partial \eta} = 0,\ T(\xi,\eta) = 1\ ,$$

$$\eta \to \infty : \frac{\partial F(\xi,\eta)}{\partial \eta} \to 0,\ T(\xi,\eta) \to 0. \qquad (2.37)$$

It should be noted that the data of any problem appear in the transformed equations only through functions $K(\xi)$ and $\omega(\xi)$, where it is understood that x is a function of ξ defined uniquely by (2.29). These functions play an important role in the analysis to follow and they will be called the Principal Functions of the problem.

5. GORTLER SERIES METHOD OF SOLUTION

For the purpose of generating series solutions for the transformed boundary layer equations (2.33) and (2.34) the forms of $K(\xi)$ and $\omega(\xi)$ should be obtained in terms of power series in ξ and hence to be determined from equation (2.29). Now, we develop the method for long horizontal cylinders of rounded-nosed cross-section and a semi-infinite vertical plate for an arbitrarily prescribed surface temperature distribution. For either of these configurations $S(x)$ is known and once $G(x)$ is fixed, we can express $K(\xi)$ and $\omega(\xi)$ in a series form.

Yang and Kelleher [11] considered the general wall temperature variations for a non-isothermal vertical plate in the form:

$$G(x) = x^n \sum_{k=0}^{\infty} a_k x^{pk(n+1)}$$

where p is any constant and n is the surface temperature variation parameter and x is the distance measured from the leading edge. The governing boundary layer equations for a non-isothermal vertical plate with the above prescribed surface temperature variation were solved for $\sigma = 0.7$ with $n = 0,\ 1/5$ and $p = 1,\ 1/2$. For our consideration of free convection over a non-isothermal vertical plate, we shall assume

$$G(x) = x \sum_{k=0}^{\infty} a_k x^{2k} \quad \text{with} \quad a_0 \neq 0.$$

For $a_k = 0$ for $k \geq 1$, it is seen that $G(x)$ varies linearly with distance from the leading edge and this distribution gives rise to a similarity solution as shown by Sparrow and Gregg [20]. This surface condition is of special significance as it yields similarity solution for the full Navier-Stokes equations governing the flow over non-isothermal vertical plate as demonstrated by Reeves and Kippemann [21].

Chiang and Kaye [4] considered laminar free convection boundary layer flow over a horizontal circular cylinder with

$$G(x) = 1 + a_1 x^2 + a_2 x^4 .$$

Later Koh and Price [5] solved the above problem for a pair of values of a_1 and a_2. For our studies on non-isothermal cylinder and a non-isothermal vertical plate, we shall take

$$G(x) = x^{\delta} \sum_{k=0}^{\infty} a_k x^{2k} , \quad a_o \neq 0 \qquad (2.38)$$

where $\delta = 1$ for vertical plate,

and $\delta = 0$ for round-nosed cylinder.

Using (2.38) and expressions for $S(x)$ in (2.29), (2.35) and (2.36), we can write $\xi, \beta(\xi)$ and $\omega(\xi)$ as a power series in x and then applying the Lagrange's formula for for reversion of power series [22] , the variable x is obtained as a power series in ξ (see Appendix A). This

series for x is used in the β and ω expansions to yield a series for β and ω in powers of ξ. The coefficients in β and ω series will ultimately be functions of the coefficients in the expansion of G and S. To obtain the required series expansions certain operations such as multiplication, division, and inversion, as well as differentiation and integration term-by-term will be performed on SG. Such operations require that the series for S and G be convergent. Also it should be noted that $a_o \neq 0$ is essential for all the operations to be meaningful. Thus $K(\xi)$ and $\omega(\xi)$ for a non-isothermal horizontal cylinder are obtained as

$$K(\xi) = K_o + K_1\xi^{3/2} + K_2\xi^3 + K_3\xi^{9/2} + K_4\xi^6 + \cdots \qquad (2.39)$$

and

$$\omega(\xi) = \omega_1\xi^{3/2} + \omega_2\xi^3 + \omega_3\xi^{9/2} + \cdots \qquad (2.40)$$

where $K_o = 3/4$ and K_j and ω_j, $j \geq 1$ are the coefficients to be calculated using the procedure given in Appendix A.

For non-isothermal vertical plate with G defined as in (2.38), we have

$$K(\xi) = \frac{3}{4} + K_1\xi^{3/2} + K_2\xi^3 + K_3\xi^{9/2} + K_4\xi^6 + \cdots \qquad (2.41)$$

and

$$\omega(\xi) = K(\xi) - 1/2, \qquad (2.42)$$

where again coefficients K_j, $j \geq 1$, are to be calculated using the procedure outlined in the Appendix A.

To solve the equations (2.33) and (2.34), we now assume the following series for $F(\xi,\eta)$ and $T(\xi,\eta)$:

$$F(\xi,\eta) = \sum_{j=0}^{\infty} F_j(\eta)\, \xi^{\alpha j}, \qquad (2.43)$$

$$T(\xi,\eta) = \sum_{j=0}^{\infty} T_j(\eta)\, \xi^{\alpha j} \qquad (2.44)$$

where $\alpha = 3/2$.

Substituting (2.39) to (2.44) in equations (2.33) and (2.34) and comparing the coefficients of like powers of ξ, we get the following system of ordinary differential equations:

(a) for vertical plate

$$F_o''' + F_o F_o'' - F_o'^2 + T_o = 0 ,$$

$$\frac{1}{\sigma} T_o'' + F_o T_o' - F_o' T_o = 0 ; \qquad (2.45)$$

for $j \geq 1$

$$F_j''' + F_o F_j'' - \frac{4}{3}(\alpha j + \frac{3}{2}) F_o' F_j' + (1 + \frac{4}{3}\alpha j) F_o'' F_j - \frac{4}{3} K_j F_o'^2 + T_j = R F_j ,$$

$$\frac{1}{\sigma} T_j'' + F_o T_j' - (1 + \frac{4}{3}\alpha j) F_o' T_j + (1 + \frac{4}{3}\alpha j) F_j T_o' - F_j' T_o - 4 K_j F_o' T_o = R T_j \qquad (2.46)$$

where

$$RF_j = \sum_{k=1}^{j-1} \left[\frac{4}{3} (\alpha k + \frac{3}{4}) F'_k F'_{j-k} - (1 + \frac{4}{3} \alpha k) F_k F''_{j-k} + \frac{4}{3} K_{j-k} \sum_{i=0}^{k} F'_i F'_{k-i} \right]$$

and

$$RT_j = \sum_{k=1}^{j-1} \left[(1 + \frac{4}{3} \alpha k) T_k F'_{j-k} - (1 + \frac{4}{3} \alpha k) F_k T'_{j-k} + 4 K_{j-k} \sum_{i=0}^{k} F'_i T_{k-i} \right] .$$

(b) for round-nosed cylinders

$$F'''_o + F_o F''_o - \frac{4}{3} K_o F'^2_o + T_o = 0 ,$$

$$\frac{1}{\sigma} T''_o + F_o T'_o = 0 ; \qquad (2.47)$$

for $j \geq 1$

$$F'''_j + F_o F''_j - \frac{4}{3} (\alpha j + 2K_o) F'_o F'_j + (1 + \frac{4}{3} \alpha j) F''_o F_j - \frac{4}{3} K_j F'^2_o + T_j = RF_j ,$$

$$\frac{1}{\sigma} T''_j + F_o T'_j - \frac{4}{3} \alpha j F'_o T_j + (1 + \frac{4}{3} \alpha j) F_j T'_o - 4 \omega_j F'_o T_o = RT_j \qquad (2.48)$$

where

$$RF_j = \sum_{k=1}^{j-1} \left[\frac{4}{3} (K_o + \alpha k) F'_k F'_{j-k} - (1 + \frac{4}{3} \alpha k) F_k F''_{j-k} + \frac{4}{3} K_{j-k} \sum_{i=0}^{k} F'_i F'_{k-i} \right]$$

and

$$RT_j = \sum_{k=1}^{j-1} \left[\frac{4}{3} \alpha k \, T_k F'_{j-k} - \left(1 + \frac{4}{3} \alpha k\right) F_k T'_{j-k} + 4 \omega_{j-k} \sum_{i=0}^{k} F'_i \, T_{k-i} \right] .$$

The boundary conditions for both the cases are

$$F_o = F'_o = 0, \quad T_o = 1 \qquad \text{at } \eta = 0$$

$$F'_o \to 0 \quad , \quad T_o \to 0 \qquad \text{as } \eta \to \infty; \tag{2.49}$$

for $j \geq 1$

$$F_j = F'_j = T_j = 0 \ , \qquad \text{at } \eta = 0$$

$$F'_j \to 0, \ T_j \to 0 \quad , \qquad \text{as } \eta \to \infty. \tag{2.50}$$

The essential feature of this Görtler type series expansion is that the zeroth-order term satisfies all the boundary conditions of the problem and hence already represents a solution to the full problem. Succeeding terms in the series only serve to improve the accuracy of the solution inside the boundary layers. These advantages in this type of series solution method have been demonstrated already in various studies on laminar free convection [7,9,10,11]. The zeroth-order equations for vertical plate (2.45) comprise the same system as investigated by Sparrow

and Gregg [20] for non-isothermal vertical plate with linearly varying surface temperature distribution. Again, the zeroth-order equations (2.47) for the cylindrical body under our consideration are the same as that studied by Chiang and Kaye [4] for free convection near the stagnation point on a horizontal circular cylinder. The system of equations for $F_j(\eta)$ and $T_j(\eta)$ for $j \geq 1$ are dependent on the nature of the driving force through the appearance of the coefficients K_j and ω_j in the equations (2.46) and (2.48). Employing the following special transformations, these coefficients are eliminated from direct consideration in the solutions of the resulting differential equations:

(i) non-isothermal vertical plate and isothermal cylinder:

$$
\begin{aligned}
F_1 &= K_1 Y_{11} \,, \\
T_1 &= K_1 Z_{11} \,; \\
F_2 &= K_1^2 Y_{21} + K_2 Y_{22} \,, \\
T_2 &= K_1^2 Z_{21} + K_2 Z_{22} \,; \\
F_3 &= K_1 K_2 Y_{31} + K_1^3 Y_{32} + K_3 Y_{33} \,, \\
T_3 &= K_1 K_2 Z_{31} + K_1^3 Z_{32} + K_3 Z_{33} \,; \\
F_4 &= K_2^2 Y_{41} + K_1^2 K_2 Y_{42} + K_1 K_3 Y_{43} + K_1^4 Y_{44} + K_4 Y_{45} \,, \\
T_4 &= K_2^2 Z_{41} + K_1^2 K_2 Z_{42} + K_1 K_3 Z_{43} + K_1^4 Z_{44} + K_4 Z_{45} \,; \qquad (2.51)
\end{aligned}
$$

and so on.

(ii) non-isothermal cylinder:

$$F_1 = K_1 Y_{11} + \omega_1 Y_{12} ,$$

$$T_1 = K_1 Z_{11} + \omega_1 Z_{12} ;$$

$$F_2 = K_1^2 Y_{21} + K_2 Y_{22} + \omega_1^2 Y_{23} + \omega_2 Y_{24} + K_1 \omega_1 Y_{25} ,$$

$$T_2 = K_1^2 Z_{21} + K_2 Z_{22} + \omega_1^2 Z_{23} + \omega_2 Z_{24} + K_1 \omega_1 Z_{25} ; \quad (2.52)$$

and so on.

The differential equations for ys and Zs together with their boundary conditions are given in Appendix B. Now these functions are universal with respect to the special data of the problem like the body contour and wall temperature. For a specific σ, they can be determined once for all and then applied to any special case of either of the two classes of problems simply by assembling the series for the stream and temperature functions. When the series is assembled, then S, G, ξ and the expansion for principal functions must be introduced for the specific problem on hand.

6. METHOD OF INTEGRATION

The non-linear partial differential equations (2.33) and (2.34) are essentially reduced by the application of series method of solution followed by special transformations to a non-linear together with a sequence of linear two-point asymptotic boundary value problems. Also, these linear equations have their coefficients determined by functional

coefficients of the preceeding terms in the series. The non-linear equations are numerically integrated using a fourth-order Runga-Kutta integration scheme with a fixed step-size. Direct numerical integration requires that the two-point non-linear boundary value problem be converted to an initial value problem by estimating two of the five required initial conditions. The exact outer boundary conditions are satisfied to an arbitrary degree of accuracy by integrating to some large value of η and using a modified Nachtsheim and Swigert [23] iteration scheme to select new values of the initial conditions until convergence is achieved. The solutions to the unknowns $F_o''(0)$ and $T_o'(0)$ are obtained accurately upto six decimal places.

The linear boundary value problems are solved by the method of complementary functions as given by Roberts and Shipman [24] and we briefly outline this technique here by applying to first-order system for isothermal cylinder (see Appendix B). We rewrite these equations as follows:

$$\begin{bmatrix} Y_{11} \\ Y_{11}' \\ Y_{11}'' \\ Z_{11} \\ Z_{11}' \end{bmatrix}' = \begin{bmatrix} 0 & 1 & 0 & 0 & 0 \\ 0 & 0 & 1 & 0 & 0 \\ -(1+\frac{4}{3}\alpha)F_o'' & \frac{4}{3}(\alpha+2K_o)F_o' & -F_o & -1 & 0 \\ 0 & 0 & 0 & 0 & 1 \\ -(1+\frac{4}{3}\alpha)\sigma T_o' & 0 & 0 & \frac{4}{3}\alpha\sigma F_o' & -\sigma F_o \end{bmatrix} \begin{bmatrix} Y_{11} \\ Y_{11}' \\ Y_{11}'' \\ Z_{11} \\ Z_{11}' \end{bmatrix} + \begin{bmatrix} 0 \\ 0 \\ \frac{4}{3}F_o'^2 \\ 0 \end{bmatrix} \qquad (2.53)$$

Boundary conditions are:

$$Y_{11}(0) = Y'_{11}(0) = Z_{11}(0) = 0$$

and

$$Y'_{11}(\infty) = Z_{11}(\infty) = 0 \,. \tag{2.54}$$

Choosing $(0,0,1,0,0)^T$ and $(0,0,0,0,1)^T$ as initial vectors and integrating the homogeneous equations obtained by dropping the non-homogeneous term in (2.53), we get two linearly independent solutions

$$\vec{Y}_r = (r_1(\eta), r_2(\eta), r_3(\eta), r_4(\eta), r_5(\eta))^T$$

and

$$\vec{Y}_s = (s_1(\eta), s_2(\eta), s_3(\eta), s_4(\eta), s_5(\eta))^T$$

respectively. Let $\vec{Y}_p = (p_1(\eta), p_2(\eta), p_3(\eta), p_4(\eta), p_5(\eta))^T$ obtained by integrating (2.53) with $(Y_{11}(0), Y'_{11}(0), 0, Z_{11}(0), 0)^T$ as initial vector, be the particular solution of (2.53).

Then $$\vec{Y} = \vec{Y}_p + C_1 \vec{Y}_r + C_2 \vec{Y}_s$$

is a solution of the linear boundary value problem (2.56) and (2.54) where C_1 and C_2 are given by

$$\begin{bmatrix} C_1 \\ C_2 \end{bmatrix} = - \begin{bmatrix} r_2(\eta_e) & s_2(\eta_e) \\ r_4(\eta_e) & s_4(\eta_e) \end{bmatrix}^{-1} \begin{bmatrix} p_2(\eta_e) \\ p_4(\eta_e) \end{bmatrix} .$$

Here η_e is the suitably chosen boundary layer edge. A step-size of 1/64 and $\eta_e = 15$ or 13 according as the Prandtl number is 0.7 or 1.0 for both classes of problems under our consideration were chosen to perform the integration of the linear equations governing the universal functions Ys and Zs. The conditions that both $|Y'_{jr}(\eta_e)|$ and $|Z_{jr}(\eta_e)|$ are less than 10^{-6}, were always satisfied for any range of values of j and r considered here. Throughout the computation, calculations were carried out upto eight decimal places in a Dec-10 computer.

As described earlier, the solutions of these linear boundary value problems are universal with respect to the special data of the problem like the body contour and wall temperature. For $\sigma = 0.7$ and 1.0, these functions have been calculated upto and including the fourth order terms for round-nosed isothermal cylinders and non-isothermal vertical plate; for non-isothermal cylinders, they have been calculated upto and including second order terms. The missing wall conditions $F''_o(0)$ and $T'_o(0)$ for zero-order solution and $Y''(0)$ and $Z'(0)$ for all universal functions are listed for $\sigma = 0.7$ and 1.0 in Table 1 for isothermal cylinder, in Table 2 for non-isothermal cylinder and in Table 3 for non-isothermal vertical plate. These values are used in the calculations of surface heat transfer characteristics of the problems.

7. RESULTS AND DISCUSSION

In order to demonstrate the usefulness and limitations of the present series solution, the method is applied to the following particular cases and the results are compared, where possible, with experimental and exact solutions:

I. Isothermal Surface Condition

(a) Horizontal circular cylinder:

We begin by presenting results for isothermal horizontal circular cylinders for which experimental and analytical results are available for comparison. The experimental data obtained by Jodlbauer [25] is used for comparison with our results obtained for the boundary layer velocities and temperatures. For high Grashof values, such as 7×10^5, we can expect the theoretical results agreeing well with experimental data.

The Shape Parameter, $K(\xi)$

First we calculate the shape parameter $K(\xi)$ for isothermal circular cylinder, for which

$$\omega(\xi) = 0,$$

and taking diameter of the cylinder as reference length,

$$x = \frac{\bar{x}}{2R} = \frac{\vartheta}{2} \quad \text{and} \quad S(x) = \sin \vartheta = \sin 2x$$

where ϑ is the angular position of the location $\bar{x}$ from the

lower stagnation point and R is the radius of the cylinder. Using $S(x)$ in (2.35), we find $K(\xi)$ at various locations on the body contour. Now we shall consider the question of how well the shape parameter $K(\xi)$ is represented by series (2.39) at downstream locations from the stagnation point. This consideration leads one to determine the radius of convergence of the series for $K(\xi)$. Since only a limited number of terms can be calculated, we assess the quality of the series by studying what happens to the sum of the series when the number of terms included is varied. For this purpose more number of coefficients K_j of the series are to be evaluated than those are already known [7]. From the general computer routine to find the coefficients K_j, we calculate K_1, K_2, K_3, K_4 for this particular case of an isothermal horizontal circular cylinder. With diameter as reference length, we obtain

$$K_1 = -0.3265986 , \quad K_2 = -0.1955556,$$

$$K_3 = -0.1263288 , \quad K_4 = -0.08378184 .$$

We observe that these coefficients show a monotonically increasing tendency and are bounded above by zero. Table 4 depicts the 2-term, 3-term, 4-term partial sums of the series for $K(\xi)$ against actual values for $K(\xi)$ obtained from (2.35) at various locations on the surface beginning from the lower stagnation point. A two-term sum approximates $K(\xi)$

very well within 1 percent error upto the downstream location $\vartheta = 50°$ from the lower stagnation point. Further downstream, it can be seen that a two-term representation for $K(\xi)$ involves increasingly large errors and so the results for flow variables and heat transfer calculations obtained by Saville and Churchill [7] beyond the location $\vartheta = 50°$ downstream carry with them this inaccurate representation for $K(\xi)$. For that matter, the five term expansion for $K(\xi)$ represents it well upto $\vartheta = 90°$ and beyond $\vartheta = 100°$ the error in representing $K(\xi)$ is large though less compared to the two term result for it. The general ability of the series representation for $K(\xi)$ can be described in terms of our findings as follows: on the lower side of the circular cylinder, $K(\xi)$ can be represented well by taking the first five terms of the series for it, while on the upper side so many additional terms of the series are needed to represent $K(\xi)$ satisfactorily that it may turn out to be impracticable owing to the tedious algebraic process involved in the calculation of K_j.

The Velocity and Temperature Profiles:

The profiles for velocity and temperature distribution in the boundary layer are calculated using the expressions:

$$\frac{\bar{u}L}{\nu\, Gr^{1/2}} = \sqrt{\frac{4}{3}\xi}\; S^{1/3}\, F_\eta$$

$$= \sqrt{\frac{4}{3}\xi}\; S^{1/3}\,[\, F_o'(\eta)+\xi^{3/2}K_1 Y_{11}'(\eta)+\xi^3(K_1^2 Y_{21}'(\eta)+K_2 Y_{22}'(\eta))$$

$$+ \xi^{9/2}(K_1K_2 Y_{31}'(\eta)+K_1^3 Y_{32}'(\eta)+K_3 Y_{33}'(\eta))$$

$$+ \xi^6(K_2^2 Y_{41}'(\eta)+K_1^2K_2 Y_{42}'(\eta)+K_1K_3 Y_{43}'(\eta)$$

$$+ K_1^4 Y_{44}'(\eta) + K_4 Y_{45}'(\eta)) + \cdots\,] \,.$$

$$\frac{t-t_\infty}{t_w-t_\infty} = T(\xi,\eta) = T_o(\eta)+\xi^{3/2}K_1 Z_{11}(\eta)+\xi^3(K_1^2 Z_{21}(\eta)+K_2 Z_{22}(\eta))$$

$$+ \xi^{9/2}(K_1K_2 Z_{31}(\eta)+K_1^3 Z_{32}(\eta)+K_3 Z_{33}(\eta))$$

$$+ \xi^6(K_2^2 Z_{41}(\eta)+K_1^2K_2 Z_{42}(\eta)+K_1K_3 Z_{43}(\eta)$$

$$+ K_1^4 Z_{44}(\eta)+K_4 Z_{45}(\eta)) + \cdots \,.$$

The velocity and temperature profiles at the location $\vartheta = 150°$ are shown in figures 3 and 4 respectively. It is seen that at this location the present results for local temperature distribution agree satisfactorily with experimental data. In the case of velocity profile, figure 3 shows a regular deviation in the sense that the measured velocities are greater than theoretically computed ones. But one significant aspect is that the position in the flow where

maximum velocity occurs do agree with the theoretical prediction as seen from figure 3. Deviations occuring at large distances for velocity measurements from the computed result may be due to the measurement of small velocities there. It is to be noted that a five-term result for velocity profile improves significantly over the corresponding two-term result around the region of maximum velocity occurrence at $\vartheta = 150°$.

Heat transfer:

In technological applications, the rate of heat transfer from the surface to the fluid is of primary importance and it can be written in terms of the local Nusselt number as

$$\frac{Nu}{Gr^{1/4}} = -(\frac{3}{4})^{1/4} \frac{S^{1/3}}{\xi^{1/4}} \left[T_o'(0)+\xi^{3/2}K_1 Z_{11}'(0)+\xi^3(K_1^2 Z_{21}'(0)+K_2 Z_{22}'(0))\right.$$

$$+ \xi^{9/2}(K_1K_2 Z_{31}'(0)+K_1^3 Z_{32}'(0)+K_3 Z_{33}'(0))$$

$$+ \xi^6(K_2^2 Z_{41}'(0)+K_1^2K_2 Z_{42}'(0)+K_1K_3 Z_{43}'(0)$$

$$\left. + K_1^4 Z_{44}'(0)+K_4 Z_{45}'(0)) +\cdots \right] .$$

Taking reference length as the diameter of the cylinder, the results for heat transfer at the surface in terms of local Nusselt number are given in Table 5 for $\sigma = 0.7$. For comparison purpose, the finite difference data is also included in this table [15]. From the table we see that the

five-term series expansion predicts heat-transfer accurately upto the location $\vartheta = 130°$ and underestimates it by about 2 per cent and $3\frac{1}{2}$ percent at $\vartheta = 140°$ and $150°$ respectively. Thus the large inaccuracy in representing heat transfer at these locations by a two-term expansion [7] is greatly reduced and thereby, it is shown that Görtler series can be used as far as the location $\vartheta = 150°$. It should be noted that the extensive calculations show though convergence is rapid in calculating heat transfer on the lower side of the cylinder, more terms are needed to reduce the inaccuracy beyond $\vartheta = 130°$.

Now we compare the mean heat transfer coefficient as obtained by the present method with that of experimental result. The average Nusselt number (averaged over the perimeter of the circle) is

$$\bar{Nu} = \frac{1}{\pi} \int_0^{\pi} Nu(x)dx \, .$$

Taking radius as reference length and using (x,ξ) transformation (2.29) to transform the integral with respect to ξ with the limits of integration given by 0 and $\xi(\pi) = 2.59$, we find

$$\frac{\bar{N}u}{Gr^{1/4}} = -\left(\frac{4}{3}\right)^{3/4} \frac{\xi^{3/4}}{\pi} \left[T_o'(0) + \frac{1}{3}\xi^{3/2} K_1 Z_{11}'(0) + \right.$$

$$+ \frac{1}{5}\xi^{3}(K_1^2 Z_{21}'(0) + K_2 Z_{22}'(0))$$

$$+ \frac{1}{7}\xi^{9/2}(K_1 K_2 Z_{31}'(0) + K_1^3 Z_{32}'(0) + K_3 Z_{33}'(0))$$

$$+ \frac{1}{9}\xi^{6}(K_2^2 Z_{41}'(0) + K_1^2 K_2 Z_{42}'(0) + K_1 K_3 Z_{43}'(0)$$

$$\left. + K_1^4 Z_{44}'(0) + K_4 Z_{45}'(0)) + \cdots \right] .$$

While a two-term sum of this series gives for $\frac{\bar{N}u}{Gr^{1/4}}$ a value 0.3027 [7], the five-term sum for it is 0.3069. Thus we see Jodlbauer data gives for average heat transfer coefficient a value 9 percent higher than a two-term sum and 7 percent higher than the five-term sum of the series.

(b) Horizontal Elliptic Cylinder:

Now that we have calculated considerable number of universal functions associated with the present series method of solution, an attempt is made here to study the applicability of this series to elliptic cylinders also. We consider the variation of heat transfer with distance from the stagnation point for a 2:1 elliptic cylinder with major axis perpendicular to the direction of gravity (see figure 2). If 2a and 2b are the lengths of major and minor axes respectively and e is the eccentricity of the elliptic section of the cylinder then $e^2 = 1 - \frac{b^2}{a^2}$. Also x and

$S(x) = \sin \varphi$ are given parametrically in terms of ϑ, the eccentric angle, by

$$x = \frac{\bar{x}}{a} = \int_0^{\vartheta} \sqrt{1-e^2 \sin^2\lambda}\, d\lambda ,$$

and

$$\sin \varphi = \frac{b}{a} \frac{\sin \vartheta}{\sqrt{1-e^2\sin^2 \vartheta}} .$$

We then transform the elliptic section into a circle and the angular displacement ξ from the stagnation point around the circle in the transformed plane is chosen as the independent variable and now it is given by

$$\xi = \int_0^{\vartheta} \left[\frac{b}{a} \sin \alpha \, (1-e^2\sin^2 \alpha)\right]^{1/3} d\alpha .$$

The coefficients K_j $(j = 1,2,3,4)$ for this problem were calculated using our general computer routine for calculation of coefficients of the principal function and they are found to be

$$K_1 = -0.8981463, \quad K_2 = -0.8955555 ,$$

$$K_3 = -0.6441484 \text{ and } K_4 = -0.08554964.$$

It is important to note that in this case a five-term sum for $K(\xi)$ could represent it well only upto $\vartheta = 45°$. Since these K_js are larger in magnitude in comparison with

those for circular cylinder, we have to do additional work in order to extend the validity of the series representation for $K(\xi)$ beyond 45°.

The heat transfer coefficient at the surface of elliptic cylinder in terms of local Nusselt number is given by

$$\frac{Nu}{Gr^{1/4}} = -(\tfrac{3}{4})^{1/4} \frac{[\frac{b}{a} \sin \vartheta (1-e^2 \sin^2 \vartheta)]^{1/3}}{\sqrt{1-e^2 \sin^2 \vartheta}}$$

$$[T_o'(0) + \xi^{3/2} K_1 Z_{11}'(0) + \xi^3 (K_1^2 Z_{21}'(0) + K_2 Z_{22}'(0))$$

$$+ \xi^{9/2} (K_1 K_2 Z_{31}'(0) + K_1^3 Z_{32}'(0) + K_3 Z_{33}'(0))$$

$$+ \xi^6 (K_2^2 Z_{41}'(0) + K_1^2 K_2 Z_{42}'(0) + K_1 K_3 Z_{43}'(0)$$

$$+ K_1^4 Z_{44}'(0) + K_4 Z_{45}'(0)) + \cdots] .$$

The results of the calculations for heat transfer coefficient, taking the length of semi-major axis as reference length, are given in Table 6 for $\sigma = 1.0$ with the finite difference data of Merkin [15]. It is seen from the table that while a two-term sum agrees with finite difference data upto about $\vartheta = 68$ deg., the five-term expansion gives sufficiently accurate results upto about $\vartheta = 115°$ beyond which the agreement between the two data rapidly deteriorates. For this blunt orientation the heat transfer coefficient first

increases with the distance from the lower stagnation point and reaches a maximum at about $\phi = 92°$ and then decreases. On the other hand, we note that there is reduction in heat transfer for circular cylinder as we go downstream locations away from the stagnation point [see figure 5] .

II Non-isothermal surface conditions

In great many technological applications the heat transferred from the surface is non-isothermal. To treat this case, we start with $G(x)$ as given by (2.38). To illustrate the application of the series, we have to fix the geometry of the body and also the coefficients in wall temperature distribution. First we shall deal with the simple geometry, namely a vertical plate and then take up the horizontal circular cylinder.

a. Vertical Plate:

To deal with this case, the universal functions associated with the series method are worked out and the missing wall values for these functions which are important in the calculation of rate of heat transfer at the surface are tabulated in Table 1. For this geometry,

$$S(x) = 1$$

and

$$\omega(\xi) = K(\xi) - 1/2.$$

We now consider the wall temperature variation of the form:

$$G(x) = \sin x.$$

Then comparing this with (2.38), we get

$$a_o = 1,\ a_1 = -\frac{1}{\lfloor 3},\ a_2 = \frac{1}{\lfloor 5},\ a_3 = -\frac{1}{\lfloor 7}\ ,\ldots\ldots.$$

With these values of the coefficients in wall temperature data, we obtain K_j(for j=1,2,3,4) as follows:

$$K_1 = -0.1154701\ ,\ K_2 = -0.02444445,$$

$$K_3 = -0.0055830 \text{ and } K_4 = -0.001309096.$$

The range of validity of the series representation for $\omega(\xi)$, which describes non-isothermal condition at the plate, can be discussed on the same lines as we have done for isothermal circular cylinder. The velocity and temperature profiles are shown in figures 6 and 7 respectively for $x = 0.8,\ 1.2$ and 1.6, x measured from the leading edge of the plate.

To facilitate comparison of our result for heat transfer at the surface with that of the finite difference data [17], we use the following expression for local Nusselt number:

$$Nu_{\bar{x}} = \frac{h\bar{x}}{\lambda}$$

where h is the heat transfer coefficient defined by

$$h(t_w(x) - t_\infty) = -\lambda\left(\frac{\partial t}{\partial \bar{y}}\right)_{\bar{y}=0}.$$

Now introducing the local Grashof number

$$Gr_{\bar{x}} = \frac{g\beta(t_w(\bar{x}) - t_\infty)\,\bar{x}^3}{\nu^2},$$

$Nu_{\bar{x}}$ may be written as

$$\frac{Nu_{\bar{x}}}{Gr_{\bar{x}}^{1/4}} = -\left(\frac{3}{4}\right)^{1/4}\frac{G^{1/3}}{\xi^{1/4}}\left[T_o'(0)+\xi^{3/2}K_1 Z_{11}'(0)+\xi^3(K_1^2 Z_{21}'(0)+K_2 Z_{22}'(0))\right.$$

$$+\xi^{9/2}(K_1K_2Z_{31}'(0)+K_1^3Z_{32}'(0)+K_3Z_{33}'(0))$$

$$+\xi^6(K_2^2Z_{41}'(0)+K_1^2K_2Z_{42}'(0)+K_1K_3Z_{43}'(0)$$

$$\left.+K_1^4Z_{44}'(0)+K_4Z_{45}'(0))+\ldots\right].$$

The results from the series solution and the finite difference data are depicted in figure 8 for $\sigma = 0.7$ and 1.0 in terms of the combined parameter $Nu_{\bar{x}}/Gr_{\bar{x}}^{1/4}$ as a function of the dimensionless distance x from the leading edge of the plate. It is clear from the figure that the results of our analysis agree well with finite difference data upto a downstream distance $x = 1.6$ from the leading edge of the plate though, of course, the ability of the series in terms of number of terms to be evaluated vary according to the location under our consideration. It is found that the two-term sum can give accurate results for the local Nusselt

number upto $x = 0.8$ while a three, four and five-term partial sum yields results accurately upto $x = 1.2$, 1.4, 1.6 respectively. Also it is clear from the figure 8 that the range of validity of the series is independent of the Prandtl number values considered here. To increase the range of validity of the series solution, it is necessary to evaluate some more additional terms. But for the range of value of x considered here, the series converges very well and the results can be considered accurate. Also, from the figure it is observed that the effect of the Prandtl number increase is to increase the heat transfer at the surface.

b. Horizontal Circular Cylinder

To illustrate the application of the series to this case, we consider some specific values for the coefficients a_j in $G(x)$. We choose two distributions of $G(x)$ by taking

(i) $a_o = 1$, $a_1 = -0.1$ and $a_j = 0$ for $j \geq 2$

and

(ii) $a_o = 1$, $a_1 = 0.2$ and $a_j = 0$ for $j \geq 2$

The radius of the cylinder is taken as reference length and the temperature at the stagnation point, T_{wo}, is taken as reference temperature T_r. In the above two cases of surface temperature distribution, $G(x)$, the coefficients K_j and ω_j are

(i) when $G(x) = 1-0.1\ x^2$,

$K_1 = -0.1847521, K_2 = -0.05442963,$

$\omega_1 = -0.07698004, \omega_2 = -0.02449383;$

(ii) when $G(x) = 1+0.2\ x^2$,

$K_1 = 0.02309401, K_2 = -0.05727407,$

$\omega_1 = 0.1539601\ , \omega_2 = -0.05056790.$

The principal function $K(\xi)$ is represented by a three-term sum of the series for $K(\xi)$ accurately upto an angular distance of 60° in both the cases and $\omega(\xi)$ is approximated well to a distance 50° from the lower stagnation point by the first two-term sum of the series for it.

The velocity and temperature profiles are calculated from the expressions

$$\frac{\bar{u}L}{\nu\, Gr^{1/2}} = \sqrt{\frac{4}{3}}\,\xi\,(SG)^{1/3}\,[\,F_o'(\eta)+\xi^{3/2}(K_1 Y_{11}'(\eta)+\omega_1 Y_{12}'(\eta))$$

$$+\,\xi^3(K_1^2 Y_{21}'(\eta)+K_2 Y_{22}'(\eta)+\omega_1^2 Y_{23}'(\eta)$$

$$+\,\omega_2 Y_{24}'(\eta)+K_1\omega_1 Y_{25}'(\eta))+\cdots\,]$$

and

$$\frac{t-t_\infty}{t_w-t_\infty} = T_o(\eta) + \xi^{3/2}(K_1 Z_{11}(\eta)+\omega_1 Z_{12}(\eta))+\xi^3(K_1^2 Z_{21}(\eta)$$

$$+\,K_2 Z_{22}(\eta)+\omega_1^2 Z_{23}(\eta)+\omega_2 Z_{24}(\eta)+K_1\omega_1 Z_{25}(\eta))+\cdots$$

for $\sigma = 0.7$ at an angular downstream distance 90° from the stagnation point when $G(x) = 1-0.1x^2$ and are shown in figures 9 and 10 respectively. We observe from the figures that two-term expansion of the series represents adequately well the local velocity and temperature distributions as far as 90° downstream from the stagnation point. It is only to be anticipated in view of the fact that the dependent and independent variables are so defined that as much information as possible is concentrated into the zeroth-order solution in the expansion of the series for flow variables, while the succeeding terms in the series only serve to improve the accuracy of the solution inside the boundary layers.

Also, we give the velocity and temperature profiles in figures 11 and 12 respectively for $\sigma = 1.0$ at the location 60° for both cases $G(x) = 1+0.2x^2$ and $G(x) = 1-0.1x^2$ including the isothermal case. An increase in wall temperature corresponds to an increase in maximum velocity while a decrease in it tends to suppress this value. Also this property holds good for the absolute value of the temperature slope near the wall.

The dimensionless heat transfer is computed in terms of local Nusselt number from the expression

$$\frac{Nu}{Gr^{1/4}} = -(\frac{3}{4})^{1/4} \frac{(SG)^{1/3}G^{1/3}}{\xi^{1/4}}[T_o'(0)+\xi^{3/2}(K_1 Z_{11}'(0)+\omega_1 Z_{12}'(0))$$

$$+\xi^3(K_1^2 Z_{21}'(0)+K_2 Z_{22}'(0)+\omega_1^2 Z_{23}'(0)$$

$$+\omega_2 Z_{24}'(0)+K_1\omega_1 Z_{25}'(0))+\ldots] .$$

The results for the heat transfer are given in figure 13 for wall temperature distribution $G(x) = 1+0.2x^2$ for $\sigma = 1.0$ and 0.7 and these are compared with those obtained in [5] for $\sigma = 1.0$. It is observed that the heat transfer increases as σ increases. In figure 14, the heat transfer is compared with that of Blasius series solution [5] for the surface temperature distribution $G(x) = 1-0.1x^2$ when $\sigma = 1.0$.

We now define a quantity q^* as follows:

$$q^* = \frac{[q/(t_w-t_\infty)Gr^{1/4}]_{\text{non-isothermal wall condition}}}{[q/(t_w-t_\infty)Gr^{1/4}]_{\text{isothermal wall condition}}},$$

where q is the surface heat-flux. This simplifies to

$$q^* = (\frac{t_{w_o} - t_\infty}{t_w - t_\infty}) \frac{(Nu/Gr^{1/4})_{\text{non-isothermal}}}{(Nu/Gr^{1/4})_{\text{isothermal}}}$$

$$= \frac{1}{G(x)} \frac{(Nu/Gr^{1/4})_{\text{non-isothermal}}}{(Nu/Gr^{1/4})_{\text{isothermal}}} .$$

q^* can then be used to give the effect of the non-isothermal

wall on heat-transfer. For $\sigma = 0.7$, fig. 15 shows the effect of non-isothermal wall at various locations for the two prescribed surface temperatures. For $G(x) = 1+0.2x^2$, the heat transfer at the location 60° from the stagnation point is 19 percent higher than that for an isothermal cylinder. When $G(x) = 1-0.1x^2$, the heat transfer at that location is 13 percent less than that for an isothermal cylinder. In other words, the heat transfer is very much influenced by the surface temperature variations.

Table 1

Missing wall values of universal functions for Isothermal cylinder

	$\sigma = 0.7$	$\sigma = 1.0$
$F_o''(0)$	0.859345	0.817010
$T_o'(0)$	-0.370234	-0.421431
$Y_{11}''(0)$	-0.091465	-0.076768
$Z_{11}'(0)$	0.032265	0.032783
$Y_{21}''(0)$	0.018443	0.014393
$Z_{21}'(0)$	-0.004615	-0.004477
$Y_{22}''(0)$	-0.076577	-0.064994
$Z_{22}'(0)$	0.027363	0.027881
$Y_{31}''(0)$	0.028544	0.022518
$Z_{31}'(0)$	-0.007031	-0.006857
$Y_{32}''(0)$	-0.00340	-0.002510
$Z_{32}'(0)$	0.000525	0.000517
$Y_{33}''(0)$	-0.066790	-0.057186
$Z_{33}'(0)$	0.023532	0.024093
$Y_{41}''(0)$	0.011210	0.008936
$Z_{41}'(0)$	-0.002728	-0.002676
$Y_{42}''(0)$	-0.007388	-0.005540

	$\sigma = 0.7$	$\sigma = 1.0$	
$Z'_{42}(0)$	0.001246	0.001206	
$Y'''_{43}(0)$	0.023434	0.018645	
$Z'_{43}(0)$	-0.005662	-0.005552	
$Y'''_{44}(0)$	0.000533	0.000370	
$Z'_{44}(0)$	-0.000041	-0.000041	
$Y'''_{45}(0)$	-0.059609	-0.051393	
$Z'_{45}(0)$	0.020615	0.021210	

Table 2

Missing wall values of universal functions
for Non-isothermal cylinder

	$\sigma = 0.7$	$\sigma = 1.0$
$F_o''(0)$	0.859345	0.817010
$T_o'(0)$	-0.370234	-0.421431
$Y_{11}''(0)$	-0.091465	-0.076768
$Z_{11}'(0)$	0.032265	0.032783
$Y_{12}''(0)$	-0.183803	-0.187802
$Z_{12}'(0)$	-0.580182	-0.637876
$Y_{21}''(0)$	0.018443	0.014393
$Z_{21}'(0)$	-0.004615	-0.004477
$Y_{22}''(0)$	-0.076577	-0.064994
$Z_{22}'(0)$	0.027363	0.027881
$Y_{23}''(0)$	0.069578	0.072933
$Z_{23}'(0)$	0.297854	0.333228
$Y_{24}''(0)$	-0.11670	-0.120081
$Z_{24}'(0)$	-0.468187	-0.514137
$Y_{25}''(0)$	0.029079	0.026188
$Z_{25}'(0)$	0.020705	0.018563

Table 3

Missing wall values of universal functions
for Non-isothermal vertical plate

	$\sigma = 0.7$	$\sigma = 1.0$
$F_o''(0)$	0.782428	0.793502
$T_o'(0)$	-0.52807	-0.595092
$Y_{11}''(0)$	-0.196956	-0.185822
$Z_{11}'(0)$	-0.356712	-0.392551
$Y_{21}''(0)$	0.071950	0.068073
$Z_{21}'(0)$	0.163080	0.178188
$Y_{22}''(0)$	-0.145781	-0.137417
$Z_{22}'(0)$	-0.307786	-0.338492
$Y_{31}''(0)$	0.096403	0.091061
$Z_{31}'(0)$	0.246494	0.269208
$Y_{32}''(0)$	-0.021996	-0.020957
$Z_{32}'(0)$	-0.069845	-0.076452
$Y_{33}''(0)$	-0.117329	-0.110569
$Z_{33}'(0)$	-0.274678	-0.302051
$Y_{41}''(0)$	0.033158	0.031281
$Z_{41}'(0)$	0.094585	0.103264
$Y_{42}''(0)$	-0.041588	-0.039532

	$\sigma = 0.7$	$\sigma = 1.0$
$Z'_{42}(0)$	-0.1463971	-0.160089
$Y'''_{43}(0)$	0.072404	0.068343
$Z'_{43}(0)$	0.200300	0.218775
$Y''''_{44}(0)$	0.005470	0.005266
$Z''_{44}(0)$	0.025073	0.027611
$Y'''_{45}(0)$	-0.098894	-0.093190
$Z'_{45}(0)$	-0.250300	-0.275260

Table 4

Shape parameter $K(\xi)$ for isothermal horizontal circular cylinder

ϑ	ξ	$K(\xi)$	From series representation of $K(\xi)$			
			two term	three term	four term	five term
0	0	0.75	0.75	0.75	0.75	0.75
10°	0.03655	0.7477	0.7477	0.7477	0.7477	0.7477
20°	0.09192	0.7407	0.7409	0.7407	0.7407	0.7407
30°	0.15729	0.7288	0.7296	0.7289	0.7288	0.7288
40°	0.22972	0.7115	0.7140	0.7117	0.7115	0.7115
50°	0.30741	0.6879	0.6943	0.6887	0.6880	0.6880
60°	0.38902	0.6571	0.6708	0.6592	0.6574	0.6571
70°	0.47343	0.6173	0.6436	0.6229	0.6185	0.6176
80°	0.55965	0.5661	0.6133	0.5790	0.5697	0.5671
90°	0.64677	0.5	0.5801	0.5272	0.5094	0.5033
100°	0.73388	0.4133	0.5447	0.4674	0.4360	0.4229
110°	0.82012	0.2968	0.5074	0.3996	0.3478	0.3223
120°	0.90453	0.1347	0.4690	0.3243	0.2439	0.1980
130°	0.98614	-0.1029	0.4307	0.2426	0.1240	-0.0469
140°	1.06383	-0.4794	0.3916	0.1562	-0.0107	-0.1321
150°	1.13626	-1.1531	0.3544	0.0675	-0.1569	-0.3372

Table 5

Local heat transfer parameter, $Nu/Gr^{1/4}$, for isothermal horizontal circular cylinder (σ=0.7)

φ	ξ	$Nu/Gr^{1/4}$				
		two term	three term	four term	five term	finite difference [15]
0°	0	0.4402	0.4402	0.4402	0.4402	0.4402
10°	0.03655	0.4397	0.4397	0.4397	0.4397	0.4395
20°	0.09192	0.4379	0.4380	0.4380	0.4380	0.4377
30°	0.15729	0.4350	0.4350	0.4350	0.4350	0.4348
40°	0.22972	0.4308	0.4309	0.4309	0.4309	0.4307
50°	0.30741	0.4254	0.4256	0.4256	0.4256	0.4255
60°	0.38902	0.4187	0.4191	0.4192	0.4192	0.4190
70°	0.47343	0.4106	0.4113	0.4114	0.4114	0.4113
80°	0.55965	0.4010	0.4021	0.4024	0.4025	0.4024
90°	0.64677	0.3899	0.3915	0.3920	0.3922	0.3922
100°	0.73388	0.3770	0.3793	0.3801	0.3805	0.3806
110°	0.82012	0.3621	0.3652	0.3666	0.3672	0.3677
120°	0.90453	0.3450	0.3489	0.3509	0.3520	0.3532
130°	0.98614	0.3252	0.3300	0.3327	0.3344	0.3370
140°	1.06383	0.3019	0.3075	0.3111	0.3135	0.3190
150°	1.13626	0.2740	0.2801	0.2845	0.2877	0.2986

Note: The diameter of the cylinder is used as reference length.

Table 6

Local heat transfer parameter, $Nu/Gr^{1/4}$, for isothermal, horizontal blunt 2:1 elliptic cylinder (σ=1.0)

ϑ	ξ	$K(\xi)$	$Nu/Gr^{1/4}$		
			two term	five term	finite difference [15]
0.0	0	0.75	0.3542	3542	0.3542
0.2	0.069284	0 .7333	0.3555	0.3555	0.3555
0.4	0.172049	0.6811	0.3589	0.3590	0.3593
0.6	0.288335	0.5871	0.3648	0.3652	0.3657
0.8	0.409145	0.4436	0.3733	0.3745	0.3747
1.0	0.528110	0.2544	0.3841	0.3872	0.3861
1.2	0.641007	0.0829	0.3954	0.4021	0.3984
1.4	0.746501	0.1340	0.4016	0.4142	0.4081
1.6	0.847175	0.5821	0.3937	0.4146	0.4088
1.8	0.948753	1.0573	0.3680	0.3997	0.3958
2.0	1.056329	1.1553	0.3318	0.3778	0.3713
2.2	1.171286	0.9443	0.2934	0.3585	0.3407
2.4	1.291330	0.5313	0.2559	0.3454	0.3081
2.6	1.411567	-0.1646	0.2190	0.3365	0.2752
2.8	1.525005	-1.6801	0.1801	0.3212	0.2418
3.0	1.621315	-8.4414	0.1301	0.2687	0.2056

Note: The length of semi major-axis of the elliptic cylinder is used as reference length.

APPENDIX - A

Expressions for $K(\xi)$ and $\omega(\xi)$ in terms of ξ

Recall the expression (2.29) for ξ, that is,

$$\xi = \int_0^x (SG)^{1/3} dx .$$

We assume the following power series for SG:

$$SG = S_1 x + S_3 x^3 + S_5 x^5 + S_7 x^7 + \cdots \tag{A1}$$

with $S_1 \neq 0$. This is true for either vertical plate or cylindrical body with necessary changes in the value of the coefficients $S_1, S_3, S_5, S_7, \cdots$

We write $P = SG$

By Lagrange's formula for reversion of power series [22], we get

$$x = \sum_{k=1}^{\infty} \alpha_k P^k \tag{A2}$$

with coefficients α_k given by

$$\alpha_k = \frac{1}{\lfloor k} H_k^{(k-1)}(0) \tag{A3}$$

where

$$H_k(t) = \frac{1}{h^k(t)} , \tag{A4}$$

with

$$h(t) = S_1 + S_3 t^2 + S_5 t^4 + S_7 t^6 + \cdots \tag{A5}$$

ξ can now be written as

$$\xi = \int_0^P P^{1/3} \frac{dx}{dP}\, dP \qquad (A6)$$

as P is analytic and $P'(0) \neq 0$.

Using (A2) in (A6), we get

$$\xi = \int_0^P P^{1/3} \left(\sum_{k=1}^{\infty} k\, \alpha_k\, P^{k-1} \right) dP .$$

On evaluating the above integral, ξ is obtained in the following series form

$$\frac{\xi}{P^{1/3}} = \frac{3}{4}\, \alpha_1 P + \frac{9\alpha_3}{10}\, P^3 + \frac{15}{16}\, \alpha_5 P^5 + \frac{21}{22}\, \alpha_7\, P^7 + \cdots \qquad (A7)$$

On cubing both sides and simplifying, it becomes

$$\frac{\xi^3}{P} = a_1 P^3 + a_2 P^5 + a_3 P^7 + a_4 P^9 + \cdots .$$

Further simplification leads to

$$\xi^{3/4} = a_1^{1/4}\, P\, (1 + g(P))^{1/4} , \qquad (A8)$$

where

$$g(P) = a_2 P^2 + a_3 P^4 + \cdots .$$

Expanding (A8), we arrive at the form

$$\xi^{3/4} = b_1 P + b_3 P^3 + b_5 P^5 + \cdots . \qquad (A9)$$

Using the fact that $\frac{d(\xi^{3/4})}{dP} = b_1$ $(\neq 0)$, we apply Lagrange's

formula to equation (A9) to obtain

$$P = C_1\xi^{3/4} + C_3\xi^{9/4} + C_5\xi^{15/4} + \cdots \qquad (A10)$$

where C_i's are to be determined in the same way as α_k's. Substituting for P in (A2) and on rearranging the coefficients of like powers of ξ, we get

$$x = P_1\xi^{3/4} + P_2\xi^{9/4} + P_3\xi^{15/4} + \cdots \qquad (A11)$$

We recall the expressions (2.35) and (2.36) which can be written as

$$K(\xi) = \frac{1}{2} + \frac{\xi}{3P^{4/3}}\frac{dP}{dx} \ , \qquad (A12)$$

and

$$\omega(\xi) = \frac{\xi}{3P^{1/3}}\frac{dG}{dx} \ . \qquad (A13)$$

Using (A10) in (A7) and (A11) in the derivative of (A1), $\frac{\xi}{3P^{4/3}}$ and $\frac{dP}{dx}$ can be written as power series in ξ

$$\frac{\xi}{3P^{4/3}} = e_1 + e_2\,\xi^{3/2} + e_3\xi^3 + \cdots \ , \qquad (A14)$$

and

$$\frac{dP}{dx} = f_1 + f_2\,\xi^{3/2} + f_3\xi^3 + \cdots \ . \qquad (A15)$$

With (A14) and (A15), (A12) gives $K(\xi)$ in the following form

$$K(\xi) = K_o + K_1\xi^{3/2} + K_2\xi^3 + K_3\xi^{9/2} + K_4\xi^6 + \cdots \qquad (A16)$$

for both vertical plate and round-nosed cylinders.

Again, expressing $x^2, x^4, \ldots$ in terms of ξ (using (A11)) and substituting in the expression for $\frac{dG}{dx}$, we obtain a power series in ξ for $\frac{dG}{dx}$. Using this expression for $\frac{dG}{dx}$ in powers of ξ, (A10) and (A14) in (A13), $\omega(\xi)$ can be written as

$$\omega(\xi) = \omega_1 \xi^{3/2} + \omega_2 \xi^3 + \ldots \quad . \tag{A17}$$

For non-isothermal vertical plate, we have

$$\omega(\xi) = K(\xi) - 1/2 \quad \text{(see 2.42)}$$

which with the help of (A16) becomes the following series in ξ

$$\omega(\xi) = (K_o - 1/2) + K_1 \xi^{3/2} + K_2 \xi^3 + K_3 \xi^{9/2} + \ldots \quad . \tag{A18}$$

APPENDIX - B

Differential equations governing the universal functions

Non-Isothermal Vertical Plate:

Using the transformations (2.51) in equations (2.46) and scaling out coefficients K_j's from the resulting equations, we get the following set of differential equations for universal functions:

$$L_1(Y_{11}, Z_{11}) = \frac{4}{3} F_o'^2 ,$$

$$L_2(Y_{11}, Z_{11}) = 4 F_o' T_o ;$$

$$L_1(Y_{22}, Z_{22}) = \frac{4}{3} F_o'^2 ,$$

$$L_2(Y_{22}, Z_{22}) = 4 F_o' T_o ;$$

$$L_1(Y_{21}, Z_{21}) = 3 Y_{11}'^2 - 3Y_{11}Y_{11}'' + \frac{8}{3} F_o' Y_{11}' ,$$

$$L_2(Y_{21}, Z_{21}) = 3Y_{11}' Z_{11} - 3Y_{11} Z_{11}' + 4F_o' Z_{11} + 4T_o Y_{11}' ;$$

$$L_1(Y_{33}, Z_{33}) = \frac{4}{3} F_o'^2 ,$$

$$L_2(Y_{33}, Z_{33}) = 4F_o' T_o ;$$

$$L_1(Y_{32}, Z_{32}) = 8Y_{11}' Y_{21}' - 3Y_{11} Y_{21}'' - 5Y_{11}'' Y_{21} + \frac{4}{3}(2F_o' Y_{21}' + Y_{11}'^2) ,$$

$$L_2(Y_{32}, Z_{32}) = 3Z_{11} Y_{21}' - 3Y_{11} Z_{21}' + 5Y_{11}' Z_{21} - 5Z_{11}' Y_{21} ;$$

$$L_1(Y_{31}, Z_{31}) = 8Y_{11}' Y_{22}' - 3Y_{11} Y_{22}'' - 5Y_{11}'' Y_{22} + \frac{8}{3} F_o'(Y_{11}' + Y_{22}') ,$$

$$L_2(Y_{31}, Z_{31}) = 3(Z_{11} Y_{22}' - Y_{11} Z_{22}') + 5(Y_{11}' Z_{22} - Z_{11}' Y_{22}) ;$$

$$+ 4[F_o'(Z_{11} + Z_{22}) + T_o(Y_{11}' + Y_{22}')]$$

$$L_1(Y_{45},Z_{45}) = \frac{4}{3} F_o'^{\,2} ,$$

$$L_2(Y_{45},Z_{45}) = 4F_o'T_o ;$$

$$L_1(Y_{44},Z_{44}) = 10Y_{11}'Y_{32}'-3Y_{11}Y_{32}''-7Y_{11}''Y_{32}+5(Y_{21}'^{\,2}-Y_{21}Y_{21}'')$$
$$+ \frac{8}{3} (F_o'Y_{32}'+Y_{11}'Y_{21}') ,$$

$$L_2(Y_{44},Z_{44}) = 3(Z_{11}Y_{32}'-Y_{11}Z_{32}')+5(Z_{21}Y_{21}'-Y_{21}Z_{21}')$$
$$+7(Y_{11}'Z_{32}-Z_{11}'Y_{32})+4(F_o'Z_{32}'+Y_{11}'Z_{21}+Z_{11}Y_{21}'+T_oY_{32}');$$

$$L_1(Y_{43},Z_{43}) = 10Y_{11}'Y_{33}'-3Y_{11}Y_{33}''+ \frac{8}{3}F_o'(Y_{11}'+Y_{33}')-7Y_{11}''Y_{33} ,$$

$$L_2(Y_{43},Z_{43}) = 3(Z_{11}Y_{33}'-Y_{11}Z_{33}')+7(Y_{11}'Z_{33}-Z_{11}'Y_{33})$$
$$+4(F_o'Z_{33}+F_o'Z_{11}+T_oY_{33}'+T_oY_{11}') ;$$

$$L_1(Y_{42},Z_{42}) = 10Y_{11}'Y_{31}'-3Y_{11}Y_{31}''+10Y_{22}'Y_{21}'-7Y_{11}''Y_{31}$$
$$-5(Y_{21}Y_{22}''+Y_{21}''Y_{22})+ \frac{4}{3}(2F_o'Y_{21}'+Y_{11}'^{\,2})$$
$$+ \frac{8}{3}(Y_{11}'Y_{22}'+F_o'Y_{31}') ,$$

$$L_2(Y_{42},Z_{42}) = 3(Z_{11}Y_{31}'-Y_{11}Z_{31}')+5(Z_{21}Y_{22}'+Z_{22}Y_{21}'-Z_{22}'Y_{21}-Y_{22}Z_{21}')$$
$$+7(Y_{11}'Z_{31}-Z_{11}'Y_{31})+4(F_o'Z_{21}+Y_{11}'Z_{11}+T_oY_{21}'$$
$$+F_o'Z_{31}+Y_{11}'Z_{22}+Z_{11}Y_{22}'+T_oY_{31}') ;$$

$$L_1(Y_{41},Z_{41}) = 5(Y_{22}'^{\,2}-Y_{22}Y_{22}'') + \frac{8}{3} F_o'Y_{22}' ,$$

$$L_2(Y_{41},Z_{41}) = 5(Z_{22}Y_{22}'-Y_{22}Z_{22}')+4(F_o'Z_{22}+T_oY_{22}') ;$$

where Ys' and Zs' satisfy

$$L_1(Y_{j-}, Z_{j-}) = Y'''_{j-} + F_o Y''_{j-} - \frac{4}{3}(\alpha j + \frac{3}{2}) F'_o Y'_{j-} + (1 + \frac{4}{3}\alpha j) F''_o Y_{j-} + Z_{j-} ,$$

$$L_2(Y_{j-}, Z_{j-}) = \frac{1}{\sigma} Z''_{j-} + F_o Z'_{j-} - (1 + \frac{4}{3}\alpha j) F'_o Z_{j-}$$

$$+ (1 + \frac{4}{3}\alpha j) T'_o Y_{j-} - T_o Y'_{j-} .$$

The boundary conditions are

$$Y_{j-}(0) = Y'_{j-}(0) = 0 = Z_{j-}(0) ,$$

$$Y'_{j-}(\infty) = 0 = Z_{j-}(\infty) .$$

Iso-Thermal Cylinder:

In this case, $\omega_j = 0$ for all j in (2.48). Using the transformations (2.51) in equations (2.48) and scaling out the coefficients K_j s from the resulting equations, we get the following sets of differential equations for universal functions:

$$L_1(Y_{11}, Z_{11}) = \frac{4}{3} F'^2_o ,$$

$$L_2(Y_{11}, Z_{11}) = 0 ;$$

$$L_1(Y_{21}, Z_{21}) = \frac{4}{3}(K_o + \alpha) Y'^2_{11} - (1 + \frac{4}{3}\alpha) Y_{11} Y'''_{11} + \frac{8}{3} F'_o Y'_{11} ,$$

$$L_2(Y_{21}, Z_{21}) = \frac{4}{3}\alpha Z_{11} Y'_{11} - (1 + \frac{4}{3}\alpha) Y_{11} Z'_{11} ;$$

$$L_1(Y_{22}, Z_{22}) = \frac{4}{3} F'^2_o ,$$

$$L_2(Y_{22}, Z_{22}) = 0 ;$$

$$L_1(Y_{31}, Z_{31}) = \tfrac{4}{3}(3\alpha+2K_o)Y'_{11}Y'_{22} - (1+\tfrac{4}{3}\alpha)Y_{11}Y''_{22} - (1+\tfrac{8}{3}\alpha)Y''_{11}Y_{22}$$
$$+ \tfrac{8}{3}F'_o(Y'_{11}+Y'_{22}),$$

$$L_2(Y_{31}, Z_{31}) = \tfrac{4}{3}\alpha Z_{11}Y'_{22} - (1+\tfrac{4}{3}\alpha)Y_{11}Z'_{22} + \tfrac{8}{3}\alpha Y'_{11}Z_{22}$$
$$- (1+\tfrac{8}{3}\alpha)Y_{22}Z'_{11};$$

$$L_1(Y_{32}, Z_{32}) = \tfrac{4}{3}(3\alpha+2K_o)Y'_{11}Y'_{21} - (1+\tfrac{4}{3}\alpha)Y_{11}Y''_{21} - (1+\tfrac{8}{3}\alpha)Y''_{11}Y_{21}$$
$$+ \tfrac{8}{3}F'_oY'_{21} + \tfrac{4}{3}Y'^2_{11},$$

$$L_2(Y_{32}, Z_{32}) = \tfrac{4}{3}\alpha Z_{11}Y'_{21} - (1+\tfrac{4}{3}\alpha)Y_{11}Z'_{21} + \tfrac{8}{3}\alpha Y'_{11}Z_{21}$$
$$- (1+\tfrac{8}{3}\alpha)Z'_{11}Y_{21};$$

$$L_1(Y_{33}, Z_{33}) = \tfrac{4}{3}F'^2_o,$$

$$L_2(Y_{33}, Z_{33}) = 0;$$

$$L_1(Y_{41}, Z_{41}) = \tfrac{4}{3}(2\alpha+K_o)Y'^2_{22} - (1+\tfrac{8}{3}\alpha)Y_{22}Y''_{22} + \tfrac{8}{3}F'_oY'_{22},$$

$$L_2(Y_{41}, Z_{41}) = \tfrac{8}{3}\alpha Z_{22}Y'_{22} - (1+\tfrac{8}{3}\alpha)Y_{22}Z'_{22};$$

$$L_1(Y_{42}, Z_{42}) = \tfrac{4}{3}(4\alpha+2K_o)Y'_{11}Y'_{31} - (1+\tfrac{4}{3}\alpha)Y_{11}Y''_{31} - (1+4\alpha)Y''_{11}Y_{31}$$
$$+ \tfrac{8}{3}(2\alpha+K_o)Y'_{22}Y'_{21} - (1+\tfrac{8}{3}\alpha)(Y_{21}Y''_{22}+Y_{22}Y''_{21})$$
$$+ \tfrac{4}{3}(2F'_oY'_{31}+Y'^2_{11}+2F'_oY'_{21}+2Y'_{11}Y'_{21}),$$

$$L_2(Y_{42}, Z_{42}) = \tfrac{4}{3}\alpha Z_{11}Y'_{31} + 4\alpha Z_{31}Y'_{11} - (1+\tfrac{4}{3}\alpha)Y_{11}Z'_{31} - (1+4\alpha)Z'_{11}Y_{31}$$
$$+ \tfrac{8}{3}\alpha(Y'_{22}Z_{21}+Y'_{21}Z_{22}) - (1+\tfrac{8}{3}\alpha)(Y_{21}Z'_{22}+Y_{22}Z'_{21});$$

$$L_1(Y_{43},Z_{43}) = \tfrac{4}{3}(4\alpha+2K_o)Y'_{11}Y'_{33}-(1+\tfrac{4}{3}\alpha)Y_{11}Y'''_{33}-(1+4\alpha)Y'''_{11}Y_{33}$$
$$+\tfrac{8}{3}(F'_oY'_{33}+F'_oY'_{11}),$$

$$L_2(Y_{43},Z_{43}) = \tfrac{4}{3}\alpha Z_{11}Y'_{33}+4\alpha Y'_{11}Z_{33}-(1+\tfrac{4}{3}\alpha)Y_{11}Z'_{33}$$
$$-(1+4\alpha)Y_{33}Z'_{11};$$

$$L_1(Y_{44},Z_{44}) = \tfrac{8}{3}(2\alpha+K_o)Y'_{11}Y'_{32}-(1+\tfrac{4}{3}\alpha)Y_{11}Y'''_{32}-(1+4\alpha)Y'''_{11}Y_{32}$$
$$+\tfrac{4}{3}(2\alpha+K_o)Y'^{2}_{22}-(1+\tfrac{8}{3}\alpha)Y_{22}Y'''_{22}+\tfrac{8}{3}(F'_oY'_{32}+Y'_{11}Y'_{22}),$$

$$L_2(Y_{44},Z_{44}) = \tfrac{4}{3}\alpha Z_{11}Y'_{32}+4\alpha Y'_{11}Z_{32}-(1+\tfrac{4}{3}\alpha)Y_{11}Z_{32}$$
$$-(1+4\alpha)Z'_{11}Y_{32}+\tfrac{8}{3}\alpha Z_{22}Y'_{22}-(1+\tfrac{8}{3}\alpha)Y_{22}Z'_{22},$$

$$L_1(Y_{45},Z_{45}) = \tfrac{4}{3}F'^{2}_o,$$

$$L_2(Y_{45},Z_{45}) = 0$$

where

$$L_1(Y_{j-},Z_{j-}) = Y'''_{j-}+F_oY''_{j-}-\tfrac{4}{3}(\alpha j+2K_o)F'_oY'_{j-}$$
$$+(1+\tfrac{4}{3}\alpha j)F''_oY_{j-}+Z_{j-},$$

$$L_2(Y_{j-},Z_{j-}) = \tfrac{1}{\sigma}Z''_{j-}+F_oZ'_{j-}-\tfrac{4}{3}\alpha jF'_oZ_{j-}+(1+\tfrac{4}{3}\alpha j)T'_oY_{j-}.$$

The boundary conditions are

$$Y_{j-}(0) = Y'_{j-}(0) = Z_{j-}(0) = 0,$$

$$Y'_{j-}(\infty) = 0 = Z_{j-}(\infty).$$

Non-Isothermal Cylinder:

Using the transformations (2.52) in equations (2.48) and scaling out coefficients K_j s and ω_j s from the resulting equations, we get the following sets of differential equations for universal functions:

$$L_1(Y_{11}, Z_{11}) = \frac{4}{3} F_o'^2 ,$$

$$L_2(Y_{11}, Z_{11}) = 0 ;$$

$$L_1(Y_{12}, Z_{12}) = 0 ;$$

$$L_2(Y_{12}, Z_{12}) = 4F_o'T_o ;$$

$$L_1(Y_{21}, Z_{21}) = \frac{4}{3}(K_o+\alpha)Y_{11}'^2 - (1+\frac{4}{3}\alpha)Y_{11}Y_{11}'' + \frac{8}{3} F_o'Y_{11}' ,$$

$$L_2(Y_{21}, Z_{21}) = \frac{4}{3}\alpha Z_{11}Y_{11}' - (1+\frac{4}{3}\alpha)Y_{11}Z_{11}' ;$$

$$L_1(Y_{22}, Z_{22}) = \frac{4}{3} F_o'^2 ,$$

$$L_2(Y_{22}, Z_{22}) = 0 ;$$

$$L_1(Y_{23}, Z_{23}) = \frac{4}{3}(K_o+\alpha)Y_{12}'^2 - (1+\frac{4}{3}\alpha)Y_{12}Y_{12}'' ,$$

$$L_2(Y_{23}, Z_{23}) = \frac{4}{3}\alpha Z_{12}Y_{12}' - (1+\frac{4}{3}\alpha)Y_{12}Z_{12}' + 4(F_o'Z_{12}+T_oY_{12}') ;$$

$$L_1(Y_{24}, Z_{24}) = 0 ,$$

$$L_2(Y_{24}, Z_{24}) = 4F_o'T_o ;$$

$$L_1(Y_{25}, Z_{25}) = \frac{8}{3}(\alpha+K_o)Y_{11}'Y_{12}' - (1+\frac{4}{3}\alpha)(Y_{11}Y_{12}''+Y_{11}''Y_{12}) + \frac{8}{3}F_o'Y_{12}'$$

$$L_2(Y_{25}, Z_{25}) = \frac{4}{3}\alpha(Y'_{11}Z_{12}+Y'_{12}Z_{11})-(1+\frac{4}{3}\alpha)(Z'_{11}Y_{12}+Y_{11}Z'_{12})$$

$$+ 4(F'_oZ_{11}+ T_oY'_{11})$$

where

$$L_1(Y_{j-}, Z_{j-}) = Y'''_{j-} +F_oY''_{j-} - \frac{4}{3}(\alpha j+2K_o)F'_oY'_{j-}$$

$$+ (1+ \frac{4}{3}\alpha j)F''_oY_{j-} +Z_{j-},$$

$$L_2(Y_{j-}, Z_{j-}) = \frac{1}{\sigma}Z''_{j-} + F_oZ'_{j-} - \frac{4}{3}\alpha jF'_oZ_{j-} +(1+ \frac{4}{3}\alpha j)T'_oY_{j-}.$$

The boundary conditions are

$$Y_{j-}(0) = Y'_{j-}(0) = Z_{j-}(0) = 0,$$

$$Y'_{j-}(\infty) = Z_{j-}(\infty) = 0.$$

REFERENCES

[1] Simon Ostrach, "Laminar flows with body forces", in Theory of Laminar Flows ed. F.K. Moore, Princeton University Press, Princeton, N.J., 528-607 (1964).

[2] Hermann, R., NACA TM 1366, (1954).

[3] Merk, H.J. and Prins, J.A., Appl. Sci. Res. 4A, 11-24, 195-206, 207-224 (1953-1954).

[4] Chiang, T. and Kaye, J., Proceedings of the 4th U.S. National Congress of Applied Mechanics, Berkeley, Calif., 1213-1219 (1962).

[5] Koh, J.C.Y. and Price, J.F., J. Heat Transfer Trans. of the ASME, 87, 237-242 (1965).

[6] Chiang, T., Ossin, A., and Tien, C.L., ibid, 86, 537-542 (1964).

[7] Saville, D.A., and Churchill, S.W., Jl. of Fluid Mechanics, 29, 391-399 (1967).

[8] Görtler, H., J. Math. Mech., 6, 1-66 (1957).

[9] Wilks, G., Int. J. Heat Mass Transfer, 15, 351-354 (1972).

[10] Lin, F.N., Letters in Heat and Mass Transfer, 3, 59-68. (1976).

[11] Kelleher, M., and Yang, K.T., Quart. J. Mech. and Appl. Math., 25, 447-457 (1972).

[12] Kuiken, H.K., Appl. Sci. Res. 20, 205-214 (1969.).

[13] Lin, F.N., and Chao, B.T., J. Heat Transfer Trans. of ASME, 96, 435-442 (1974).

[14] Lin, F.N., and Chern, S.Y., ibid 103, 819-821 (1981).

[15] Merkin, J.H., ibid 99, 453-457 (1977).

[16] Merkin, J.H., "Free convection Boundary Layer on an Isothermal Horizontal Cylinder", Presented at the ASME-AICHE Heat Transfer Conference, St. Louis, Mo., August(1976).

[17] Na, T.Y., Appl. Sci. Res. 33, 519-554 (1978).

[18] Tollmien, W., Grengschichttheorie. Handl. Exper. physik, 4, Pt. 1, 248 (1931).

[19] Goldstein, S., Ed. Modern Developments in Fluid Dynamics. Clarendon Press, Oxford (1938).

[20] Sparrow, E.M., and Gregg, J.L., Trans. Am. Soc. Mech. Engrs. 80, 379 (1958).

[21] Reeves, B.L., and Kippenhan, J., JASS 29, 38-47 (1962).

[22] Copson, E.T., An introduction to the theory of function of a complex variable, Oxford, The clarendon press, 123-125 (1960).

[23] Nachtsheim, P.R. and Swigert, P., Development in Mechanics 1, 361-367 (1965).

[24] Roberts, S.M. and Shipman, J.S., Two-point Boundary Value Problems: Shooting methods American Elsevier, N.Y. (1972).

[25] Jodlbauer, K., Das Temperatur -und Geschwindigkeitsfeld um ein geheiztes Rohr bei freier konvektion Forsch. Ing. Wes. 4, 157 (1933).

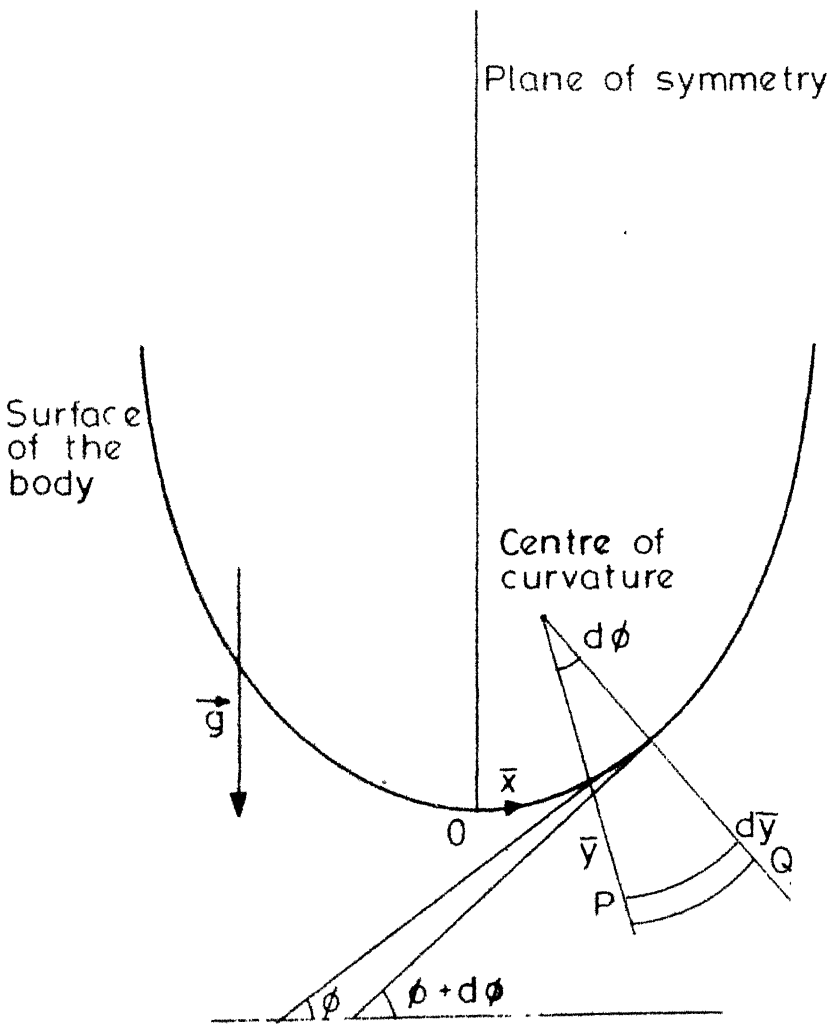

Fig. 1 Physical model and coordinate system: $t_w > t_\infty$

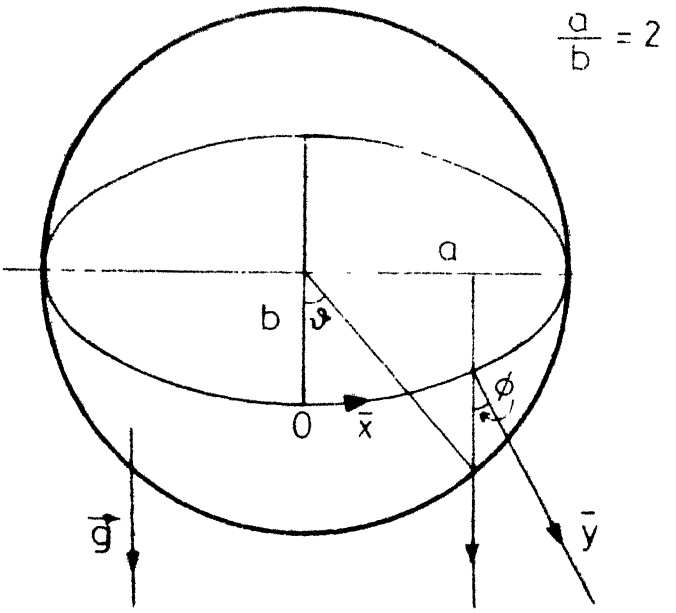

Fig. 2 Cross-section of a blunt horizontal elliptical cylinder with major-axis perpendicular to the direction of gravity

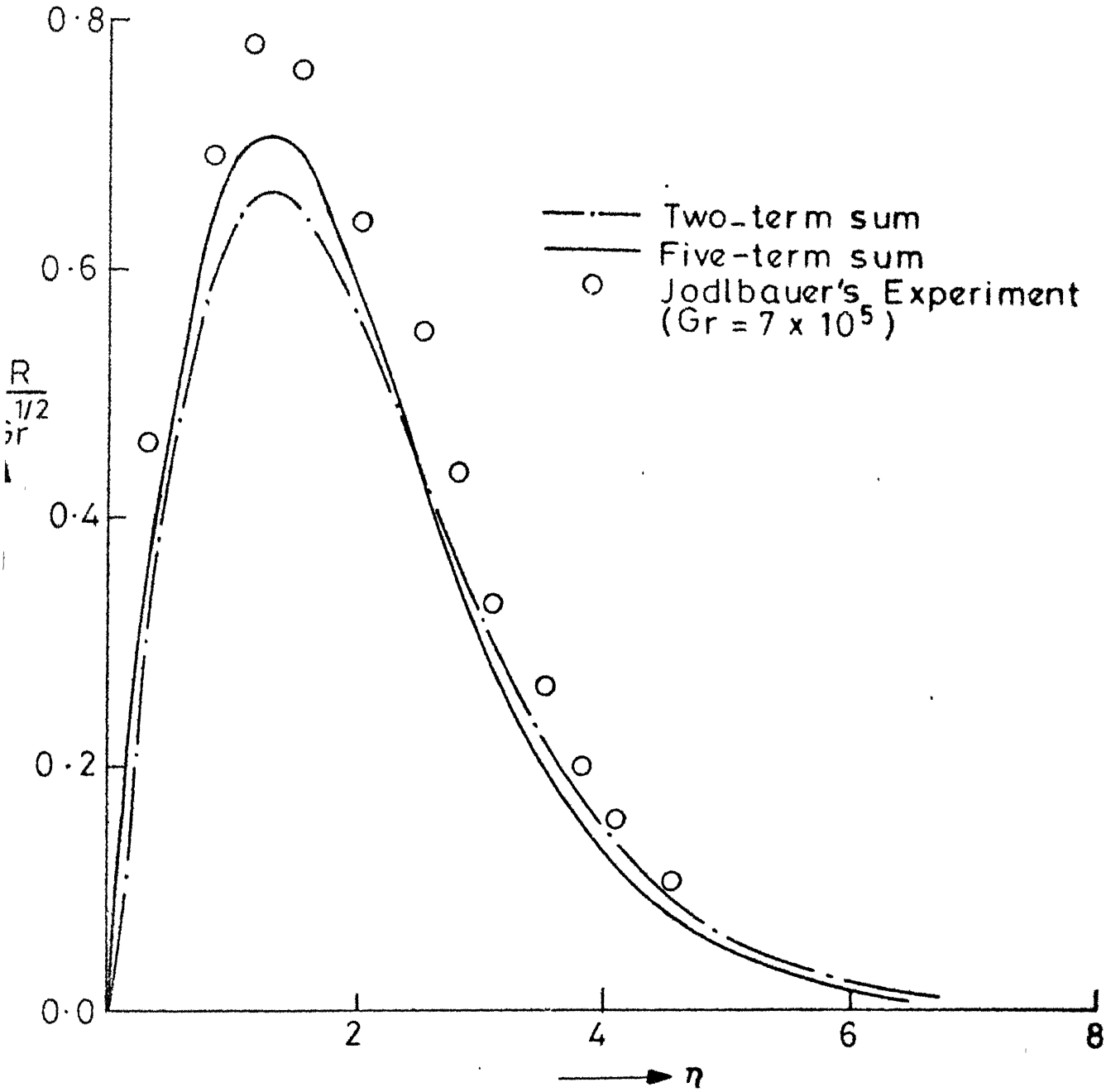

g. 3 $\bar{u}$ - velocity distribution around a heated isothermal circular cylinder; $\vartheta = 150°$ and $\sigma = 0{\cdot}7$.

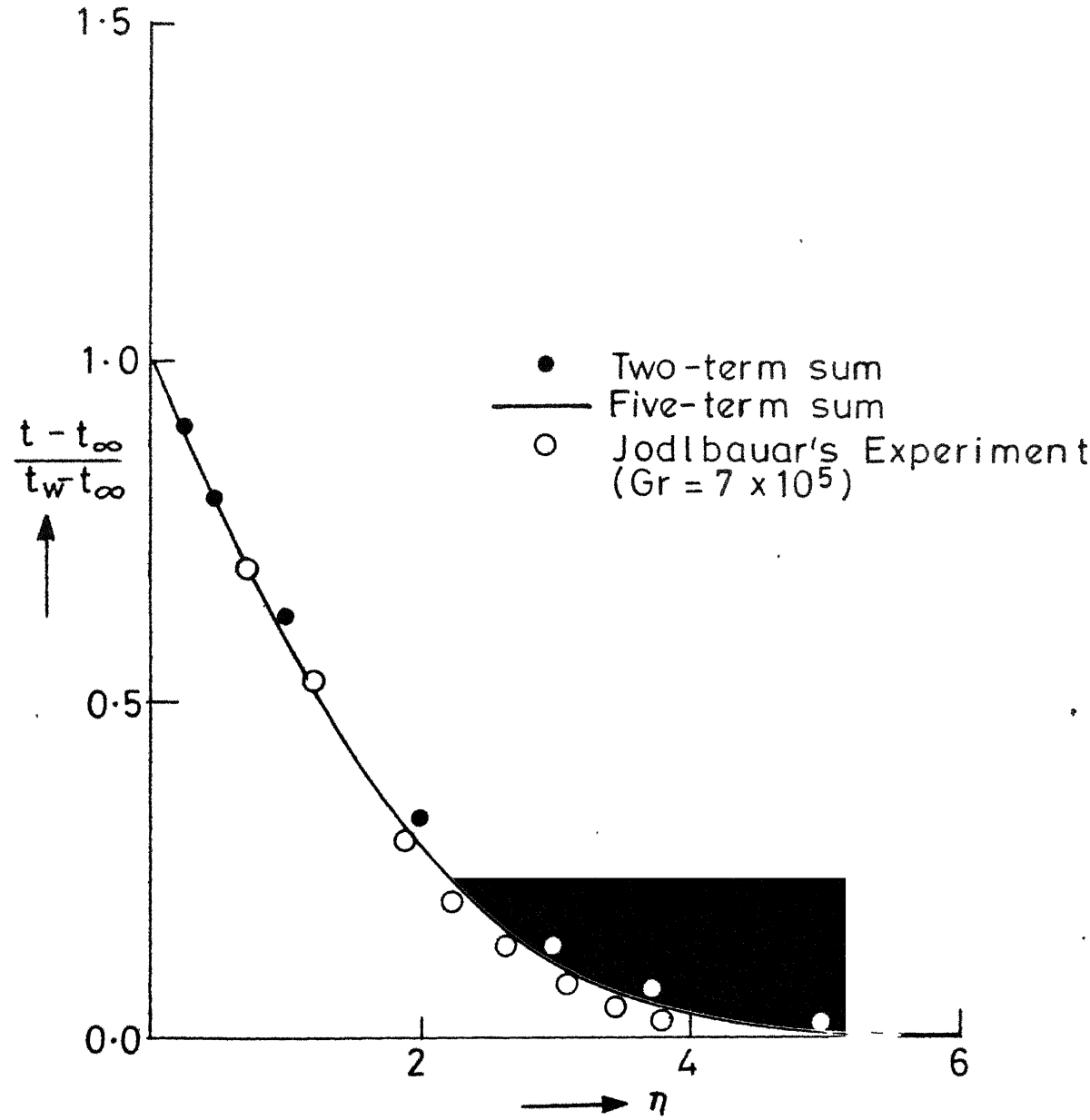

Fig. 4 Temperature distribution around a heated isothermal circular cylinder; $\vartheta = 150°$ and $\sigma = 0·7$.

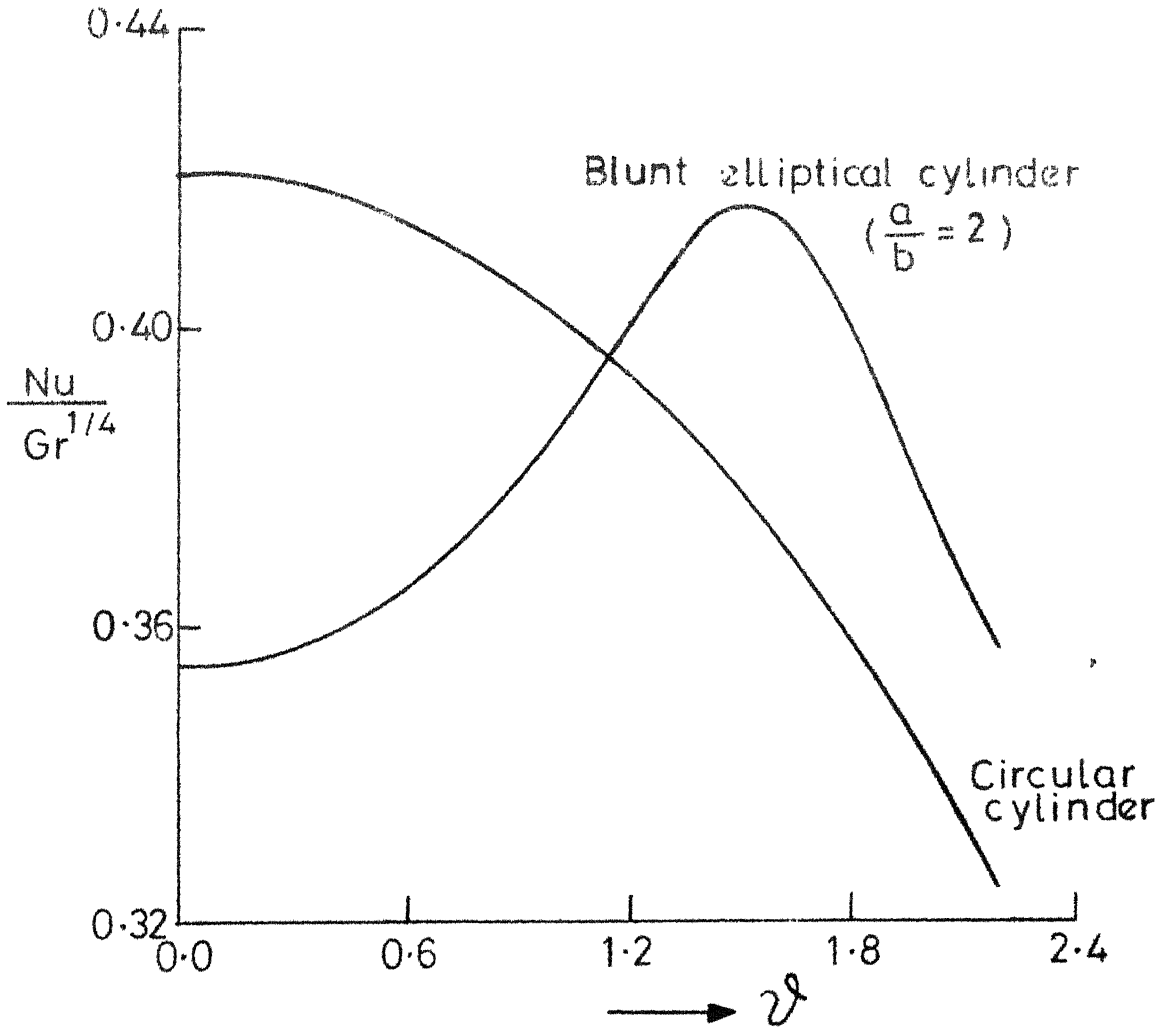

Fig. 5 Heat transfer over isothermal circular and elliptical cylinders; $\sigma = 1 \cdot 0$.

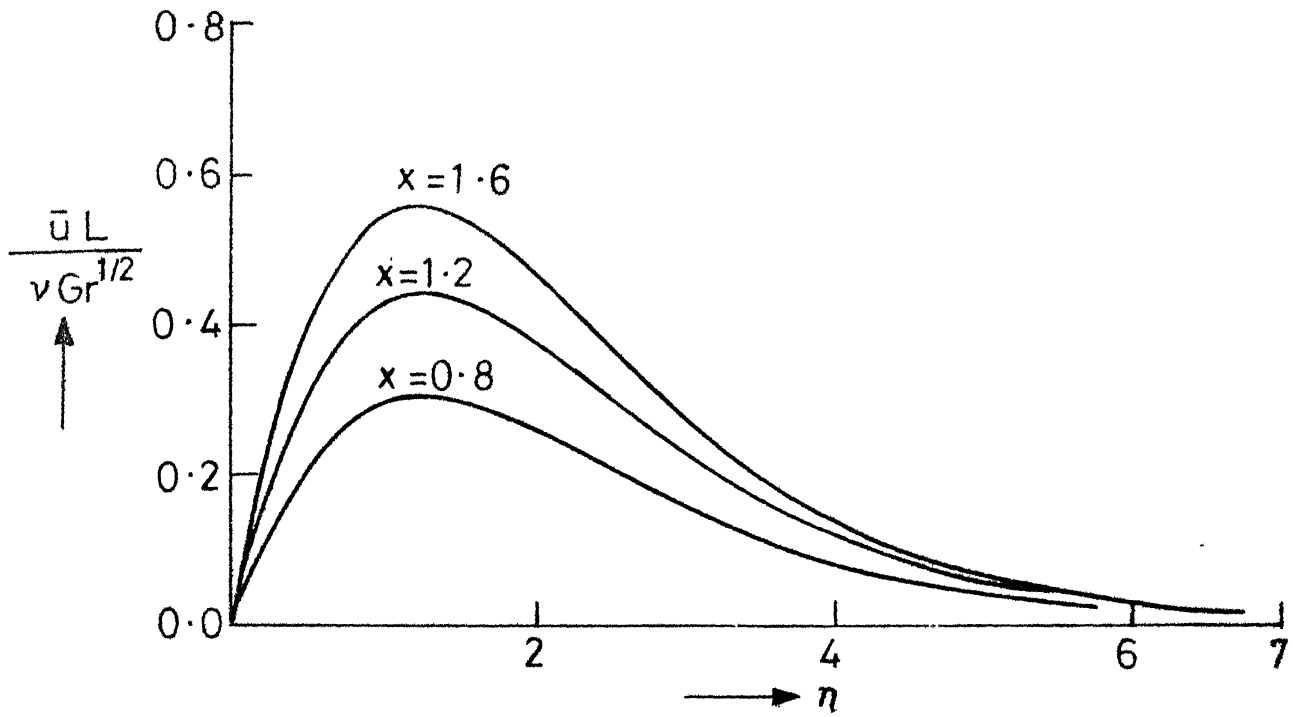

Fig. 6 ū - velocity distribution for a non-isothermal vertical plate; G(x) = Sinx and $\bar{\sigma} = 0 \cdot 7$.

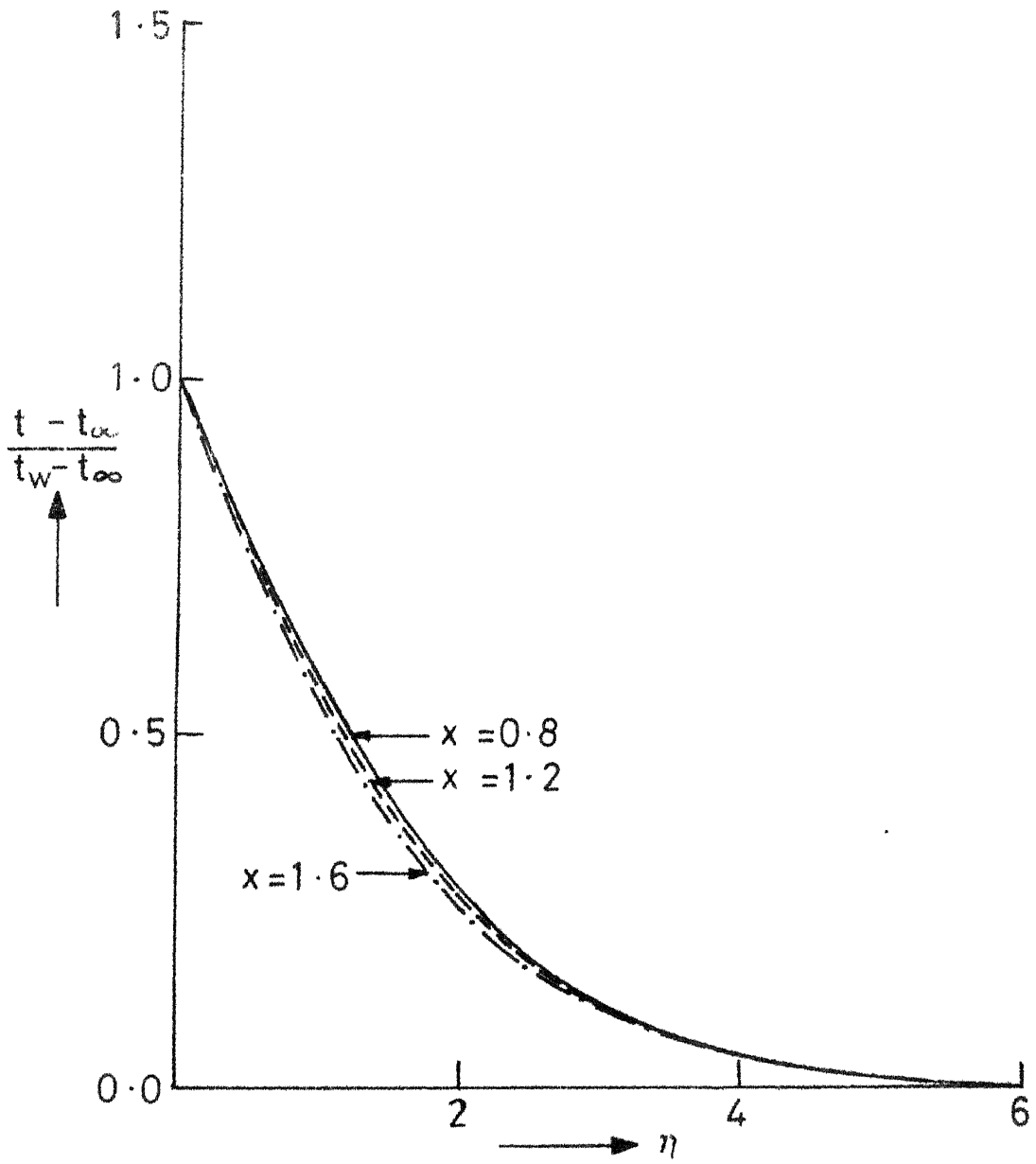

Fig. 7 Temperature distribution for a non-isothermal vertical plate; $G(x) = \sin x$ and $\sigma = 0{\cdot}7$.

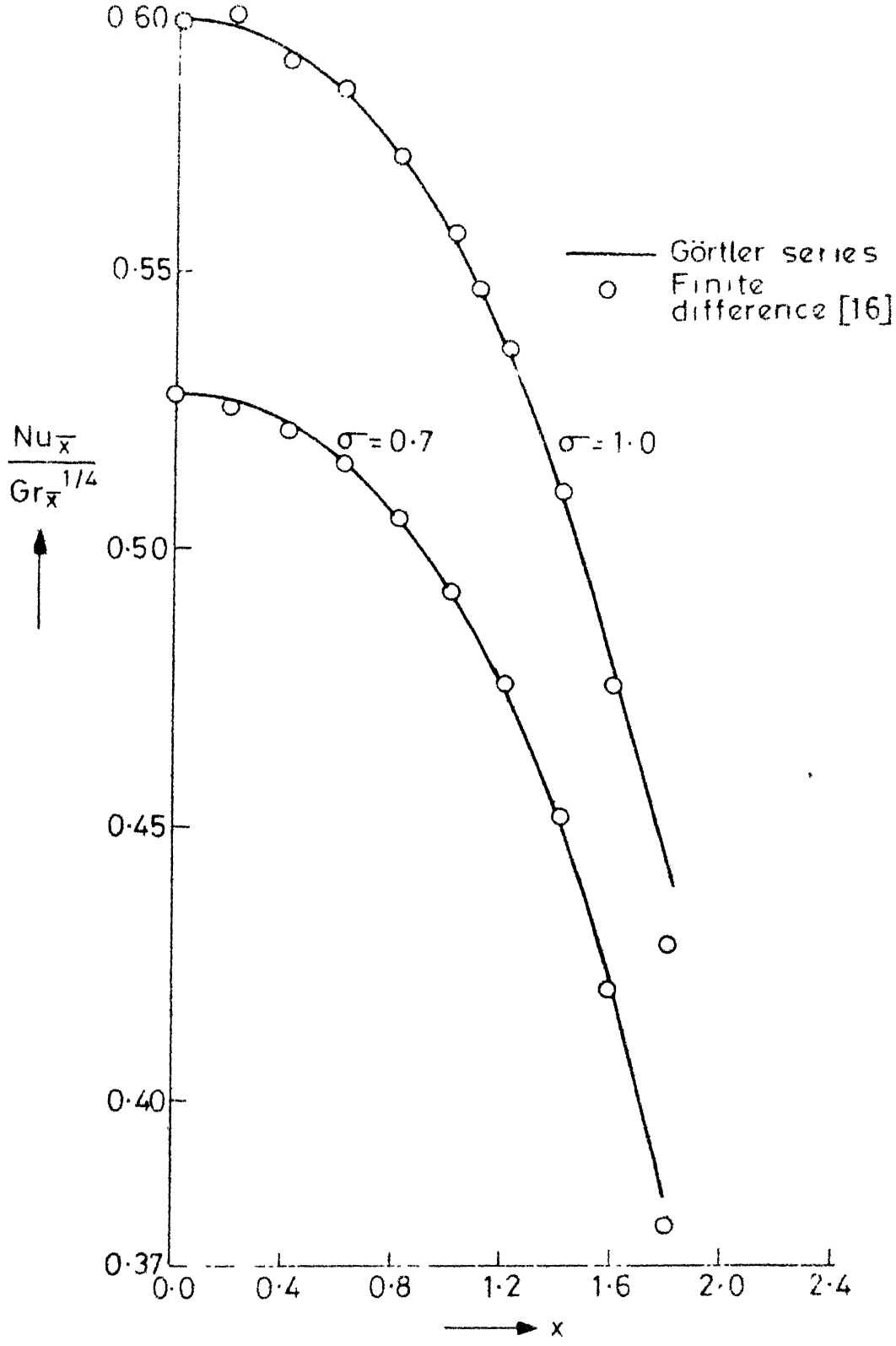

Fig. 8 Comparison of Heat transfer variation for non-isothermal vertical plate; $G(x) = \sin x$.

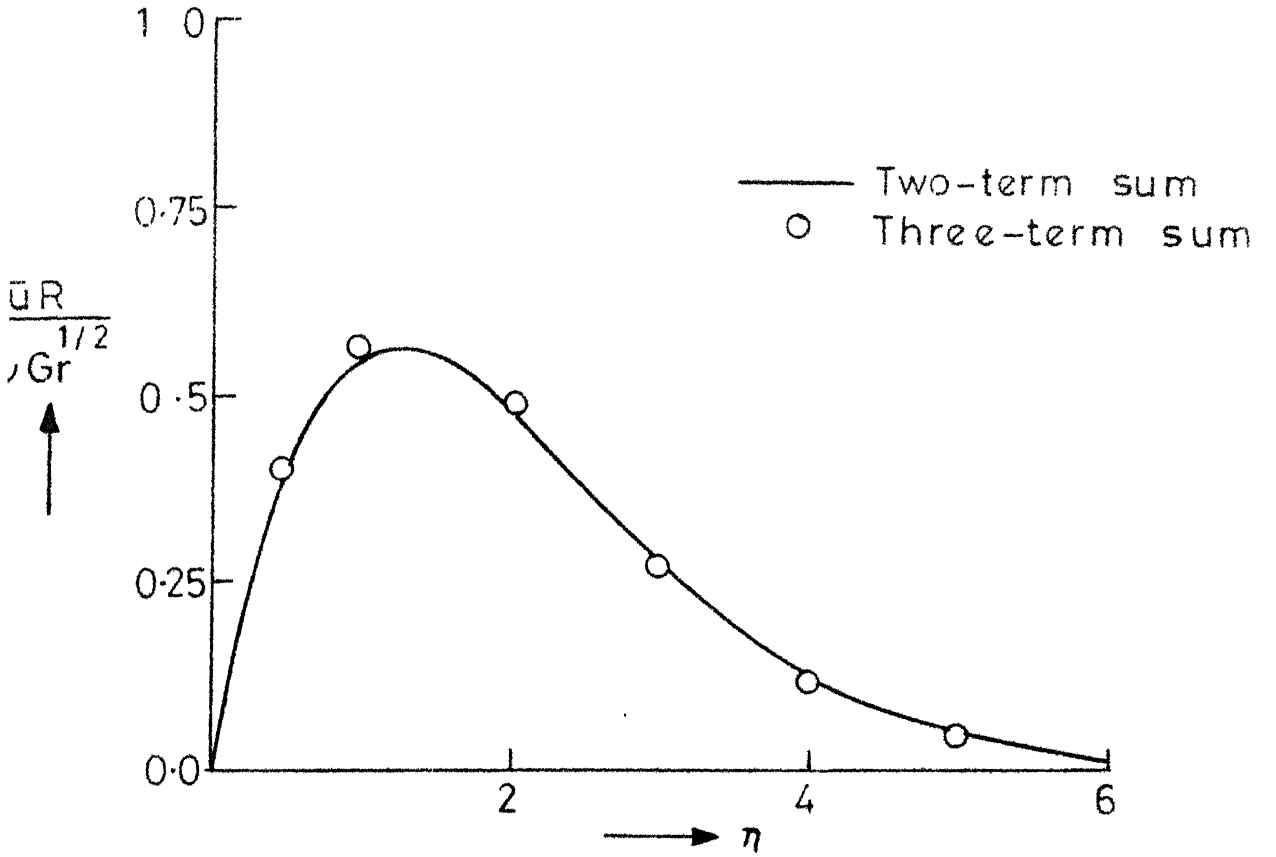

Fig. 9 ū-velocity distribution around a non-isothermal circular cylinder; $G(x) = 1 - 0{\cdot}1\,x^2$, $\vartheta = 90°$ and $\bar{\sigma} = 0{\cdot}7$.

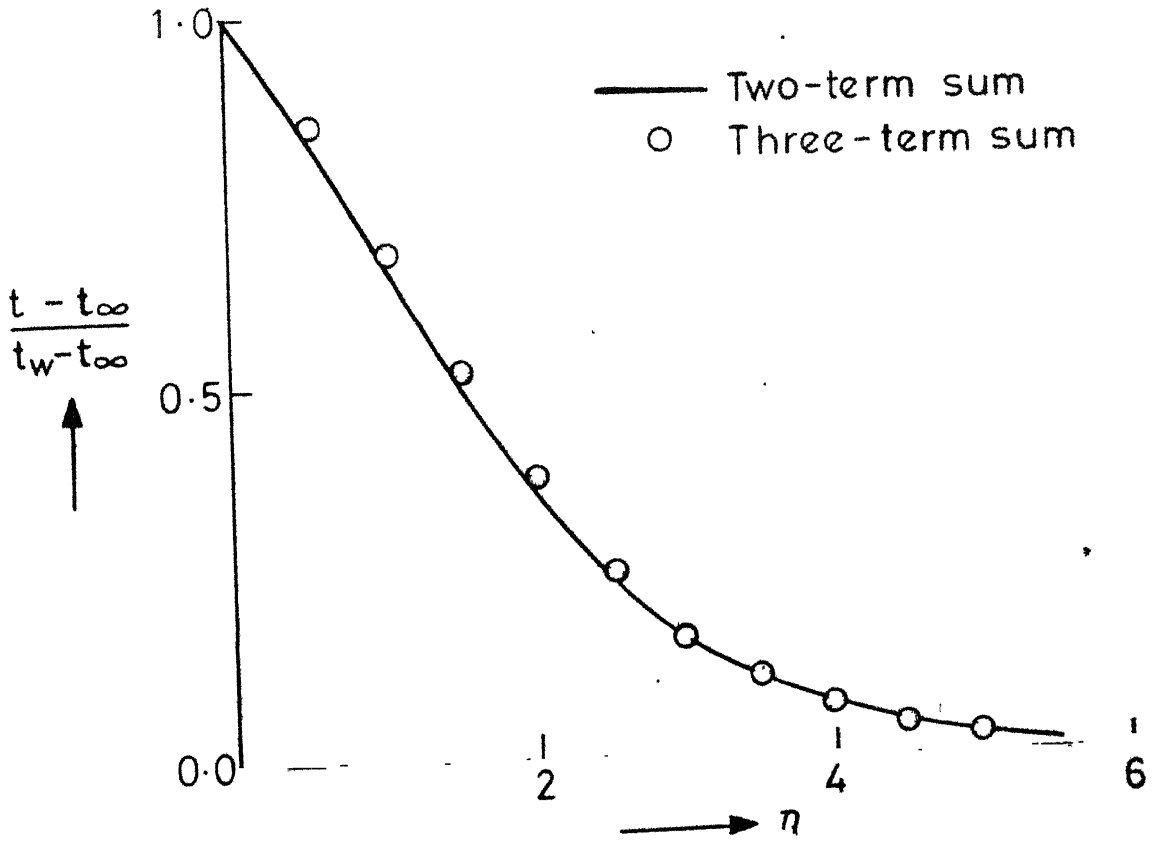

Fig. 10 Temperature distribution around a non-isothermal circular cylinder; $G(x) = 1 - 0{\cdot}1\,x^2$, $\vartheta = 90°$ and $\bar{\sigma} = 0{\cdot}7$.

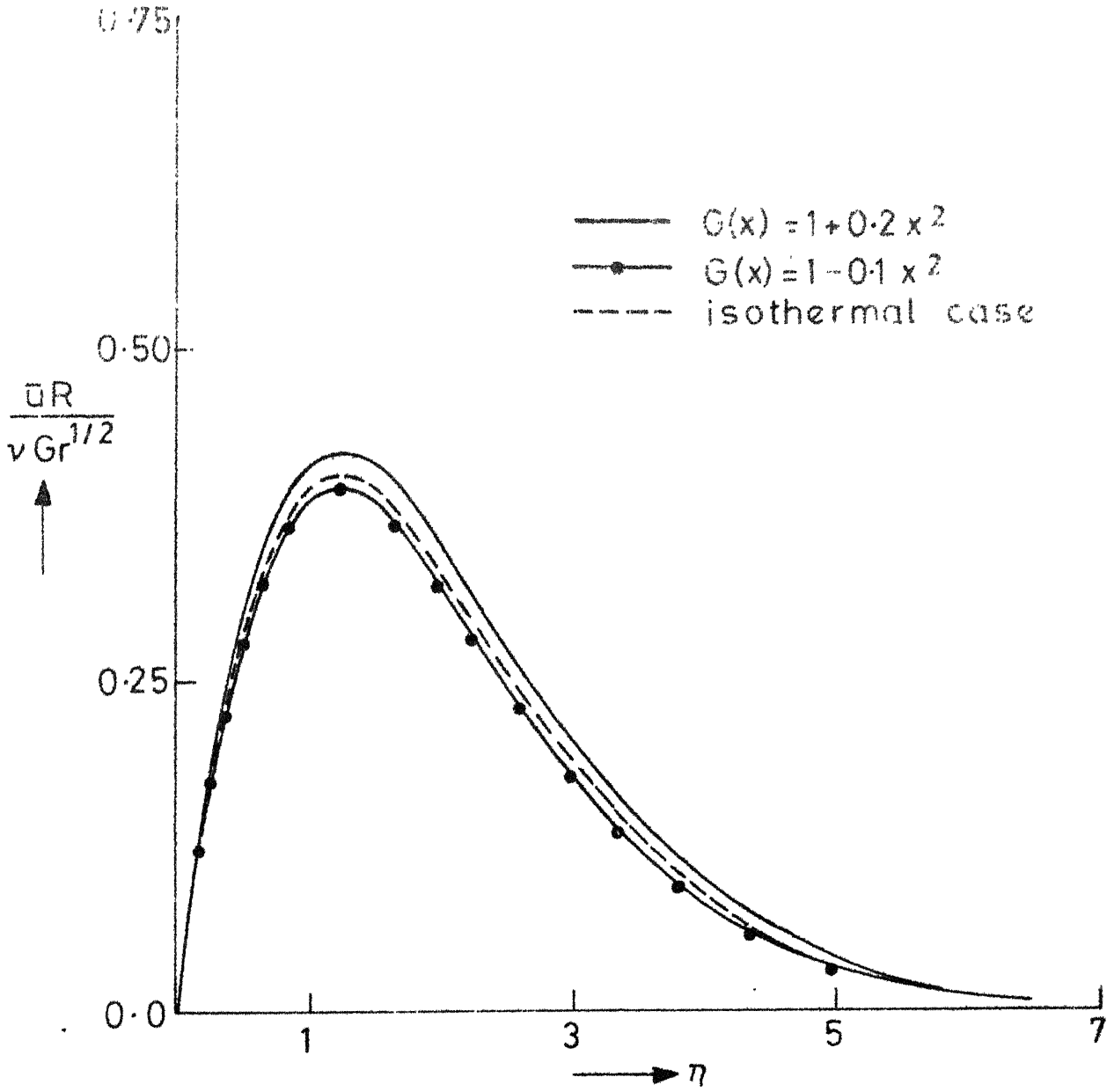

Fig. 11 $\bar{u}$-velocity distribution around a non-isothermal circular cylinder ; $\vartheta = 60°$ and $\sigma = 1{\cdot}0$.

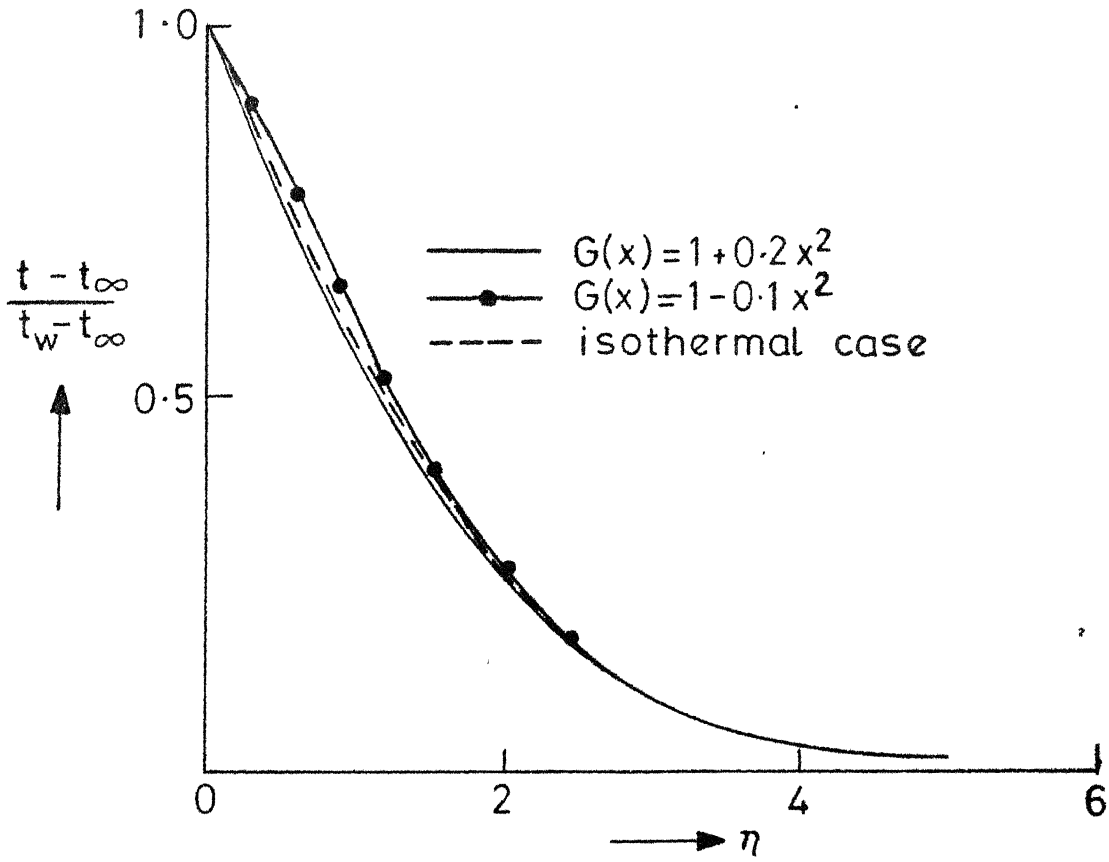

Fig. 12 Temperature distribution around a non-isothermal circular cylinder; $\vartheta = 60°$ and $\sigma = 1·0$.

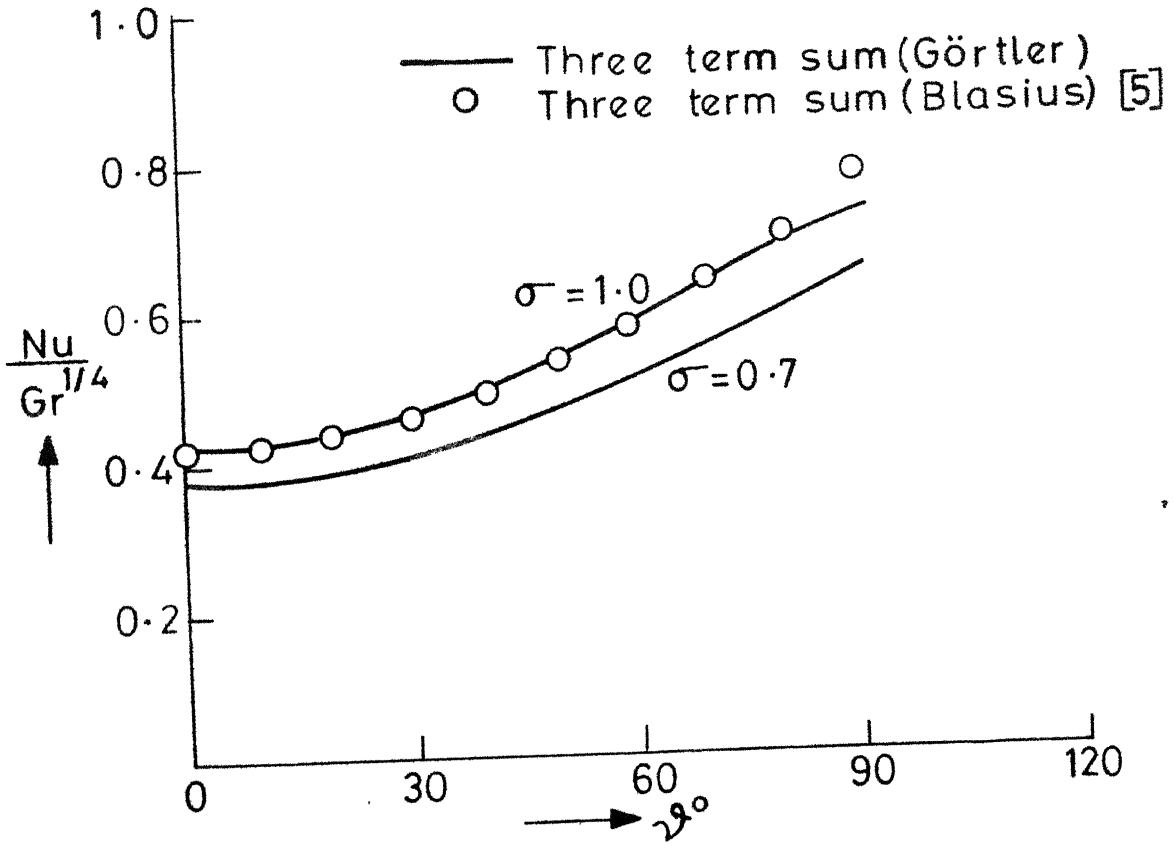

Fig. 13 Heat transfer variation over a non-isothermal circular cylinder; $G(x) = 1{\cdot}0 + 0{\cdot}2\,x^2$.

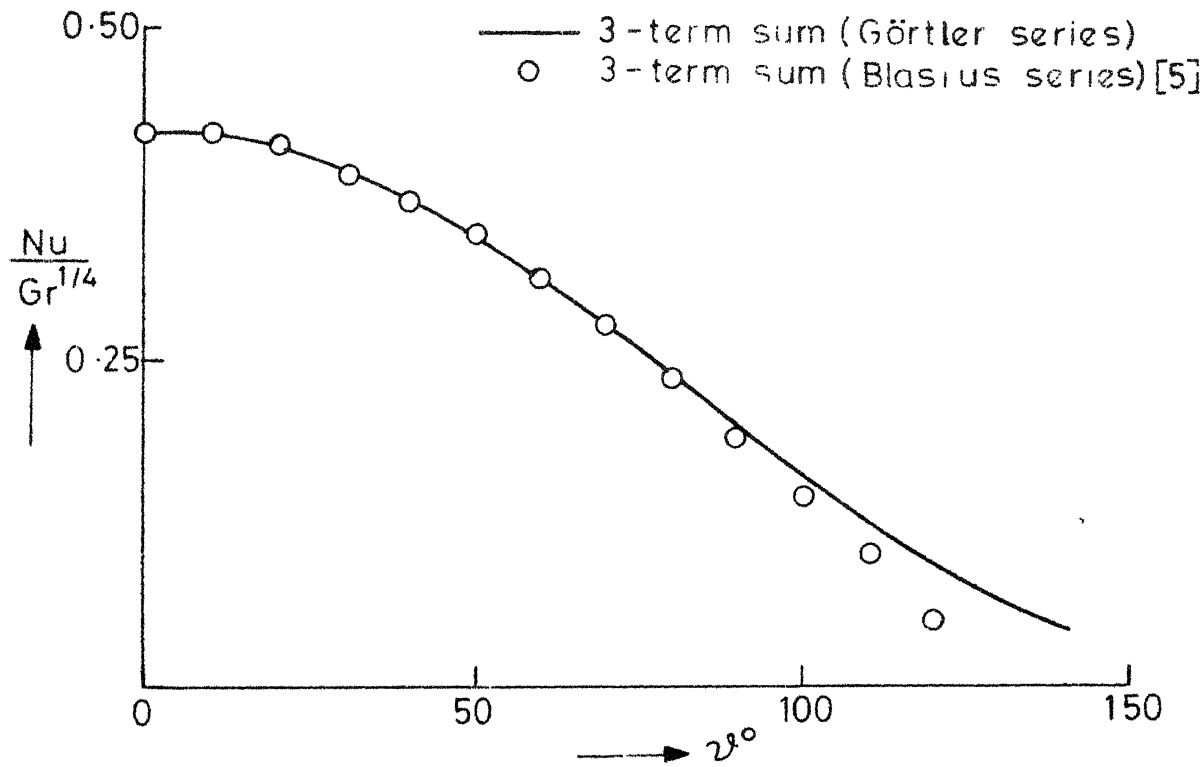

Fig. 14 Heat transfer variation over non-isothermal circular cylinder ; $G(x) = 1 - 0{\cdot}1\,x^2$ and $\bar{\sigma} = 1{\cdot}0$.

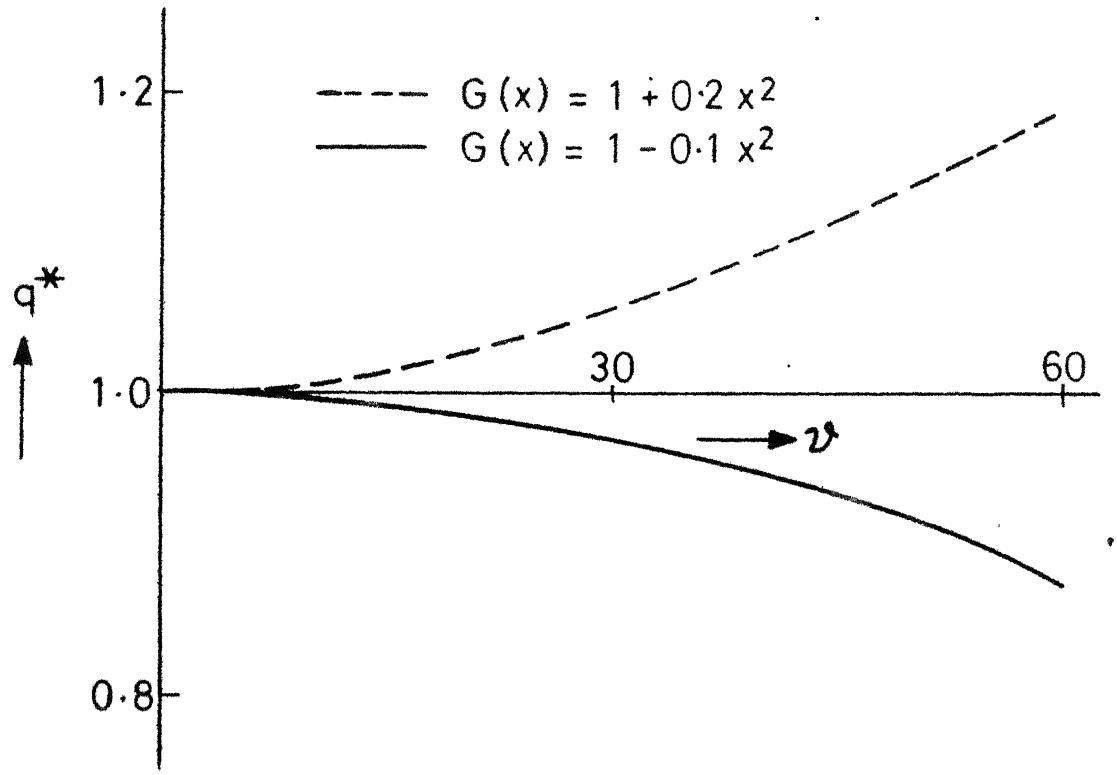

Fig.15 Effect of non-isothermal wall condition on heat transfer; $\sigma = 0{\cdot}7$.

CHAPTER III

LOCAL NON-SIMILARITY SOLUTION OF FREE CONVECTION FLOW AND HEAT TRANSFER FROM AN ISOTHERMAL PLATE INCLINED AT A SMALL ANGLE TO THE HORIZONTAL

1. INTRODUCTION

In this chapter, we study analytically the laminar free convection boundary layer flow over a flat surface that is inclined at a small angle to the horizontal. Surface inclination results in a pressure gradient across the boundary layer (being induced by the surface normal component of the buoyancy force) and leads to a theoretical analysis more complicated than that for vertical surfaces. In the case of heated vertical surfaces maintained at a temperature greater than the surrounding fluid, a local region of lower density produces an upward buoyancy force and a boundary layer is formed over the body which is driven directly by this force. But if the surface is horizontal or nearly so, the buoyancy force along the surface is very small and a very different kind of flow drive arises. In the particular case of a horizontal surface, there is no component of the buoyancy force along the surface and there is no direct drive of any tangential flow that may result. Rotem and Claassen [1] carried out a flow visualization experiment using a semifocussing Schlieren system which clearly indicated the existence of a boundary layer near the leading edge on the upperside of the heated horizontal surface though its horizontal extent is limited. Stewartson [2] was the first to give a theoretical description of a boundary layer over horizontal surfaces under the action of buoyancy force. Since there is no component of buoyancy

along the surface, the accelerating flow must be driven indirectly by a buoyancy - induced pressure gradient. Stewartson's analysis contains a sign error in the pressure gradient term of the horizontal momentum equation and thus condition for existence of such a boundary layer is that the heated plate is to face downwards. Later, this error was corrected by Gill, Zeh and del-casal [3] and one finds a horizontal boundary layer above the heated plate driven by a negative pressure gradient. This is called ''indirect - drive'' and is due to the pressure deficiency in the thermal transport region next to the surface with respect to the ambient medium. It is indirect in that the buoyancy force does not drive the flow. Rather, it produces a pressure field which induces such a flow.

For a heated plate inclined at a small positive angle α to the horizontal, the boundary layer flow is driven not only by the above-mentioned indirect mechanism but also by a component of the buoyancy force B_t along the surface. Jones [4] made an analysis of this type of flow by considering that except in the neighbourhood of the leading edge, the direct drive due to B_t dominates the induced pressure effects, which can therefore be neglected. The resulting flow far downstream in his analysis is then what is described by the classical free convection solution along a vertical plate. Pera and Gebhart [5] considered the free convection

flow over a horizontal and slightly inclined surfaces. The effect of inclination on the flow and transport is analysed by perturbing flow over horizontal surface. Their study includes experimental data for the temperature distributions and heat transfer parameter. When the inclination of the plate is negative, the pressure gradient associated with the indirect-drive is favourable for motion while the component of the buoyancy force along the surface is opposing the motion. Jones [4] demonstrated that in this case the flow eventually separates though, of course, separation is not accompained by the development of a singularity in the solution of the governing equations.

In this chapter, the boundary layer in free convection flow over the upper surface of a heated semi-infinite horizontal plate inclined at a small angle α with the horizontal is studied analytically by the local non-similarity method of solution [6]. The range of α considered here, as obtained from the analysis, is defined by the requirement that Λ, the limit of $Gr^{1/5} \tan \alpha$ as $Gr \to \infty$, be $O(1)$, where Gr is a suitably defined Grashof number. The conservation equations are transformed such that they can lend themselves to local non-similarity solutions. In this method of solution, all the terms in the transformed conservation equations are retained and terms are selectively neglected only in the subsidiary equations. This solution

method, in general, offers to non-similar convective heat transfer problems many of the advantages of similarity analysis while at the same time, providing an assessment of accuracy of the results obtained within the method itself. The forms of the local non-similarity method considered here are the two and three-equation models obtained by retaining the transformed conservation equations as such and only selectively neglecting terms in the derived subsidiary equations at the second and third level of the successive approximations in this method of solution. The corresponding two-point non-linear boundary value problems for these two models at a streamwise location are solved by the initial value technique as modified by Nachtsheim and Swigert [6]. Particularly, the application of this numerical procedure for the highly non-linear three-equation model was commenced at some downstream location with good initial estimates of missing wall conditions generated by quasilinearization technique [7]. Numerical results for the local surface heat-transfer, wall shear-stress and velocity and temperature distributions are presented for Prandtl number 0.72 and 1.0 when $\Lambda = 1$ and -1.

For small positive angle of inclination, our study makes no assumption on the neglect of induced pressure effects from some distance downstream away from the leading edge of the plate and the method of analysis adopted here facilitates solving for the entire region of flow. On the other hand,

Jones [4] had covered the whole region by working with two sets of transformed boundary layer equations in order to give non-similar corrections which bridge the gap between his series solutions, one valid near the leading edge and the other far downstream of the flow. It is shown that our results for transport rates at the surface and also the velocity and temperature distributions compares well with that of Jones in the entire flow region. When the angle of inclination is negative, our method of solution predicts the point of separation of the flow and notably, for the case of air, the two-equation model locates this point within an error of $1\frac{1}{2}$ percent from the exact value as reported by Jones [4]. This stands in sharp contrast to its behaviour in the case of forced flow over a circular cylinder, where this technique yields large deviation in the boundary layer characteristics of the flow while approaching the region near separation point. Perhaps, this behaviour may be due to the fact that there is no evidence of singularity at the separation point, unlike in forced flow, where a classical singular behaviour is to be expected in skin-friction factor near the point of separation.

2. BASIC EQUATIONS

We consider the steady two-dimensional free convection flow over a semi-infinite flat plate inclined at an angle α to the horizontal placed in an infinite expanse of fluid.

The plate is maintained at a temperature T_w which is different from the ambient temperature T_∞ of the fluid. The Boussinesq form of the governing equations for the flow as derived from equations(1.9), (1.13) and (1.11) in cartesian coordinates $\bar{x}$ and $\bar{y}$, along and normal to the plate respectively, with origin at the leading edge may be written as:

$$\frac{\partial \bar{u}}{\partial \bar{x}} + \frac{\partial \bar{v}}{\partial \bar{y}} = 0, \tag{3.1}$$

$$\bar{u}\frac{\partial \bar{u}}{\partial \bar{x}} + \bar{v}\frac{\partial \bar{u}}{\partial \bar{y}} = -\frac{1}{\rho}\frac{\partial \bar{P}}{\partial \bar{x}} + \nu\left(\frac{\partial^2 \bar{u}}{\partial \bar{x}^2} + \frac{\partial^2 \bar{u}}{\partial \bar{y}^2}\right) + g\beta \sin\alpha\,(T-T_\infty), \tag{3.2}$$

$$\bar{u}\frac{\partial \bar{v}}{\partial \bar{x}} + \bar{v}\frac{\partial \bar{v}}{\partial \bar{y}} = -\frac{1}{\rho}\frac{\partial \bar{P}}{\partial \bar{y}} + \nu\left(\frac{\partial^2 \bar{v}}{\partial \bar{x}^2} + \frac{\partial^2 \bar{v}}{\partial \bar{y}^2}\right) + g\beta \cos\alpha\,(T-T_\infty) \tag{3.3}$$

$$\bar{u}\frac{\partial T}{\partial \bar{x}} + \bar{v}\frac{\partial T}{\partial \bar{y}} = \bar{\alpha}\left(\frac{\partial^2 T}{\partial \bar{x}^2} + \frac{\partial^2 T}{\partial \bar{y}^2}\right) . \tag{3.4}$$

Here quantities $\bar{u}$ and $\bar{v}$ are the components of velocity in the directions along and normal to the plate respectively, $\bar{P}$ and T are respectively the pressure and temperature fields induced by motion, ν and $\bar{\alpha}$ are the appropriate transport coefficients, ρ the density and α the angle of inclination of the plate with the horizontal.

The variables are now non-dimensionalized and stretched in the following way:

$$\bar{x} = \frac{\bar{x}}{L}\ ,\ y = \frac{\bar{y}}{LGr^{-1/5}}\ ,\ u = \frac{\bar{u}L}{\nu Gr^{2/5}}\ ,\ v = \frac{\bar{v}L}{\nu Gr^{1/5}}$$

$$p = \frac{\bar{p}L^2}{\rho\nu Gr^{4/5}} \text{ and } \theta = \frac{T - T_\infty}{T_w - T_\infty} \tag{3.5}$$

where L is a characteristic length along the surface and Gr is the Grashof number given by

$$Gr = \frac{g\beta(T_w - T_\infty)\ L^3 \cos\alpha}{\nu^2} \tag{3.6}$$

Using(3.5), equations (3.1) to (3.4) are reduced to

$$\frac{\partial u}{\partial x} + \frac{\partial v}{\partial y} = 0\ , \tag{3.7}$$

$$u\frac{\partial u}{\partial x} + v\frac{\partial v}{\partial y} = -\frac{\partial P}{\partial x} + \frac{\partial^2 u}{\partial y^2} + \frac{\partial^2 u}{\partial x^2} Gr^{-2/5} + Gr^{1/5}\tan\alpha\ \theta\ , \tag{3.8}$$

$$u\frac{\partial v}{\partial x} + v\frac{\partial v}{\partial y} = -\frac{\partial P}{\partial y} Gr^{2/5} + \theta Gr^{2/5} + \frac{\partial^2 v}{\partial y^2} + Gr^{-2/5}\frac{\partial^2 v}{\partial x^2}\ , \tag{3.9}$$

$$u\frac{\partial \theta}{\partial x} + v\frac{\partial \theta}{\partial y} = \frac{1}{\sigma}\left[\frac{\partial^2 \theta}{\partial y^2} + Gr^{-2/5}\frac{\partial^2 \theta}{\partial y^2}\right] \tag{3.10}$$

where σ is the Prandtl number of the fluid.

The boundary conditions in terms of non-dimensional variables are

$$u = 0 = v \text{ and } \theta = 1 \text{ on } y = 0 \text{ for } x > 0,$$
$$u, \theta, p \to 0 \text{ as } y \to \infty \tag{3.11}$$

and

$$u = p = \theta = 0 \quad \text{on} \quad x = 0 \text{ for } y > 0 \,. \tag{3.12}$$

By ignoring terms which are $O(Gr^{-2/5})$ relative to those retained in the limit $Gr \to \infty$, we get the boundary layer equations

$$\frac{\partial u}{\partial x} + \frac{\partial v}{\partial y} = 0 \,, \tag{3.13}$$

$$u \frac{\partial u}{\partial x} + v \frac{\partial u}{\partial y} = - \frac{\partial p}{\partial x} + \Lambda \theta + \frac{\partial^2 u}{\partial y^2} \,, \tag{3.14}$$

$$0 = - \frac{\partial p}{\partial y} + \theta \,, \tag{3.15}$$

$$u \frac{\partial \theta}{\partial x} + v \frac{\partial \theta}{\partial y} = \frac{1}{\sigma} \frac{\partial^2 \theta}{\partial y^2} \tag{3.16}$$

where the range of angle of inclination α considered here is defined by the requirement that

$$\Lambda = \lim_{Gr \to \infty} Gr^{1/5} \tan \alpha$$

be $O(1)$ so that the buoyancy force term is formally comparable with the induced pressure gradient along the plate. For $\Lambda = 0$, the flow is over a horizontal surface and for $\Lambda \to \infty$ we will get the classical free convection problem for which the scalings used here become inappropriate.

We now choose the stream function Ψ which satisfies the continuity equation (3.13) and now the boundary layer equations become

$$\Psi_y \Psi_{xy} - \Psi_x \Psi_{yy} = -p_x + \Psi_{yyy} + \Lambda\theta \,, \tag{3.17}$$

$$p_y = \theta \,, \tag{3.18}$$

$$\Psi_y \theta_x - \Psi_x \theta_y = \frac{1}{\sigma} \theta_{yy} \,, \tag{3.19}$$

with boundary conditions:

$$\Psi = 0 = \Psi_y, \quad \theta = 1 \quad \text{on} \quad y = 0 \text{ for } x > 0 \,, \tag{3.20}$$

$$\Psi_y, p, \theta \to 0 \quad \text{as} \quad y \to \infty$$

and

$$\Psi_y = p = \theta = 0 \quad \text{on} \quad x = 0 \text{ for } y > 0 \,. \tag{3.21}$$

3. TRANSFORMATION OF BOUNDARY LAYER EQUATIONS

We now introduce the following transformations

$$\eta = y\, x^{-2/5} \,, \tag{3.22}$$

$$\Psi = x^{3/5} F(x,\eta) \,,$$

$$p = x^{2/5} G(x,\eta) \,,$$

$$\theta = H(x,\eta) \tag{3.23}$$

to transform the boundary layer equations (3.17) to (3.19) into non-similar form:

$$5F''' + 3FF'' - F'^2 + 2\eta G' - 2G + 5\Lambda x^{3/5} H = 5x\left(\frac{\partial G}{\partial x} + F' \frac{\partial F'}{\partial x} - F'' \frac{\partial F}{\partial x}\right) \tag{3.24}$$

$$G' = H \tag{3.25}$$

$$5H'' + 3\sigma FH' = 5x\left(F' \frac{\partial H}{\partial x} - H' \frac{\partial F}{\partial x}\right) . \qquad (3.26)$$

In the foregoing equations, the primes denote partial differentiation with respect to η. The boundary conditions are, now:

$$F(x,0) = F'(x,0) = 0, \quad H(x,0) = 1 ,$$

$$F'(x,\infty) = G(x,\infty) = H(x,\infty) = 0 . \qquad (3.27)$$

Here η would be a similarity variable if $\Lambda = 0$, as in that case the boundary layer over horizontal isothermal semi-infinite plate is similar. Otherwise, the transformed momentum and energy equations remain a system of partial differential equations with $\frac{\partial}{\partial x}$ terms on the right hand side providing the major obstacle to the solution. We say this set of equations is in non-similar form, the non-similarity arising as a consequence to $\Lambda \neq 0$.

4. LOCAL NON-SIMILARITY MODEL

To correct the drawbacks of the local similarity model, Sparrow, Quack and Boerner [8], described a local non-similarity method for obtaining solutions of the non-similar boundary layer equations. This preserves the most attractive features of the local similarity model (that is, quasi odes and locally independent solutions), while retaining all of the non-similarity terms in the conservation equations. The

departure from local similarity is accounted for through a sequence of successive approximations as explained in [8]. Only terms in the equations subsidiary to the conservation equations are selectively neglected. This technique is particularly useful for solving problems in which many unknowns appear and for which forward marching technique needs considerable computation procedure in knowing the solution at downstream locations. Moreover, in this method, manipulation to introduce a finite difference expression is not necessary and the derived ordinary differential equations can be directly integrated numerically. The formulation of the system of equations for the local non-similarity models will proceed as follows. Taking

$$\Omega = \Lambda x^{3/5} \tag{3.28}$$

and

$$f = \frac{\partial F}{\partial x} \quad \text{and} \quad g = \frac{\partial G}{\partial x} \ , \tag{3.29}$$

the boundary layer equations and boundary conditions can be written as

$$F''' + \frac{3}{5} FF'' - \frac{1}{5} F'^2 + (\Omega + \frac{2}{5} \eta) G' - \frac{2}{5} G = x(g + F'f' - F''f) \ , \tag{3.30}$$

$$G''' + \frac{3}{5} \sigma FG'' = \sigma x(F'g' - G''f) \ , \tag{3.31}$$

$$F(x,0) = F'(x,0) = 0 \quad G'(x,0) = 1$$

and

$$F'(x,\infty) = G(x,\infty) = G'(x,\infty) = 0 \tag{3.32}$$

Differentiating the above set of equations and boundary conditions with respect to x and taking $Q_1 = \Lambda x^{-2/5}$ we get

$$f''' + \frac{3}{5} Ff'' - \frac{7}{5} F'f' + \frac{8}{5} F''f - \frac{7}{5} g + (\frac{2}{5}\eta + Q)g' + \frac{3}{5} Q_1 G' = x \frac{\partial}{\partial x} (g + F'f' - F''f) , \qquad (3.33)$$

$$g''' + \frac{3}{5} \sigma F g'' + \frac{8}{5} \sigma G''f - \sigma F'g' = \sigma x \frac{\partial}{\partial x} (F'g' - G''f) , \qquad (3.34)$$

$$f(x,0) = f'(x,0) = g'(x,0) = 0$$

and

$$f'(x,\infty) = g(x,\infty) = g'(x,\infty) = 0 \qquad (3.35)$$

F, f, G and g appear in the equations (3.30) to (3.35). If not for the presence of the term $x \frac{\partial}{\partial x}(g + F'f' - F''f)$ and $\sigma x \frac{\partial}{\partial x}(F'g' - G''f)$, these equations could be treated as ordinary differential equations and solved locally. To provide the desired local autonomy to equations (3.30), (3.31), (3.33) and (3.34), it is now assumed that the terms $x \frac{\partial}{\partial x} (g + F'f' - F''f)$ and $\sigma x \frac{\partial}{\partial x} (F'g' - G''f)$ can be dropped from these equations. This reduction is readily justifiable for x-values that are close to 0, whereas when x is not small, we can invoke the postulate that the dropped ones are small.

The philosophy behind the reduction is similar to that employed in deriving the local similarity model, but with a fundamental difference in the outcome. In the case of the

local similarity, it is postulated that for x not small, $g - fF'' + F'f'$ and $F'g' - G''f$ are small so that right hand side of (3.30) and (3.31) can be approximated by zero. Thus the approximation introduced leaves the boundary layer equations truncated. Whereas in the non-similarity model, the equations (3.30) and (3.31) are left intact and the approximation is introduced only in the subsidiary equations (3.33) and (3.34). Thus we can anticipate that local non-similarity method will yield accurate results for boundary layer characteristics than the local similarity model can give.

Thus the governing equations for local non-similarity model are now given by

(i) Equations (3.30), (3.31) and boundary conditions (3.32) and

(ii) approximating equations

$$f''' + \frac{3}{5} Ff'' - \frac{7}{5} F'f' + \frac{8}{5}F''f - \frac{7}{5}g + (\frac{2}{5}\eta + Q)g' + \frac{3}{5} Q_1 G' = 0 ,$$

$$g''' + \frac{3}{5} \sigma Fg'' + \frac{8}{5} \sigma G''f - \sigma F'g' = 0$$

and boundary conditions (3.35).

For a given Λ, Q and Q_1 would be known at any streamwise position x. Therefore, at a fixed streamwise position, x, Q and Q_1 may be regarded as known constants and equations (3.30), (3.31), (3.33) and (3.34) can be treated as a system of ordinary differential equations.

Solutions of such equations are straightforward by techniques regularly employed for similarity boundary layer equations. Equations (3.30), (3.31), (3.33) and (3.34) with boundary condition (3.32) and (3.35) constitute what is known as the two-equation local non-similarity model for our free convection problem. It represents the first stage in a succession of locally applicable multi-equation systems which are expected to provide increasingly accurate results.

We now derive the Three-equation model for the problem.

Put $$\bar{g} = \frac{\partial g}{\partial x} \quad \text{and} \quad \bar{f} = \frac{\partial f}{\partial x} \tag{3.36}$$

so that

$$x \frac{\partial}{\partial x} (g + F'f' - F''f) = x(\bar{g} - \bar{f}F'' + \bar{f}'F' - ff'' + f'^2)$$

and

$$\sigma x \frac{\partial}{\partial x} (F'g' - fG'') = \sigma x (f'g' - fg'' + F'\bar{g}' - \bar{f}G'')$$

Then differentiating (3.33), (3.34) and (3.35) with respect to x and taking $Q_2 = \Lambda x^{-7/5}$, we obtain

$$\bar{f}''' + \frac{3}{5}F\bar{f}'' - \frac{12}{5} F'\bar{f}' + \frac{13}{5} F''\bar{f} - \frac{12}{5} \bar{g} + (\frac{2}{5}\eta + Q)\bar{g}' + \frac{6}{5} Q_1 g'$$

$$- \frac{6}{25} Q_2 G' + \frac{16}{5} ff'' - \frac{12}{5} f'^2 = x \frac{\partial}{\partial x} (\bar{g} - \bar{f}F'' + \bar{f}'F' - ff'' + f'^2), \tag{3.37}$$

$$\bar{g}''' + \frac{3}{5} \sigma F\bar{g}'' + \frac{13}{5} \sigma \bar{f}G'' - 2\sigma(F'\bar{g}' + f'g') + \frac{16}{5} \sigma fg''$$

$$= \sigma x \frac{\partial}{\partial x}(f'g' - fg'' + F'\bar{g}' - \bar{f}G'') \tag{3.38}$$

$$\bar{f}(x,0) = \bar{f}'(x,0) = \bar{g}'(x,0) = 0,$$

$$\bar{f}'(x,\infty) = \bar{g}(x,\infty) = \bar{g}'(x,\infty) = 0. \qquad (3.39)$$

To make the system locally autonomous, we drop right hand sides of (3.36) and (3.37). On the other hand, all the terms in the transformed boundary layer equations (3.30) and (3.31) and in the first subsidiary equations (3.33) and (3.34) are retained. Since approximation is made in the secondarily subsidiary equations (3.37) and (3.38), the boundary layer characteristics should be even more accurate than those of the two-equation model.

Thus the three-equation model comprises of the following three sets of equations and their boundary conditions:

(i) equations (3.30) and (3.31) with boundary conditions (3.32)

(ii) equations (3.33) and (3.34) with boundary conditions (3.35)

and (iii) the approximating equations

$$\bar{f}''' + \frac{3}{5}F\bar{f}'' - \frac{12}{5}F'\bar{f}' + \frac{13}{5}F''\bar{f} - \frac{12}{5}\bar{g} + (\frac{2}{5}\eta + Q)\bar{g}' + \frac{6}{5}Q_1 g'$$

$$- \frac{6}{25}Q_2 G' + \frac{16}{5}ff'' - \frac{12}{5}f'^2 = 0 \qquad (3.40)$$

and

$$\bar{g}''' + \frac{3}{5}\sigma F\bar{g}'' + \frac{13}{5}\sigma\bar{f}G'' - 2\sigma F'\bar{g}' - 2\sigma f'g' + \frac{16}{5}\sigma fg'' = 0 \qquad (3.41)$$

with boundary conditions (3.39).

5. NUMERICAL SOLUTIONS

We have already seen that the application of non-similarity method of solution to this problem, the two and three-equation models give rise to four and six coupled equations respectively to be solved in each case as non-linear simultaneous equations. To initiate forward integration of the sets of equations in these two models requires N numerical values for the functions and their derivatives at $\eta = 0$ where N is the total order of the system of equations in each case. Thus, for example, for the three-equation model, a total of eighteen function and derivative values are needed at $\eta = 0$ but only nine of them are available from equations (3.32), (3.35) and (3.39). Therefore it was necessary to determine simultaneously the nine missing starting values. We are not aware of previously published boundary value problems where it has been solved for as many as nine simultaneously unknown starting values. Each of the systems of equations for the above forms of the local non-similarity method was solved by employing the Runga-Kutta integration scheme in conjunction with Newton-Raphson shooting method as modified by Nachtsheim and Swigert [6] so as to fulfill the boundary conditions at the edge of the boundary layer . By solving directly the original equations in these models through the initial value technique, we retain the main feature of local non-similarity method that no approximation is made in the conservation

equations. This is in sharp contrast to the numerical method of solution, namely the selected points method of Lanczos, used by Jones where it is necessary to go in for linearized form of the conservation equations at each location of the downstream flow. Also, unlike his numerical method of solution where the downstream region is to be covered in steps, these local non-similarity forms offer scope to solve the problem at any downstream point independently of the other when the estimates of the missing wall conditions there, are available. But, because of the highly non-linear character of the sets of equations in the two forms of the local non-similarity method, it was essential to have good initial estimates of the missing wall values to enable us to integrate the sets of equations in these two models. We obtained good estimates of missing wall conditions for the two-equation model by considering the reduced linear boundary value problem obtained after dropping off non-linear terms in this model. The solution of the linearized problem thus obtained is

$$F(\eta) = \frac{1}{300\eta_\infty}\left(2 - \frac{1}{\eta_\infty}\right)\eta^5 + \frac{Q}{24\eta_\infty}\eta^4 - \frac{1}{6}\left(\frac{1}{5}\eta_\infty + Q\right)\eta^3 + \frac{1}{30}\eta_\infty^2\eta^2 + \frac{1}{6}\eta_\infty\left(\frac{1}{20} + Q\right)\eta^2$$

$$G(\eta) = \eta - \frac{1}{2}\eta_\infty - \frac{1}{2\eta_\infty^2}\eta^2$$

$$f(\eta) = \frac{1}{10} Q_1 \eta_\infty \left(2\eta - 3 \frac{1}{\eta_\infty} \eta^2 + \frac{1}{\eta_\infty^2} \eta^3\right),$$

$$g(\eta) = 0,$$

where η_∞ is an arbitrarily guessed value for the edge of the boundary layer η_e. At the downstream location $x = 0.1$, when $\Lambda = 1$, the initial guesses for $\eta_\infty = 1$ are

$$F''(x,0) = 0.160706, \quad G(x,0) = -0.5, \quad G'(x,0) = -1.0,$$

$$f''(x,0) = 0.50238, \quad g(x,0) = g''(x,0) = 0.$$

We used these initial values to integrate the non-linear equations of the Two-equation model across the boundary layer region in steps by successively increasing the range of integration until the correct missing wall conditions and the edge of the boundary layer are found by some convergence criterion. The solution is taken to be convergent if the boundary conditions and the edge of the boundary layer are found by some convergence criterion. The solution is taken to be convergent if the boundary conditions

$$|F''(x,\infty)|, \ |G(x,\infty)|, \ |G'(x,\infty)| < 5 \times 10^{-4}$$

and

$$|f''(x,\infty)|, \ |g(x,\infty)|, \ |g'(x,\infty)| < 5 \times 10^{-3}$$

are all satisfied simultaneously. Once this is done at $x = 0.1$, the resulting solution provides good initial estimates of wall values for other streamwise locations

and the initial value techniques can be used to solve the corresponding non-linear boundary value problem.

In solving the non-linear boundary value problem for the three-equation model at any streamwise location it was necessary to obtain very good initial estimates for the nine missing wall conditions which allow integration of the equations in the model over some interval $[0,\eta_\infty]$ across the boundary layer region. We generated these estimates by applying quasilinearization process [7] to the non-linear boundary value problem in this model. Before proceeding to give an outline of this numerical technique, we shall first write

$$\vec{Y} = (F,F',F'',G,G',G'',f,f',f'',g,g',g'',\bar{f},\bar{f}',\bar{f}'',\bar{g},\bar{g}',\bar{g}'')$$

The essential idea in applying this technique is that given one approximate solution $\bar{Y}_i$ to the system, we approximate the differential equation for $\vec{Y}$ near $\vec{Y}_i$ by the linear differential equation in $\vec{Y}_{i+1}$. These are

$$F'''_{i+1} + (\tfrac{3}{5} F_i + xf_i) F''_{i+1} - (\tfrac{2}{5} F'_i + xf_i) F'_{i+1} + \tfrac{3}{5} F''_i F_{i+1} - \tfrac{2}{5} G_{i+1}$$

$$+ (\tfrac{2}{5}\eta + Q) G'_{i+1} + xF''_i f_{i+1} - xF'_i f'_{i+1} - xg_{i+1}$$

$$= (\tfrac{3}{5} F_i + xf_i) F''_i - xF'_i f'_i - \tfrac{1}{5} (F'_i)^2 \quad ,$$

$$\tfrac{1}{\sigma} G'''_{i+1} + (\tfrac{3}{5} F_i + xf_i) G''_{i+1} + \tfrac{3}{5} G''_i F_{i+1} - xg'_i F'_{i+1} + xG''_i f_{i+1} - xF'_i g'_{i+1}$$

$$= \tfrac{3}{5} F_i G''_i + xG''_i f_i - xF'_i g'_i \quad .$$

$$f'''_{i+1} + \left(\frac{3}{5} F_i + \frac{8}{5} f_i + x\bar{f}_i\right)F''_{i+1} - \left(\frac{7}{5} f'_i + x\bar{f}'_i\right) F'_{i+1} + \frac{3}{5} F''_i F_{i+1}$$

$$+ \frac{3}{5} Q_1 G'_{i+1} + \left(\frac{8}{5} F''_i + xf''_i\right) f_{i+1} - \left(\frac{7}{5} F'_i + 2xf'_i\right) f'_{i+1} + xf_i f''_{i+1}$$

$$- \frac{7}{5} g_{i+1} + \left(\frac{2}{5}\eta + Q\right) g'_{i+1} + xF''_i \bar{f}_{i+1} - xF'_i \bar{f}'_{i+1} - x\bar{g}_{i+1}$$

$$= \frac{3}{5} F''_i F_i + \frac{8}{5} F''_i f_i + xf_i f''_i - \frac{7}{5} f'_i F'_i - x\left(f'_i\right)^2$$

$$+ xF''_i \bar{f}_i - xF'_i \bar{f}'_i \,,$$

$$\frac{1}{\sigma} g'''_{i+1} + \frac{3}{5} g''_i F_{i+1} - \left(g'_i + x\bar{g}_i\right)F'_{i+1} + \left(\frac{8}{5} f_i + x\bar{f}_i\right) G'_{i+1} + \left(\frac{8}{5} G''_i + xg''_i\right) f_{i+1}$$

$$- x g'_i f'_{i+1} - \left(F'_i + xf'_i\right) g'_{i+1} + \left(\frac{3}{5} F_i + xf_i\right) g'_{i+1} + xG'_i \bar{f}_{i+1}$$

$$- x F'_i \bar{g}_{i+1} = \frac{8}{5} f_i G''_i - g'_i F'_i - xg'_i f'_i + \frac{3}{5} g''_i F_i$$

$$+ xf_i g''_i + xG''_i \bar{f}_i - xF'_i \bar{g}'_i \,,$$

$$\bar{f}'''_{i+1} + \frac{3}{5} \bar{f}''_i F_{i+1} - \frac{12}{5} \bar{f}'_i F'_{i+1} + \frac{13}{5} \bar{f}_i F''_{i+1} - \frac{6}{25} Q_2 G'_{i+1} + \frac{16}{5} f''_i f_{i+1}$$

$$- \frac{24}{5} f'_i f'_{i+1} + \frac{16}{5} f_i f''_{i+1} + \frac{6}{5} Q_1 g'_{i+1} + \frac{13}{5} F''_i \bar{f}_{i+1} - \frac{12}{5} F'_i \bar{f}'_{i+1}$$

$$+ \frac{3}{5} F_i \bar{f}''_{i+1} - \frac{12}{5} \bar{g}_{i+1} + \left(\frac{2}{5}\eta + Q\right)\bar{g}'_{i+1}$$

$$= \frac{12}{5} \left(f'_i\right)^2 - \frac{16}{5} f_i f''_i + \frac{13}{5} F''_i \bar{f}_i - \frac{12}{5} \bar{f}'_i F'_i - \frac{3}{5} F_i \bar{f}''_i \,,$$

$$\frac{1}{\sigma}\bar{g}''_{i+1} + \frac{3}{5}\bar{g}''_i F_{i+1} - 2\bar{g}'_i F_{i+1} + \frac{13}{5}\bar{f}_i G''_{i+1} + \frac{16}{5} g''_i f_{i+1}$$

$$-2g'_i f'_{i+1} - 2f'_i g'_{i+1} + \frac{16}{5} f_i g''_{i+1} + \frac{13}{5} G''_i \bar{f}_{i+1} - 2F'_i \bar{g}_{i+1} + \frac{3}{5} F_i \bar{g}''_{i+1}$$

$$= -2f'_i g'_i + \frac{16}{5} g''_i f_i + \frac{13}{5} G''_i \bar{f}_i - 2F'_i \bar{g}'_i + \frac{3}{5} F_i \bar{g}''_i \quad , \qquad (3.42)$$

The linearized equations comprise a linear two-point boundary value problem for $\vec{Y}_{i+1}$ along with boundary conditions

$$F_{i+1}(x,0) = F'_{i+1}(x,0) = 0 \ , \ G'_{i+1}(x,0) = 1$$

$$f_{i+1}(x,0) = f'_{i+1}(x,0) = g'_{i+1}(x,0) = 0$$

$$\bar{f}_{i+1}(x,0) = \bar{f}'_{i+1}(x,0) = \bar{g}'_{i+1}(x,0) = 0$$

and

$$F'_{i+1}(x,\infty) = G_{i+1}(x,\infty) = G_{i+1}(x,\infty) = 0$$

$$f'_{i+1}(x,\infty) = g_{i+1}(x,\infty) = g'_{i+1}(x,\infty) = 0$$

$$\bar{f}'_{i+1}(x,\infty) = \bar{g}_{i+1}(x,\infty) = \bar{g}'_{i+1}(x,\infty) = 0 \qquad (3.43)$$

As usual with Newton's method, the hope is that the sequence of functions

$\vec{Y}_o, \vec{Y}_1, \cdots \vec{Y}_i, \cdots$ converge to $\vec{Y}$, solving the original problem. Thus, we have reduced the original non-linear boundary value problem to the transformed problem: solve

a sequence of linear boundary value problem for $\vec{Y}_o, \vec{Y}_1, \cdots$ converging to $\vec{Y}$. From the equations (3.42) it is clear that out of 18 boundary conditions required only 9 are prescribed at $\eta = 0$. As described in Chapter II, we proceed by assuming the solution into 10 linear parts, 9 of which are complementary solutions and one is a particular solution. Complementary solutions are obtained by dropping non-homogeneous terms from the equations and assuming one of the unknowns as unity and the rest zero at a time. The particular solution is obtained by retaining the non-homogeneous terms and taking all the unknown conditions as zero. Then the solution $\vec{Y}$ is given by

$$\vec{Y}_{i+1} = \sum_{r=1}^{9} C_r \vec{Y}_{h_r} + \vec{Y}_p$$

where $\vec{Y}_{h_r}$, r = 1 to 9, are complementary solutions and $\vec{Y}_p$ the particular solution. The constants C_r(r = 1 to 9) can be obtained by satisfying 9 boundary conditions at η_e. To start the quasilinearization process at the downstream location $x = 1.0$ when $\Lambda = 1.0$, we supplied the initial profile by combining the solution for F, G, f, g as given by the two-equation model at that location together with $\bar{f} = \bar{g} = 0$ over the interval of integration $[0,1]$. If the maximum of the absolute difference between the two trial solutions for the missing initial conditions is greater than $\varepsilon = 10^{-6}$, the process is repeated till the desired accuracy is achieved. From Table1(a),we note that the iterative process converged in only 3 trials. We then form the initial profile

$\vec{Y}_o$ for an application of the technique for the extended interval $[0,2]$ by combining the stored final trial solution $\vec{Y}_F$ over $[0,1]$ with $\vec{Y}_o(\eta) = \vec{Y}_F(1)$ for $1 \leq \eta \leq 2$. We observe again from Table1(b)that the quasilinearization process converged for the same ε in 5 trials. With the final trial values for missing wall conditions thus obtained in quasilinearization process, we now switch over to the initial value technique and solve the non-linear boundary value problem for the three-equation model at $x = 1.0$ when $\Lambda = 1.0$. The initial value technique is taken to converge if

$$|F''(x,\infty)|,\ |G(x,\infty)|,|G'(x,\infty)| \leq 5 \times 10^{-4}$$

$$|f''(x,\infty)|,\ |g(x,\infty)|,|g'(x,\infty)| \leq 5 \times 10^{-3},$$

and

$$|\bar{f}''(x,\infty)|,\ |\bar{g}(x,\infty)|,|\bar{g}'(x,\infty)| \leq 5 \times 10^{-2}$$

are all satisfied simultaneously. The solution thus obtained at $x = 1.0$ was used to solve by initial value technique at other location and the process is thus extended to all other streamwise locations. Our numerical experimentation shows that the computer time taken at any location in the streamwise direction to solve the three-equation model is very large in comparison with that for the two-equation model. Moreover, as will be seen in the next section, the two-equation model gives result for temperature distribution and heat transfer rate very accurately while the skin friction and velocity

distribution are of accuracy somewhat enough for the purposes of engineering applications. Hence we found solutions to the two-equation model only for other cases $\Lambda = -1$ and $\Lambda = 1$ when $\sigma = 0.72$, 1.0 and $\sigma = 1.0$ respectively.

6. RESULTS AND DISCUSSION

Numerical results were obtained for Prandtl numbers 0.72 and 1.0 when $\Lambda = 1.0$ and -1.0. The numerical values of missing wall conditions for the two and three-equation models are listed in Tables 2,3,4,5,6. The tabulated information has been used for the preparation of graphs which depict the trend for skin-friction and heat-transfer variations at the surface in the streamwise distance x from the leading edge of the plate.

First, we shall consider the case when $\Lambda = 1$. Figures 1 and 2 show skin-friction and heat-transfer at the plate as a function of x. The results from the three-equation model are seen to be in close agreement with those from the Selected Points method of Lanczos. The two-equation model, on the other hand, is observed to provide results that are enough for practical purposes in engineering applications. We note here that near the leading edge, the results from the two and three-equation models agree well among themselves and with the series solution of Jones. The skin-friction trends as predicted by the local non-similarity method of solution

for $\sigma = 0.72$ and 1.0 are consistent with the expected effects of buoyancy force after a short distance x in downstream of the flow. This component of buoyancy force modifies the shear stress at the wall at a short distance x in the sense that the decreasing values for skin-friction near the leading edge of the inclined plate starts increasing as seen from the figure 1. An inspection of the same figure also reveals that at a fixed point x the buoyancy force is seen to have a larger influence on the friction factor for $\sigma = 0.72$ than for $\sigma = 1.0$. This is only to be expected as air is comparatively of lesser density and hence greatly sensitive to buoyancy force effect, thereby causing large changes in velocity gradients at the wall which is thus reflected in the wall shear results. Also shown in figure 1(b) are results for large downstream distances and the series solution results at those locations as obtained by Jones are also included for comparison. It is seen that there is a good agreement between results from our method of analysis and the series expansion in this region also.

Within the scale of the figure, the results from the two and three-equation models for heat transfer coefficient at various streamwise locations are indistinguishable and therefore they are plotted as a single curve in figure 2. The agreement between results from local non-similarity and selected points method as seen from the figure 2 indicates

the high accuracy of our method of solution. Also, at large downstream distances, the series result coincides with that given by the local non-similarity method. (see fig. 2b) The close agreement of results for skin-friction and heat-transfer between our method of solution and that used by Jones is somewhat remarkable and quite surprising. It is thus shown that the non-similar equations formulated on the basis of a horizontal scale, when analysed by the local non-similarity method of solution predicts with reasonable accuracy the boundary layer characteristics of the flow in the entire region as covered here. Again, an inspection of the figure indicates that the heat transfer rate at the surface for $\sigma = 1.0$ is larger than that for air. This is because as the Prandtl number increases the thermal layer thickness decreases and the surface temperature gradient increases which results in a high rate of heat transfer from the surface.

Representative velocity and temperature profiles for several values of x for $\sigma = 0.72$ and 1.0 are shown in figures (3:12). The velocity gradient at the wall increases in downstream direction of the flow. This is accompanied by increase in velocity near the surface and decrease in thickness of the velocity layer. The results of the present analysis are compared with those of Jones in figures 11 and 12, the coordinates of the figure being those interpreted

in terms of that author. In terms of the present analysis, the ordinate and abscissa groupings may be written as

$$\bar{\eta} = x^{3/20}\eta \quad , \quad \bar{F}_{\bar{\eta}} = x^{-3/10} F_{\eta}$$

The velocity profile calculated in the two-equation model at $x = 4.5$ is seen to agree satisfactorily with that given by using the selected points method of Lanczos for the non-similar formulation of the problem, wherein the neglect of induced pressure effects has been assumed. In our coordinate system, we find the agreement between the three-equation model and the selected points method of Lanczos for the velocity profile at $x = 10.0$ is highly satisfactory as seen from figure 10. Also seen in the same figure is that the three-equation model somewhat over corrects the two-equation model and provide results of significantly greater accuracy.

With regard to temperature profiles, the temperature gradient at the wall is seen to increase as x increases with an accompanying decrease in the thermal layer thickness. It is noted from figure 9 that the temperature gradient at the wall for $\sigma = 1.0$ is somewhat steeper than that for $\sigma = 0.72$ as is to be expected. Since the two and three-equation models predict temperature distributions which are almost identical, we plotted this as a single curve at $x = 4.5$ in terms of Jones variables (see figure 12). The comparison of results from the local non-similarity with the

Jones results shows very good agreement and thus the capability of the local non-similarity method to predict boundary layer characteristics is again supported.

We shall now examine the free convection phenomena when the angle of inclination of the plate is negative and given by $\Lambda = -1$. For this case, the buoyancy force component along the surface now opposes the motion and hence both the Nusselt number and skin-friction factor decrease in down-stream direction of the flow as seen from figure 13 and 14 and ultimately the flow separates. The two-equation model predicts this point of separation at $x = 3.65$ for $\sigma = 0.72$ and $x = 3.15$ for $\sigma = 1.0$. It is noted from the figure 13 that the separation of the flow is not accompained by any singularity. But the numerical method converges near separation point only after a large number of iterations than that is required in the region near the leading edge of the plate. Analogous to the characteristic behaviour near the separation point - the skin friction and heat transfer coefficient were found to behave in a regular manner - was also encountered in other boundary layer studies such as in the study of interaction between a laminar boundary layer and a moderately strong shock [9] and also in the study based upon an incompressible boundary layer calculation where it is insisted that the displacement thickness associated with the boundary layer behaves regularly at separation [10].

Contrary to this findings for flow under consideration, most boundary layer calculations including those with heat transfer exhibit singular behaviour at the point of zero skin-friction. This was the case for the mixed convection flow over an isothermal vertical plate placed in a uniform stream parallel to it with buoyancy force opposing the motion. Merkin [11] has shown that the skin-friction behaves like $\sqrt{x_s - x}$ near the separation point x_s. This is the classical singular behaviour to be expected when there is no heat transfer. Also Buckmaster, [12], has proved analytically that when there is heat transfer at a plate cooler than the fluid outside the boundary layer and the pressure gradient is prescribed, then a singularity of the type $\sqrt{x_s - x}\ \log\ (x_s - x)$ may be expected. In the light of these discussions, it is no wonder that the local non-similarity method as applied to this problem can go up to separation point unlike in the case of forced flow over a circular cylinder [8]. While the selected point method of Lanczos predicts the point of separation of the flow for air at $x = 3.704$, our method of solution puts it at $x = 3.65$ and thus deviating from exact result just by $1\frac{1}{2}$ per cent only.

The velocity and temperature profiles in this case, $\Lambda = -1$, are shown in figures 15-22 for several values of x and $\sigma = 0.72$ and 1.0. The effects of opposing buoyancy force on the fluid motion is to reduce the velocities and

the velocity gradients at the wall in the downstream direction. The velocity profiles corresponding to the locations $x = 3.65$ and $x = 3.15$ for $\sigma = 0.72$ and 1.0 respectively are typical of that which is obtained at the point of separation. With regard to temperature profiles, the temperature gradient at the wall now decreases with accompanying increase in the thermal boundary layer thickness for increasing downstream distances.

Table 1

Convergence history of quasilinearization process applied to the three-equation model at $x = 1.0$ and $\sigma = 0.72$

1(a) Interval of integration $[0,1]$:

Missing wall values at $\eta = 0$	Trial Number		
	1	2	3
$F''(x,0)$	0.582515	0.582444	0.582443
$G(x,0)$	-0.506109	-0.506795	-0.506796
$G''(x,0)$	-1.011215	-1.009053	-1.009052
$f''(x,0)$	0.147377	0.148055	0.148055
$g(x,0)$	0.001001	0.000674	0.000674
$g''(x,0)$	-0.003494	-0.002439	-0.002439
$\bar{f}''(x,0)$	-0.030106	-0.030003	-0.030003
$\bar{g}(x,0)$	-0.000183	-0.000305	-0.000305
$\bar{g}''(0)$	0.000659	0.001095	0.001095

1(b) Interval of integration [0,2]

Missing wall values at $\eta = 0$	Trial Number				
	1	2	3	4	5
$F''(x,0)$	1.133427	1.172933	1.173112	1.173112	1.173112
$G(x,0)$	-0.904286	-0.948659	-0.948649	-0.948649	-0.948648
$G''(x,0)$	-0.596535	-0.557730	-0.557663	-0.557664	-0.557664
$f''(x,0)$	0.220240	0.232218	0.231951	0.231953	0.231954
$g(x,0)$	0.019520	0.011932	0.011946	0.011945	0.011945
$g''(x,0)$	-0.018744	-0.012028	-0.012005	-0.012005	-0.012005
$\bar{f}''(x,0)$	-0.038858	-0.044931	-0.044745	-0.044745	-0.044746
$\bar{g}(x,0)$	-0.009545	-0.005668	-0.005615	-0.005615	-0.005616
$\bar{g}''(x,0)$	0.008501	0.005210	0.005161	0.005161	0.005162

Table 2

Missing wall values for the two-equation model at various streamwise locations when $\Lambda = 1.0$ and $\sigma = 0.72$

x	$F''(x,0)$	$G(x,0)$	$G'(x,0)$	$f''(x,0)$	$g(x,0)$	$g'(x,0)$
0.01	1.012956	-1.719960	-0.360899	1.724501	0.753051	-0.186420
0.05	1.069364	-1.696415	-0.366502	0.907459	0.378576	-0.095723
0.10	1.116645	-1.677632	-0.371126	0.688496	0.276625	-0.071170
0.35	1.272207	-1.620259	-0.385624	0.454658	0.166785	-0.044162
0.50	1.342495	-1.596513	-0.391889	0.361759	0.123178	-0.034248
0.95	1.513424	-1.543596	-0.406458	0.278862	0.084736	-0.024862
1.0	1.529997	-1.538736	-0.407811	0.273060	0.082115	-0.024214
1.5	1.680533	-1.497327	-0.419839	0.230984	0.063333	-0.019518
2.0	1.810740	-1.464564	-0.429767	0.204758	0.052066	-0.016637
2.5	1.927391	-1.437320	-0.438322	0.186252	0.044410	-0.014637
3.5	2.133092	-1.393490	-0.452706	0.161074	0.034513	-0.011979
4.5	2.313399	-1.358878	-0.464654	0.144211	0.028308	-0.010253
5.0	2.396558	-1.343969	-0.469977	0.137598	0.025985	-0.009591
6.0	2.551901	-1.317677	-0.479260	0.126757	0.022328	-0.008526
8.0	2.829239	-1.275195	-0.495994	0.111112	0.017421	-0.007043
10.0	3.074487	-1.241664	-0.509654	0.100127	0.014266	-0.006045
12.0	3.296487	-1.214052	-0.521440	0.091848	0.012064	-0.005321
14.0	3.500643	-1.190646	-0.531842	0.085311	0.010438	-0.004768
16.0	3.690517	-1.170367	-0.541174	0.079976	0.009188	-0.004329
18.0	3.868646	-1.152512	-0.549652	0.075512	0.008198	-0.003972
20.0	4.036892	-1.136586	-0.557431	0.071704	0.007394	-0.003675
25.0	4.422832	-1.103071	-0.574515	0.064192	0.005922	-0.003111

Table 3

Missing wall values for the three-equation model at various streamwise locations when $\Lambda = 1.0$ and $\sigma = 0.72$

3(a)

Missing wall values	x				
	0.01	0.05	0.35	0.95	1.0
$F''(x,0)$	1.011986	1.065471	1.263427	1.497710	1.5139758
$G(x,0)$	-1.720237	-1.715802	-1.622007	-1.545579	-1.540737
$G''(x,0)$	-0.360887	-0.362808	-0.385377	-0.406105	-0.407474
$f''(x,0)$	1.869169	0.978137	0.454658	0.304145	0.297836
$g(x,0)$	0.829650	0.419790	0.166785	0.095255	0.092318
$g''(x,0)$	-0.201031	-0.101215	-0.044162	-0.027186	-0.026478
$\bar{f}''(x,0)$	-54.410390	-5.647714	-0.371913	-0.093376	-0.087040
$\bar{g}(x,0)$	-23.711487	-2.558342	-0.178260	-0.044936	-0.041819
$\bar{g}''(x,0)$	6.154328	0.635890	0.044219	0.011178	0.010414

3(b)

Missing wall values	x				
	2.0	3.0	4.5	5.0	10.0
$F''(x,0)$	1.782448	2.006773	2.281138	2.515875	3.031266
$G(x,0)$	-1.483585	-1.414805	-1.358816	-1.316811	-1.239290
$G''(x,0)$	-0.424620	-0.445793	-0.464810	-0.480017	-0.510572
$f''(x,0)$	0.221720	0.187483	0.1565577	0.137270	0.107781
$g(x,0)$	0.058825	0.043658	0.031723	0.024914	0.015746
$g''(x,0)$	-0.017794	-0.014386	-0.011194	-0.009285	-0.006540
$\bar{f}''(x,0)$	-0.033752	-0.019734	-0.011505	-0.007849	-0.003966
$\bar{g}(x,0)$	-0.015539	-0.003841	-0.004538	-0.002862	-0.001217
$\bar{g}''(x,0)$	0.003876	0.001073	0.001252	0.000820	0.000379

3(c)

Missing wall values	x				
	12.0	14.0	16.0	18.0	20.0
$F''(x,0)$	3.250478	3.452147	3.639764	3.815818	3.982125
$G(x,0)$	-1.211157	-1.187328	-1.166708	-1.148574	-1.132414
$G''(x,0)$	-0.522571	-0.533159	-0.542656	-0.551283	-0.559196
$f''(x,0)$	-0.098623	0.091401	0.085517	0.080601	0.076415
$g(x,0)$	0.013252	0.011417	0.010012	0.008902	0.008004
$g''(x,0)$	-0.005741	-0.005131	-0.004648	-0.004256	-0.003931
$\bar{f}''(x,0)$	-0.003101	-0.002516	-0.002097	-0.001784	-0.001542
$\bar{g}(x,0)$	-0.000886	-0.000675	-0.000531	-0.000429	-0.000353
$\bar{g}''(x,0)$	0.000286	0.000224	0.000181	0.000150	0.000127

Table 4

Missing wall values for the two-equation model at various streamwise locations when $\Lambda = 1.0$ and $\sigma = 1.0$

x	F''(x,0)	G(x,0)	G'(x,0)	f''(x,0)	g(x,0)	g'(x,0)
0.01	0.897840	-1.556704	-0.394791	1.662952	0.762325	-0.225220
0.05	0.952344	-1.533030	-0.401577	0.875860	0.381551	-0.115461
0.10	0.997883	-1.514165	-0.407106	0.664845	0.277932	-0.085758
0.35	1.148327	-1.457100	-0.424540	0.403675	0.148450	-0.048685
0.75	1.313259	-1.402417	-0.442347	0.297050	0.096073	-0.033511
0.9	1.365020	-1.386699	-0.447686	0.275809	0.085873	-0.030508
1.0	1.397551	-1.377138	-0.450985	0.264179	0.080349	-0.028870
2.0	1.668790	-1.305718	-0.476958	0.198017	0.050219	-0.019710
2.5	1.781351	-1.279797	-0.487019	0.180057	0.042612	-0.017299
3.0	1.884238	-1.257697	-0.495893	0.166433	0.037076	-0.015504
3.5	1.979606	-1.238433	-0.503863	0.155602	0.032845	-0.014103
4.5	2.153136	-1.206048	-0.517789	0.139214	0.026771	-0.012034
5.0	2.33085	-1.192163	-0.523975	0.132786	0.024509	-0.011242
6.0	2.382333	-1.167790	-0.535165	0.122248	0.020965	-0.009972
7.5	2.585286	-1.137501	-0.549700	0.110309	0.017215	-0.008579
10.0	2.883433	-1.097999	-0.567800	0.096376	0.013232	-0.007026
12.0	3.095916	-1.072863	-0.583328	0.088341	0.011144	-0.006171
15.0	3.383422	-1.042151	-0.600712	0.079294	0.008986	-0.005249
17.5	3.601155	-1.021040	-0.613251	0.073523	0.007722	-0.004684
20.0	3.803352	-1.002860	-0.624460	0.068824	0.006760	-0.004240

Table 5

Missing wall values for the two-equation model at various streamwise locations when $\Lambda = -1.0$ and $\sigma = 0.72$

x	$F''(x,0)$	$G(x,0)$	$G'(x,0)$	$f''(x,0)$	$g(x,0)$	$g'(x,0)$
0.01	0.943830	-1.750323	-0.353826	-1.719238	-0.795719	0.191783
0.05	0.887897	-1.776237	-0.347923	-0.900073	-0.437562	0.103122
0.1	0.841584	-1.798698	-0.342903	-0.679722	-0.344704	0.079693
0.2	0.772022	-1.834286	-0.335747	-0.511752	-0.277228	0.062213
0.55	0.605718	-1.929735	-0.315390	-0.333371	-0.214694	0.044624
1.0	0.456267	-2.030749	-0.295935	-0.253277	-0.195101	0.037544
2.0	0.228145	-2.222106	-0.262401	-0.173744	-0.187952	0.031515
2.5	0.144948	-2.305768	-0.248838	-0.149781	-0.189038	0.029916
3.0	0.075563	-2.381886	-0.236951	-0.130560	-0.190945	0.028689
3.5	0.17220	-2.45035	-0.226594	-0.114546	-0.193116	0.027695
3.6	0.00668	-2.46309	-0.22469	-0.11166	-0.19355	0.02752
3.65	0.00125	-2.46923	-0.22370	-0.11034	-0.19377	0.02745

Table 6

Missing wall values for the two-equation model at various streamwise locations when $\Lambda = -1.0$ and $\sigma = 1.0$

x	$F''(x,0)$	$G(x,0)$	$G'(x,0)$	$f''(x,0)$	$g(x,0)$	$g'(x,0)$
0.01	0.831200	-1.587410	-0.386230	-1.655614	-0.809931	0.232119
0.1	0.732990	-1.636616	-0.373036	-0.652926	-0.353640	0.096678
0.2	0.666422	-1.672996	-0.363666	-0.490486	-0.285961	0.075578
0.55	0.508456	-1.771033	-0.339859	-0.317114	-0.224295	0.054337
1.0	0.368555	-1.874817	-0.316634	-0.238451	-0.205926	0.045732
1.5	0.251956	-1.976660	-0.295481	-0.191185	-0.200758	0.041099
2.0	0.160522	-2.068045	-0.277639	-0.159536	-0.200465	0.038241
2.5	0.086696	-2.149706	-0.262430	-0.135806	-0.201903	0.036207
2.75	0.054921	-2.186870	-0.255688	-0.125898	-0.202881	0.035386
3.0	0.026692	-2.219176	-0.250236	-0.117154	-0.203735	0.034678
3.15	0.009902	-2.241192	-0.245980	-0.112070	-0.204562	0.034267

REFERENCES

[1] Rotem, Z. and Claassen, L. , J. Fluid Mech., 39, 173-192, (1969).

[2] Stewartson, K., Z.A.M.P., 9a, 276-282, (1958).

[3] Gill, W.N., Zeh, D.W. and del-casal, E., ibid 16, 539-541, (1965).

[4] Jones, D.R., Quart. J. Mech. Appl. Math., 26, 77-98, (1973).

[5] Pera, L. and Gebhart, B., Int. J. Heat Mass Transfer, 16, 1131-1146, (1973).

[6] Nachtsheim, P. R. and Swigert, P., Development of Mechanics, 1, 361-367, (1965).

[7] Roberts, S.M. and Shipman, J.S., Two-point Boundary Value Problems: Shooting methods, American Elsevier, New York, 87 -107 (1972).

[8] Sparrow, E.M., Quack, H., and Boerner, C.J., AIAA J1 8, 1936-1942, (1970).

[9] Stewartson, K. and Williams, P.G., Proc. R. Soc. A312, 181-206, (1969).

[10] Catherall, D., and Mangler, K.W., J. Fluid Mech., 26, 163-182, (1966).

[11] Merkin, J.H., ibid 35, 439-450 (1969).

[12] Buckmaster, J., ibid 44, 237-247, (1970).

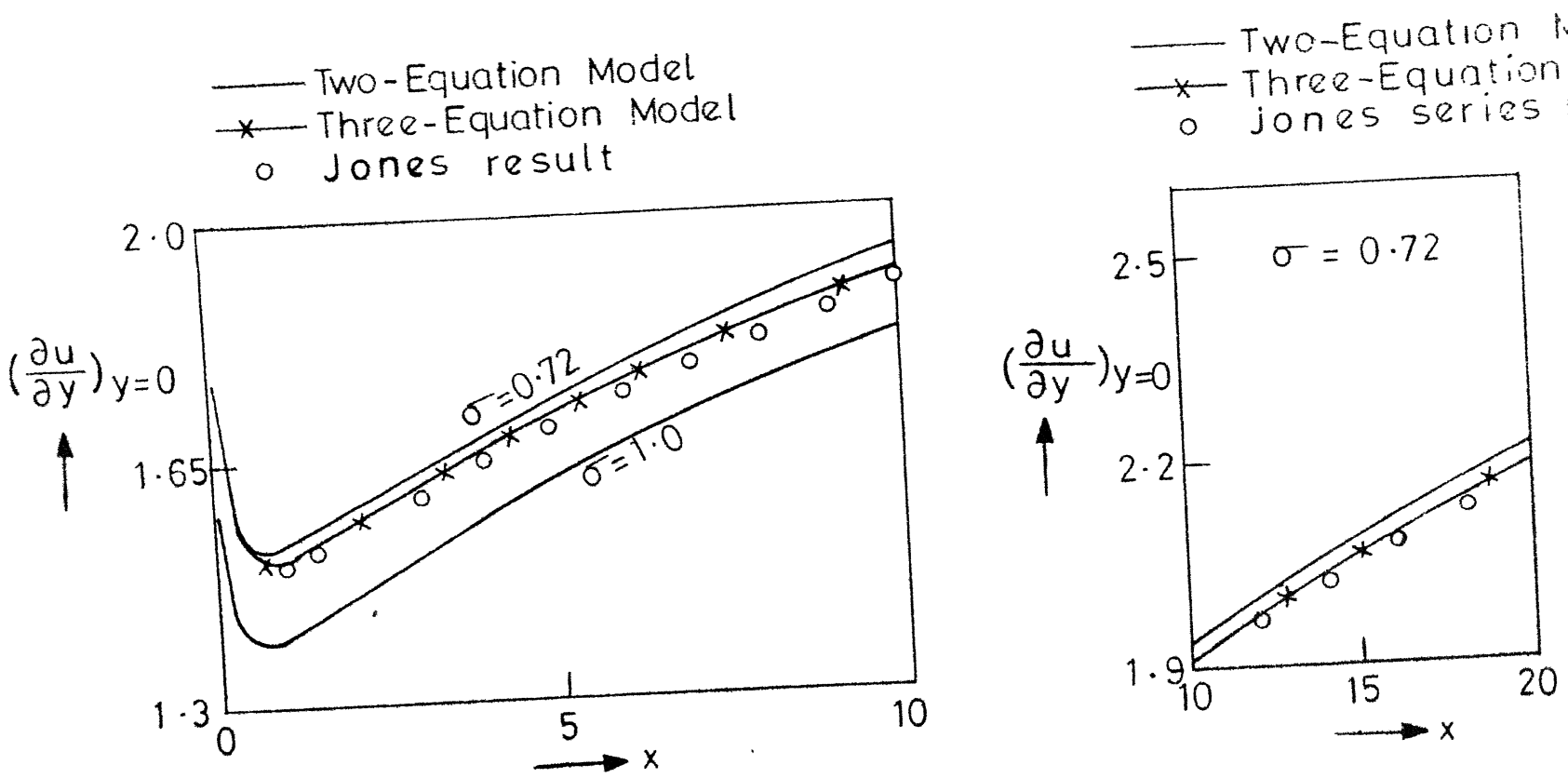

Fig.1 Variation of skin-friction with x when $\Lambda = 1 \cdot 0$.

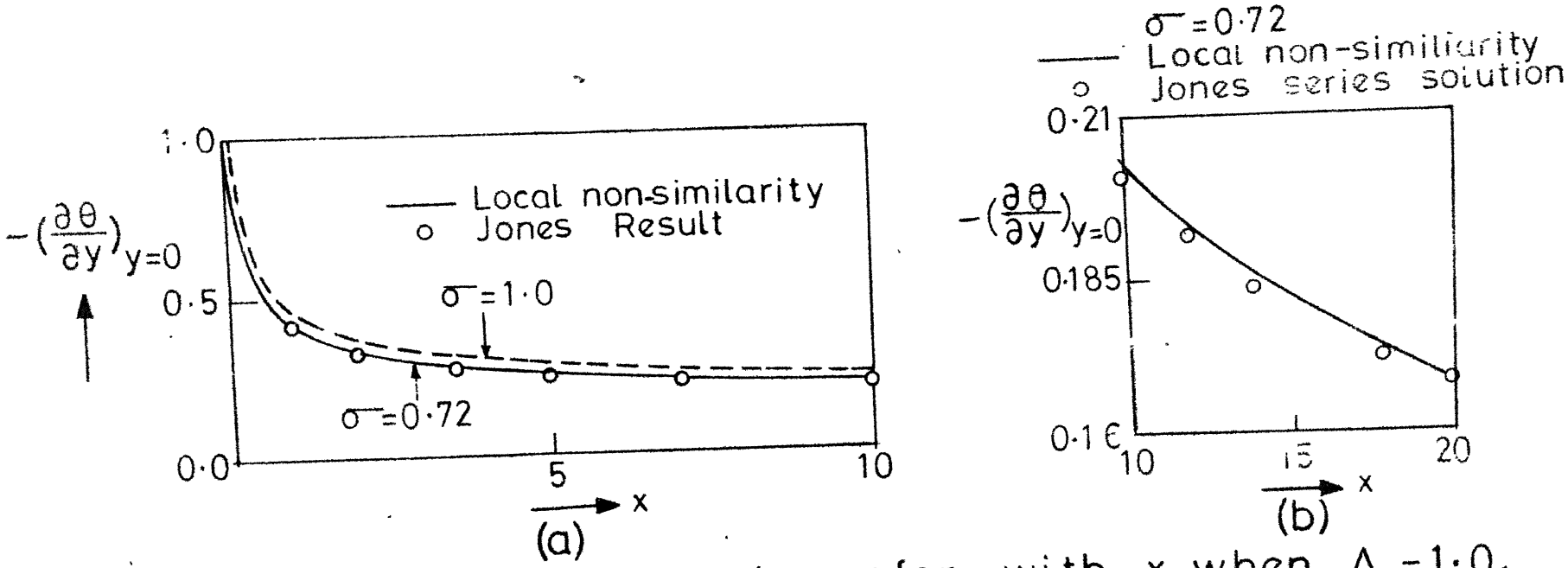

Fig. 2 Variation of heat transfer with x when $\Lambda = 1\cdot0$.

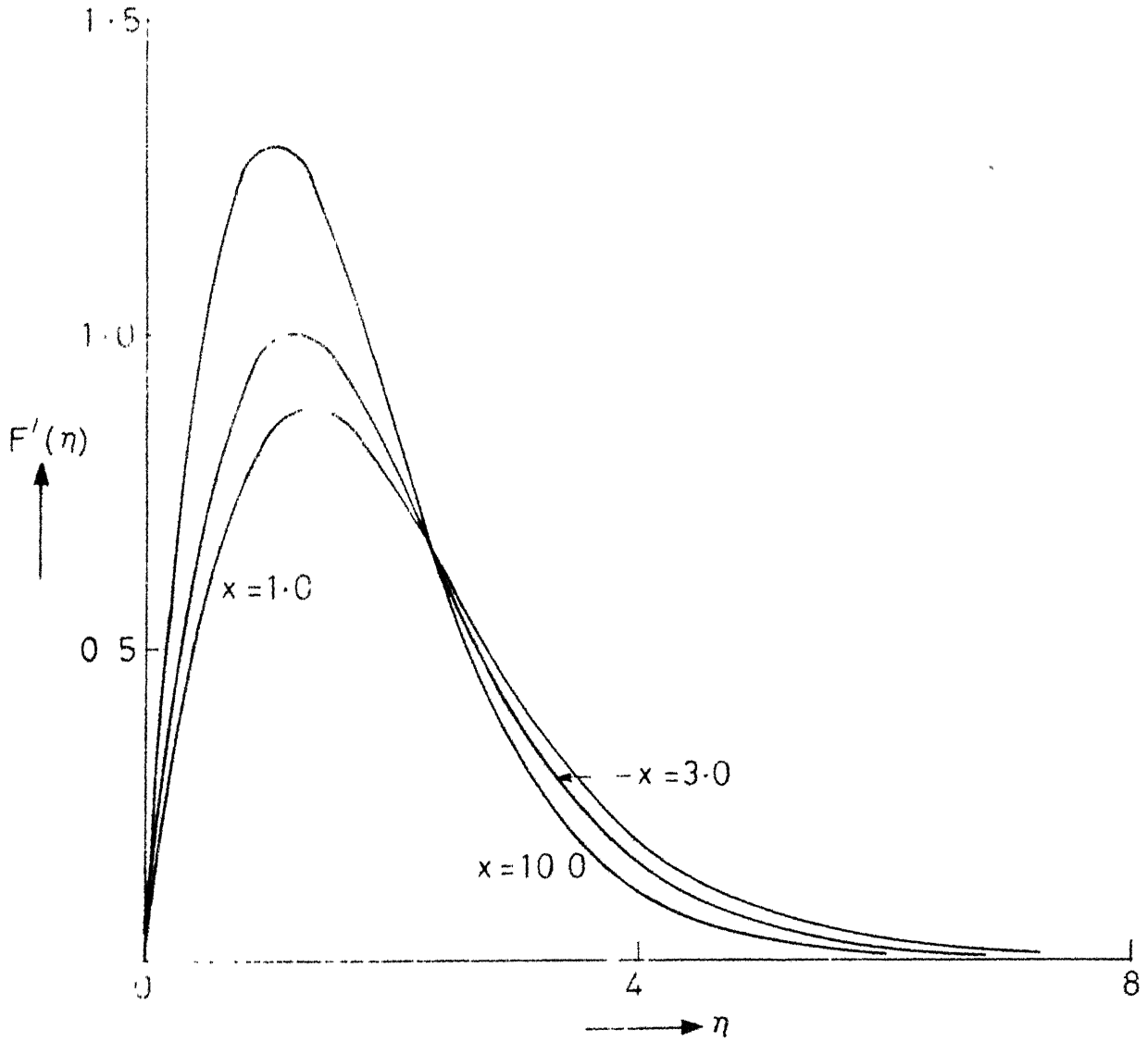

Fig. 3 Velocity profiles when $\Lambda = 1 \cdot 0$ and $\bar{\sigma} = 0 \cdot 72$ Two-Equation Model.

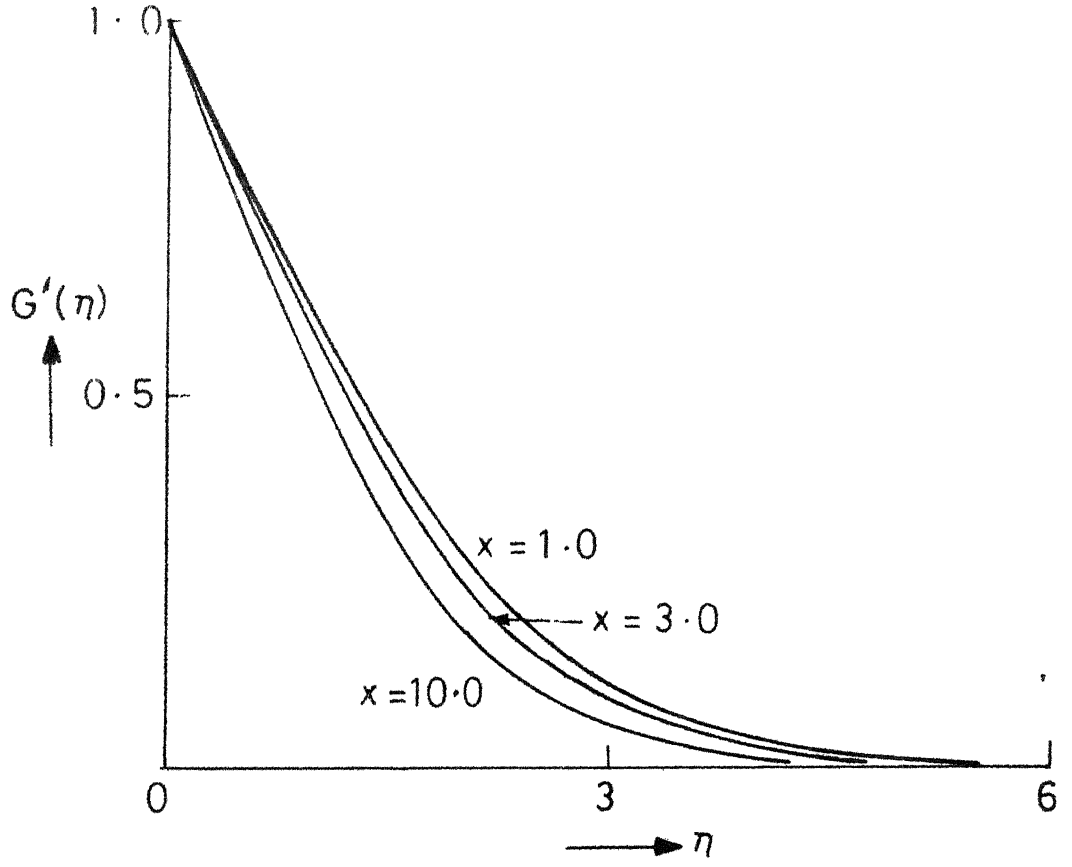

Fig. 4 Temperature profiles when $\Lambda = 1{\cdot}0$ and $\sigma = 0{\cdot}72$.

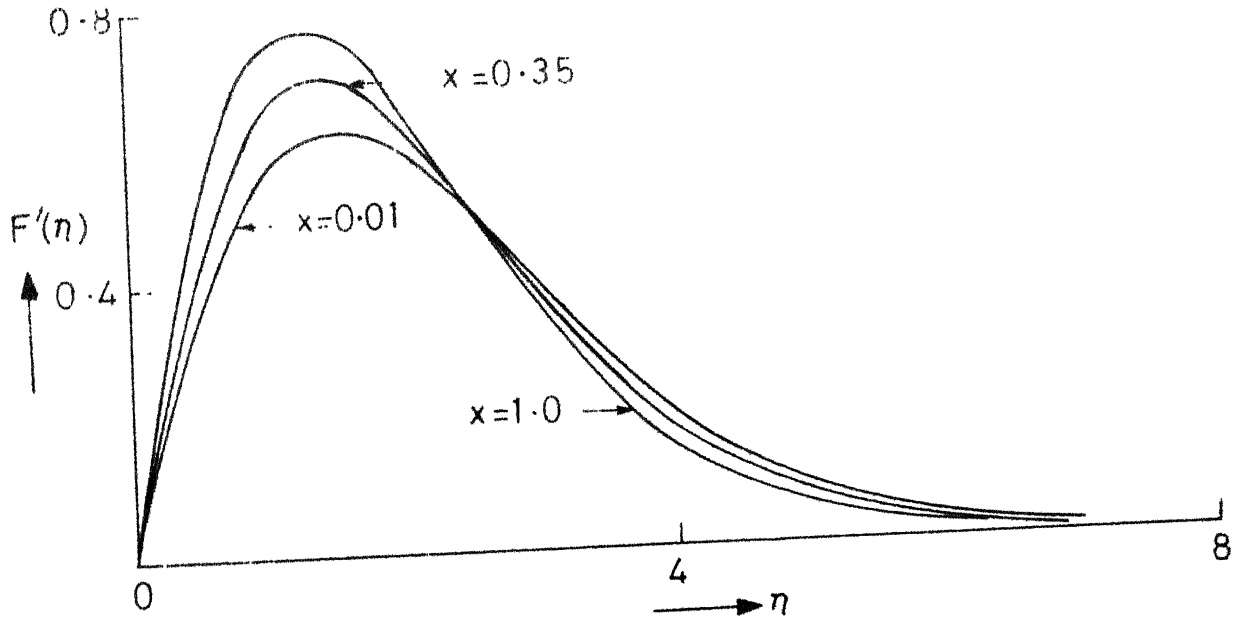

Fig.5 Velocity profiles when $\Lambda=1\cdot0$ and $\overline{\sigma}=1\cdot0$.

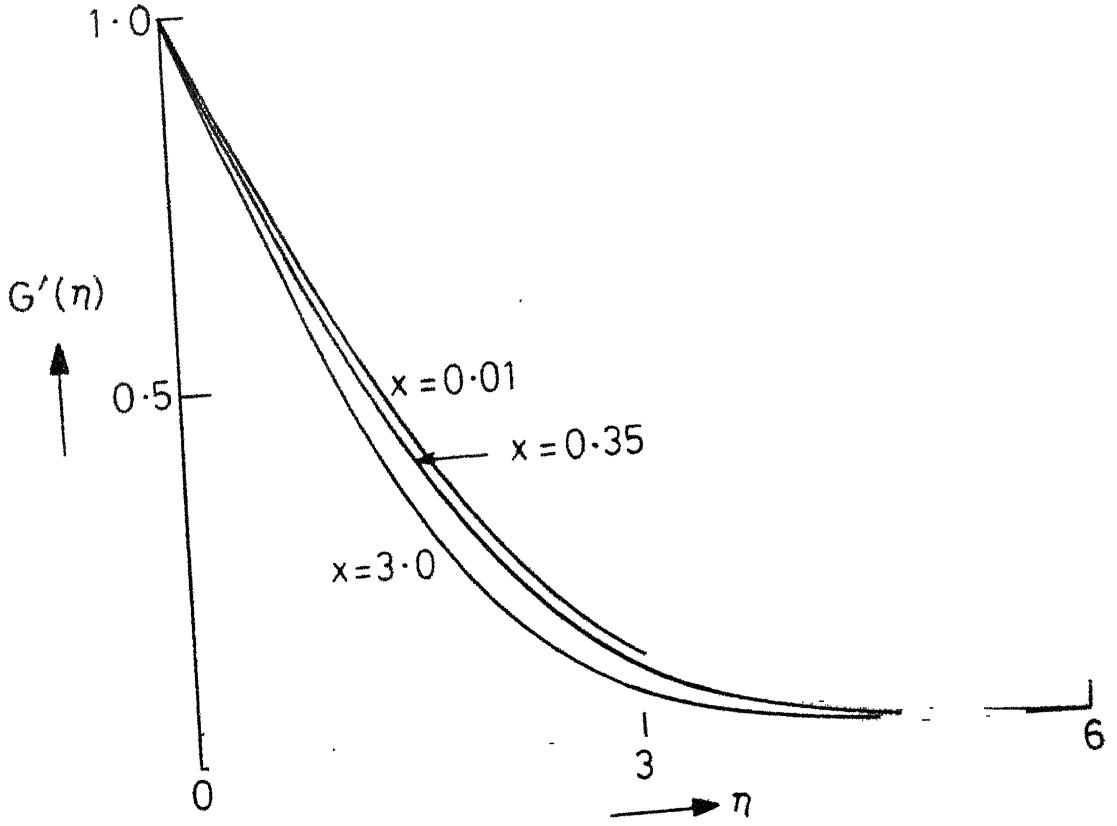

Fig. 6 Temperature profiles when $\Lambda = 1 \cdot 0$ and $\sigma = 1 \cdot 0$

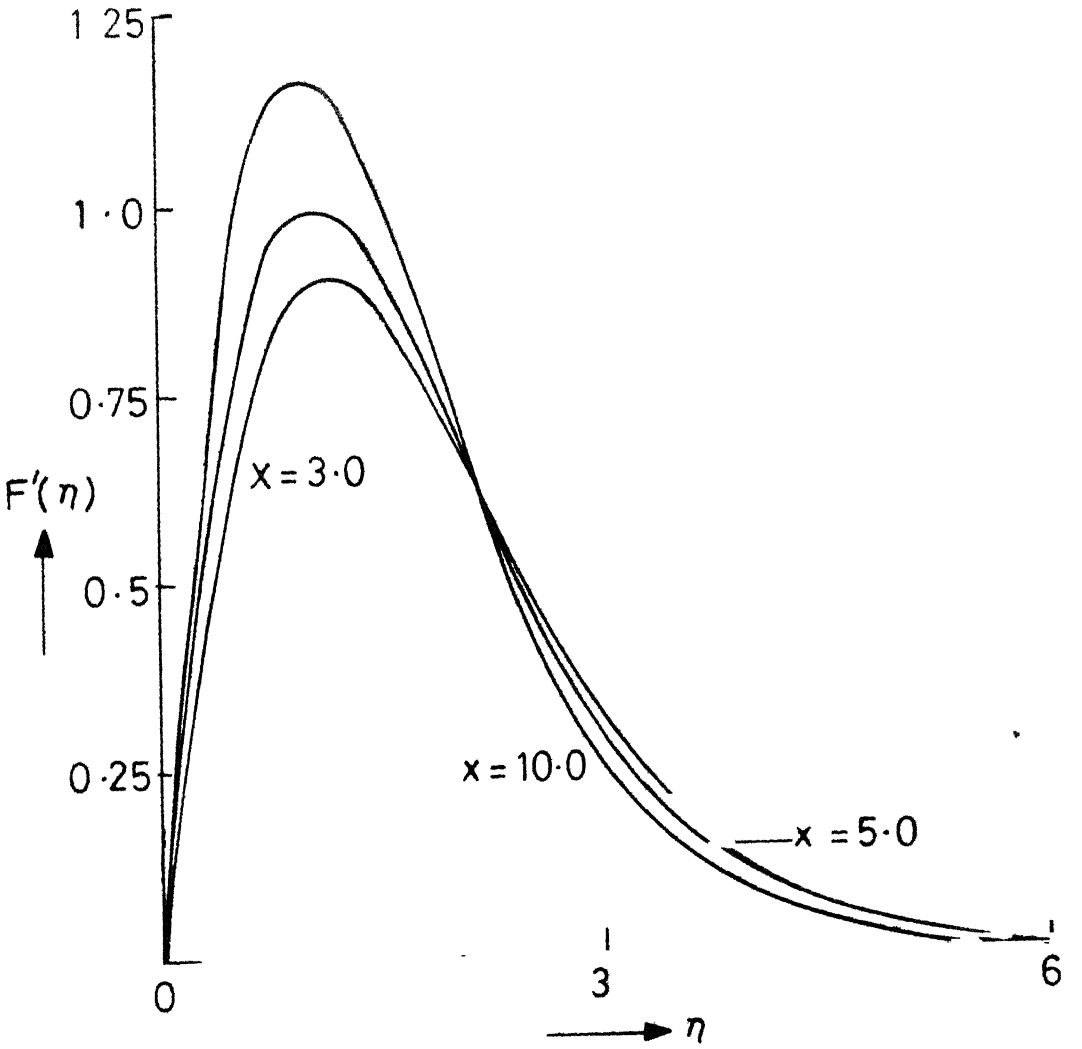

Fig. 7 Velocity profiles when $\Lambda = 1 \cdot 0$ and $\sigma = 1 \cdot 0$.

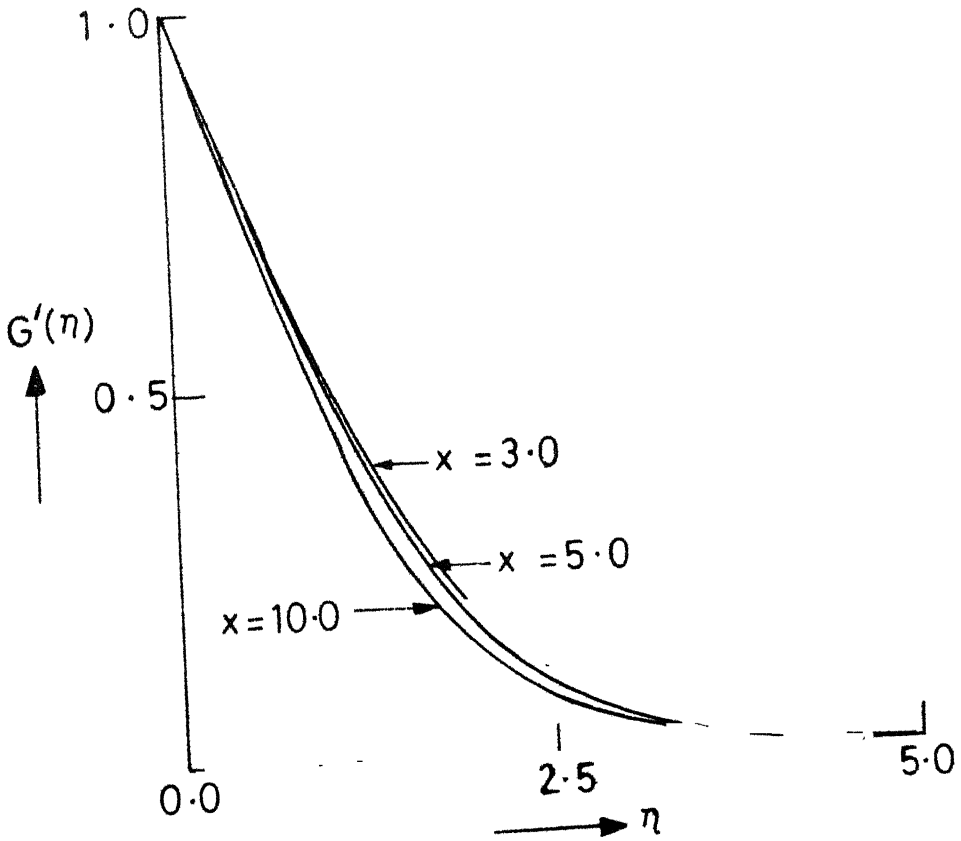

Fig. 8 Temperature profiles when $\Lambda = 1{\cdot}0$ and $\sigma = 1{\cdot}0$.

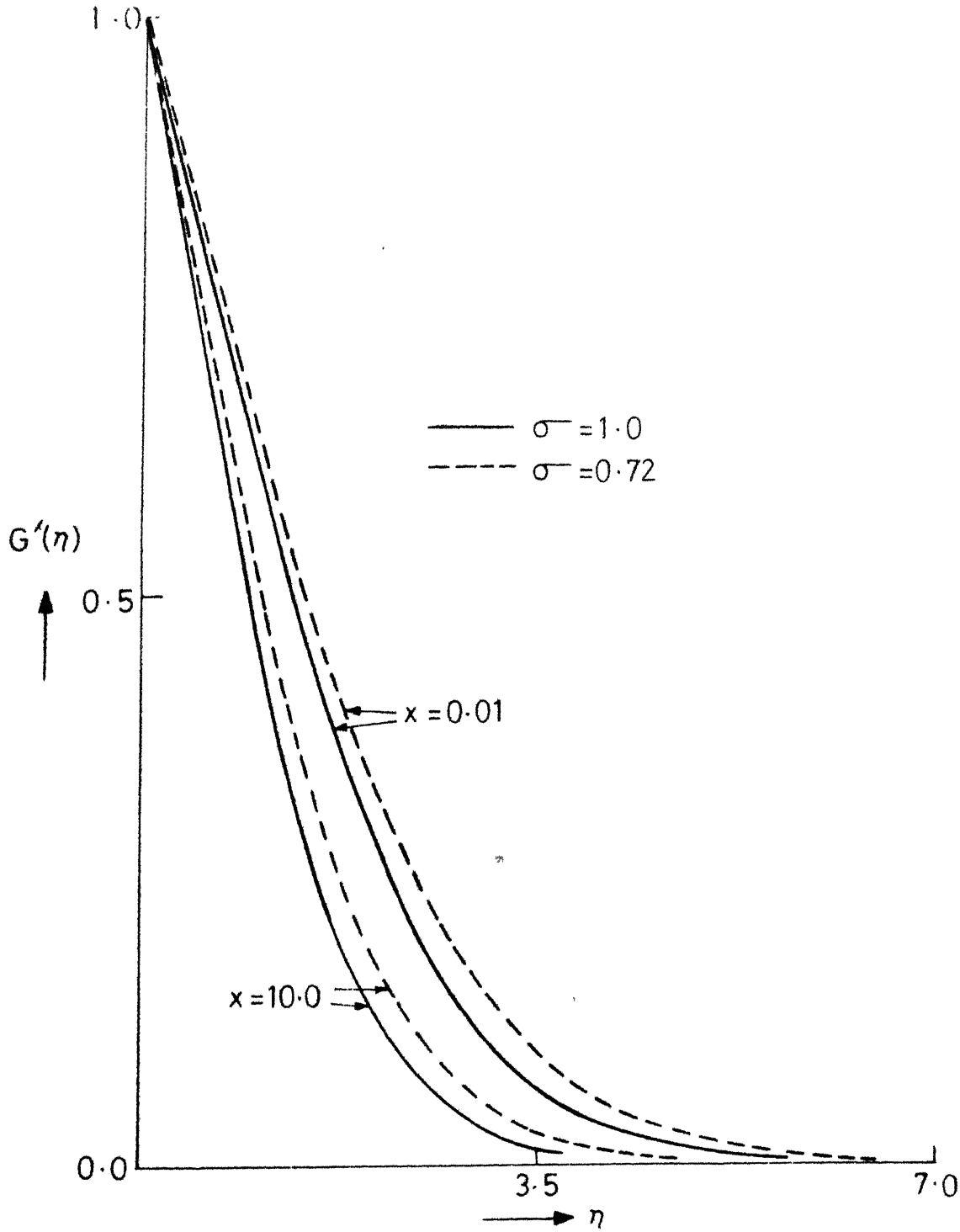

Fig. 9 Temperature profiles when $\Lambda = 1{\cdot}0$.

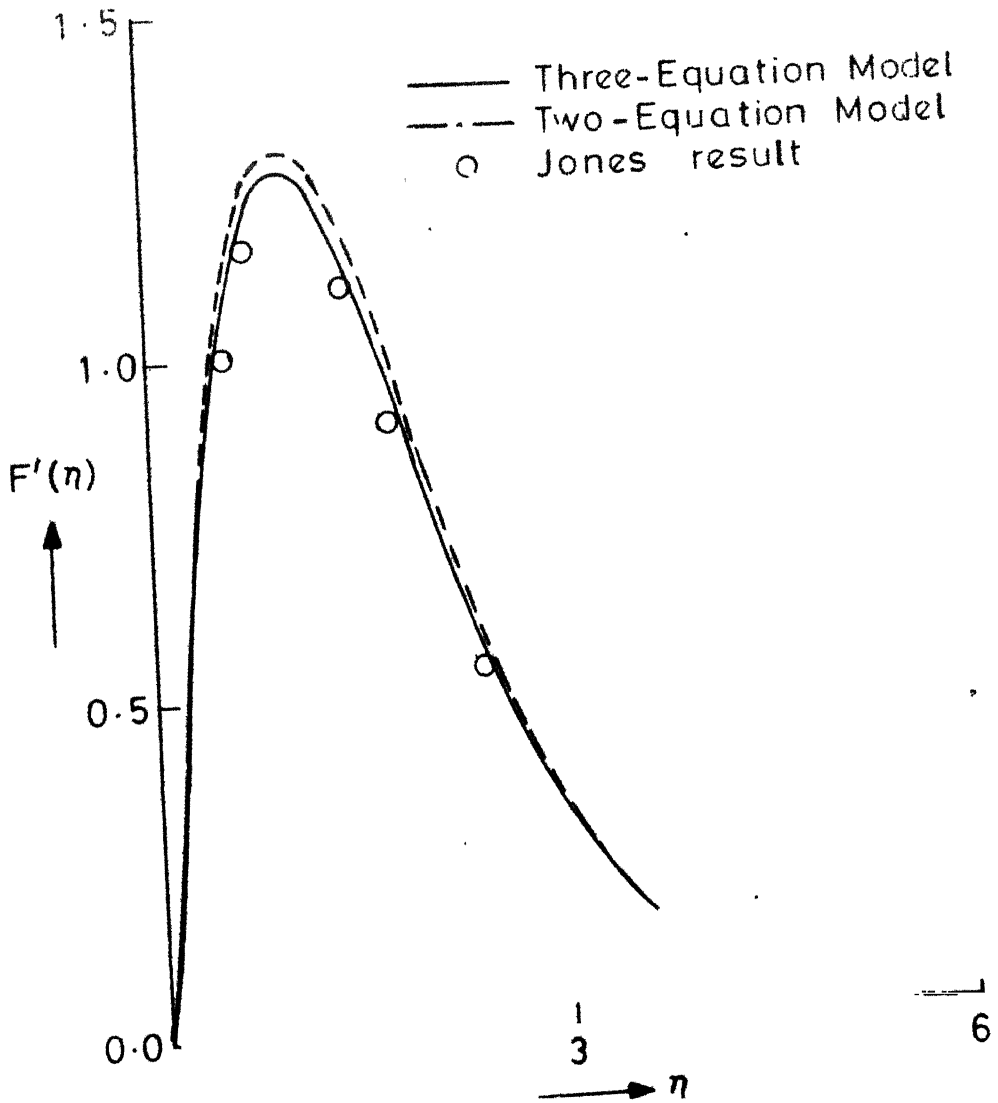

Fig. 10 Velocity profiles when $\Lambda=1\cdot0$, $\sigma=0\cdot72$ and $x=10\cdot0$.

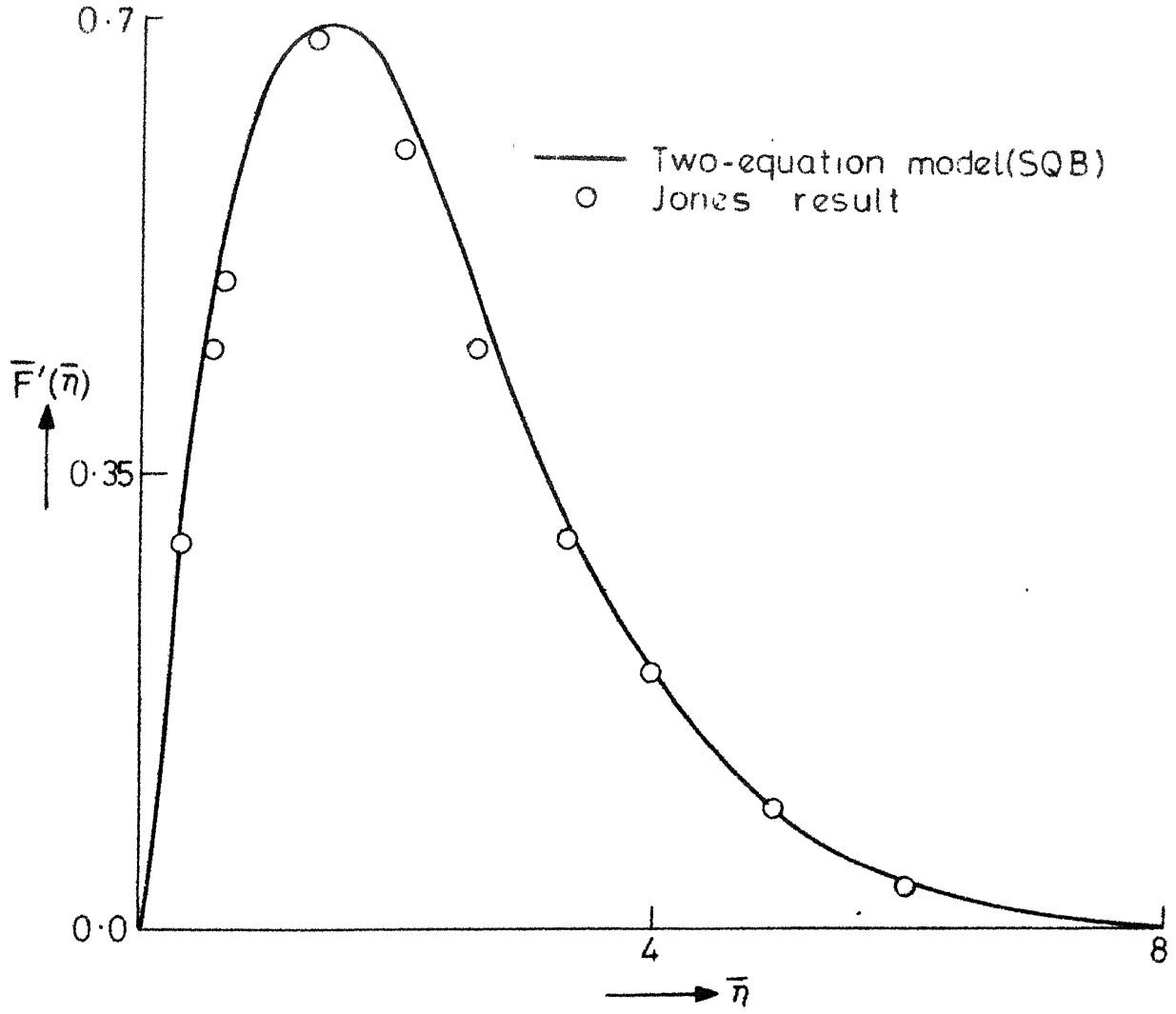

Fig. 11 Velocity profiles when $\Lambda = 1 \cdot 0$, $\bar{\sigma} = 0 \cdot 72$ and $x = 4 \cdot 5$.

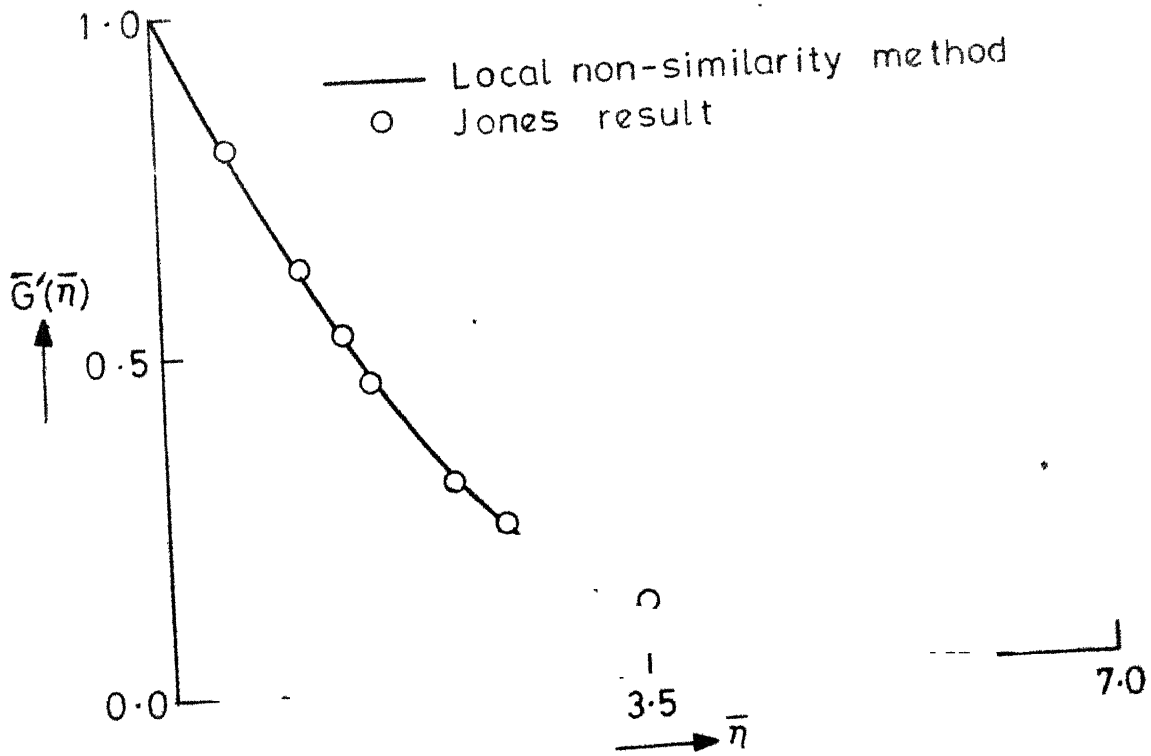

Fig. 12 Temperature profiles when $\Lambda = 1{\cdot}0$, $\bar{\sigma} = 0{\cdot}72$ and $x = 4{\cdot}5$.

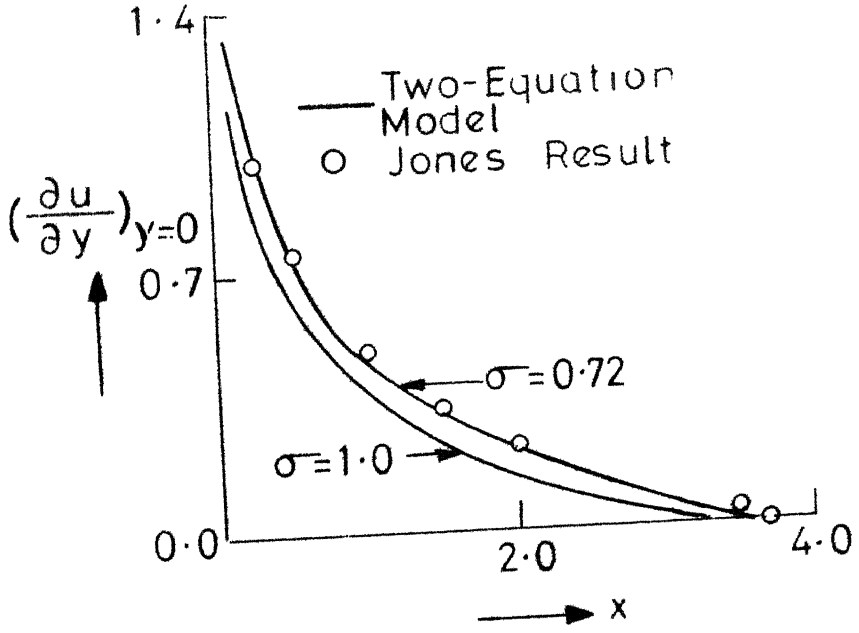

Fig. 13 Variation of skin-friction with x when $\Lambda = -1{\cdot}0$.

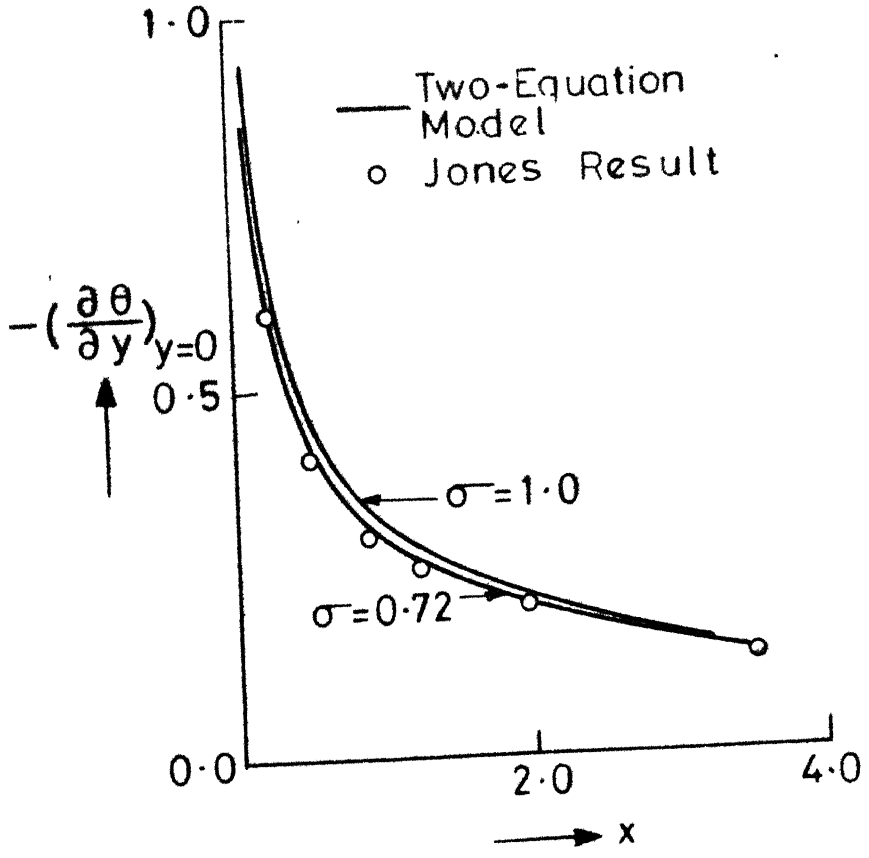

Fig. 14 Variation of heat transfer with x when $\Lambda = -1{\cdot}0$.

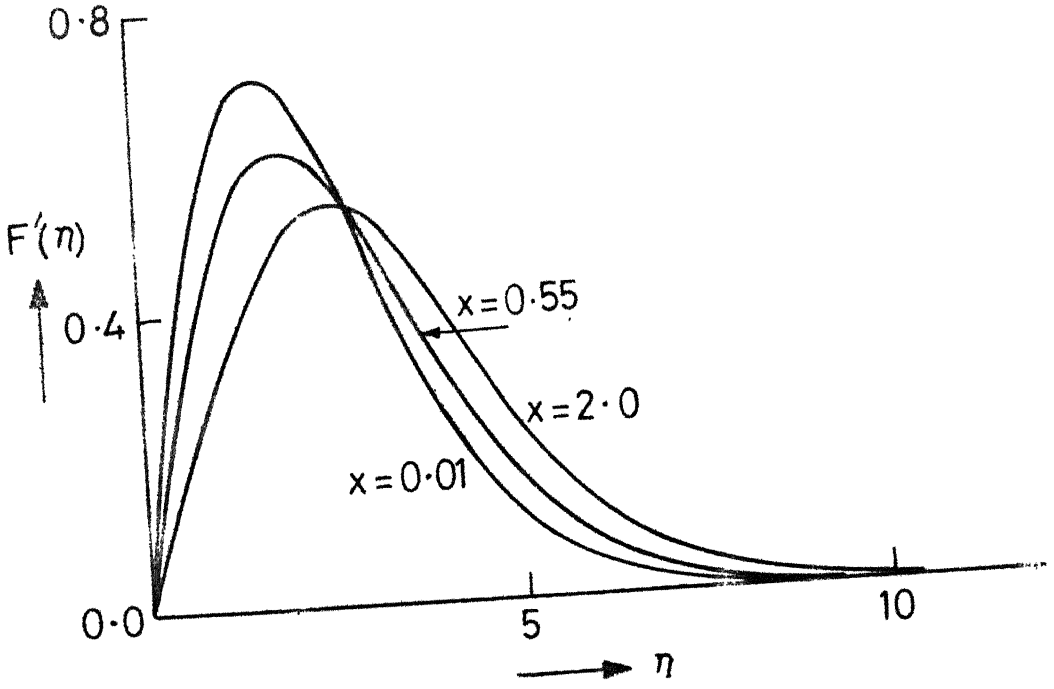

Fig.15 Velocity profiles when $\Lambda = -1\cdot0$ & $\sigma = 0\cdot72$.

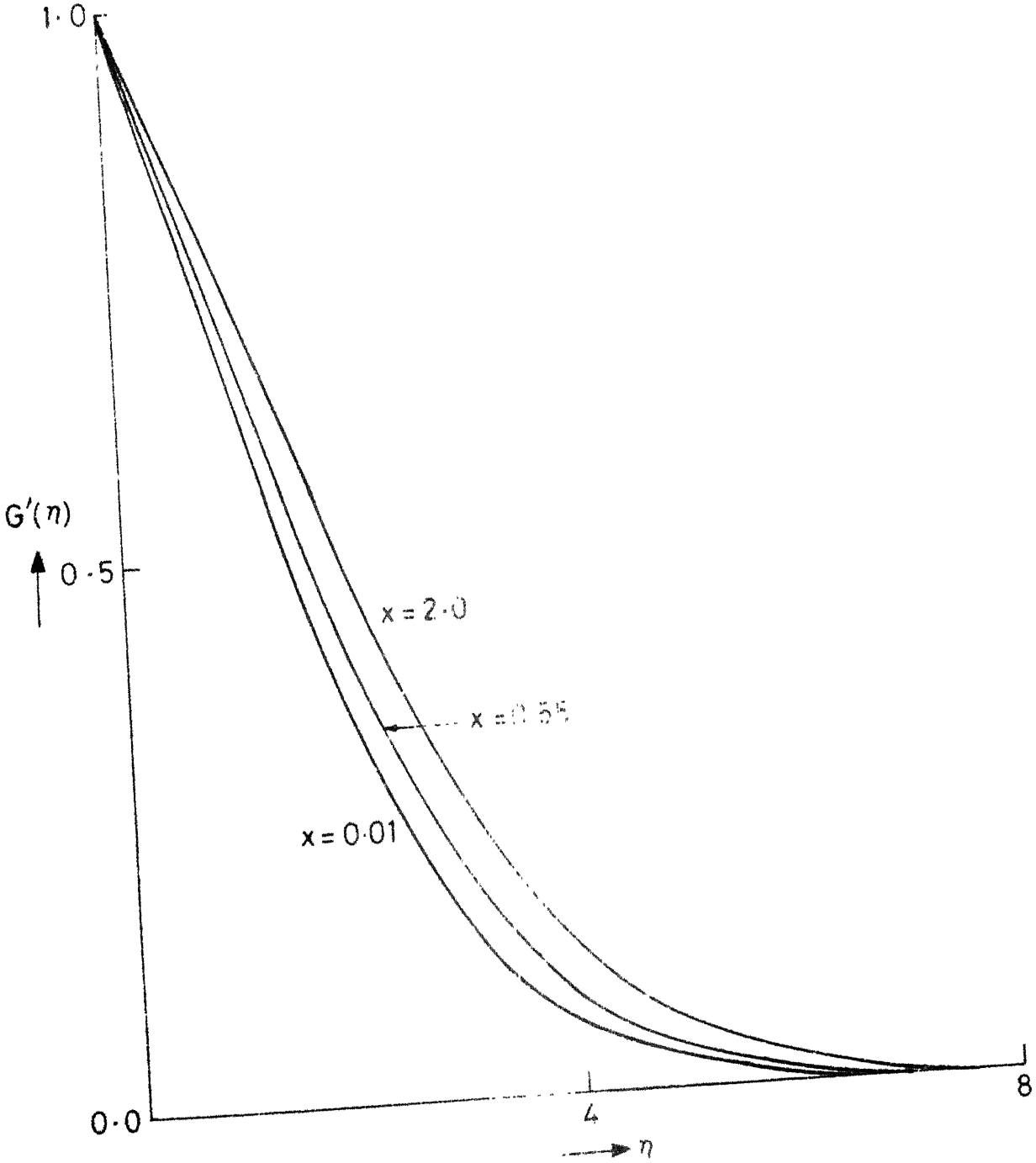

Fig. 16 Temperature profiles when $\Lambda = -1.0$ & $\sigma = 0.72$.

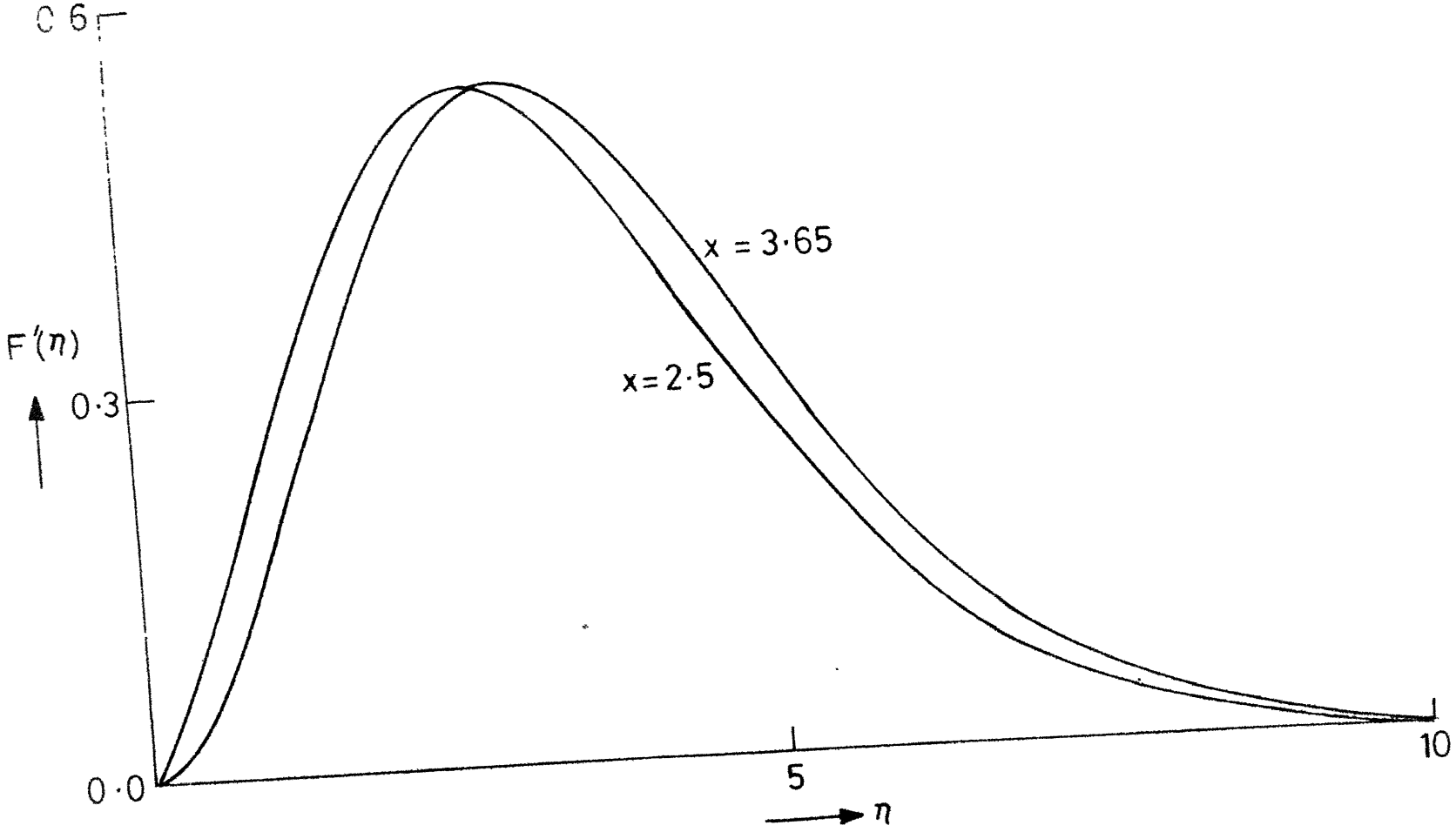

Fig.17 Velocity profiles when $\Lambda = -1.0$ and $\sigma = 0.72$.

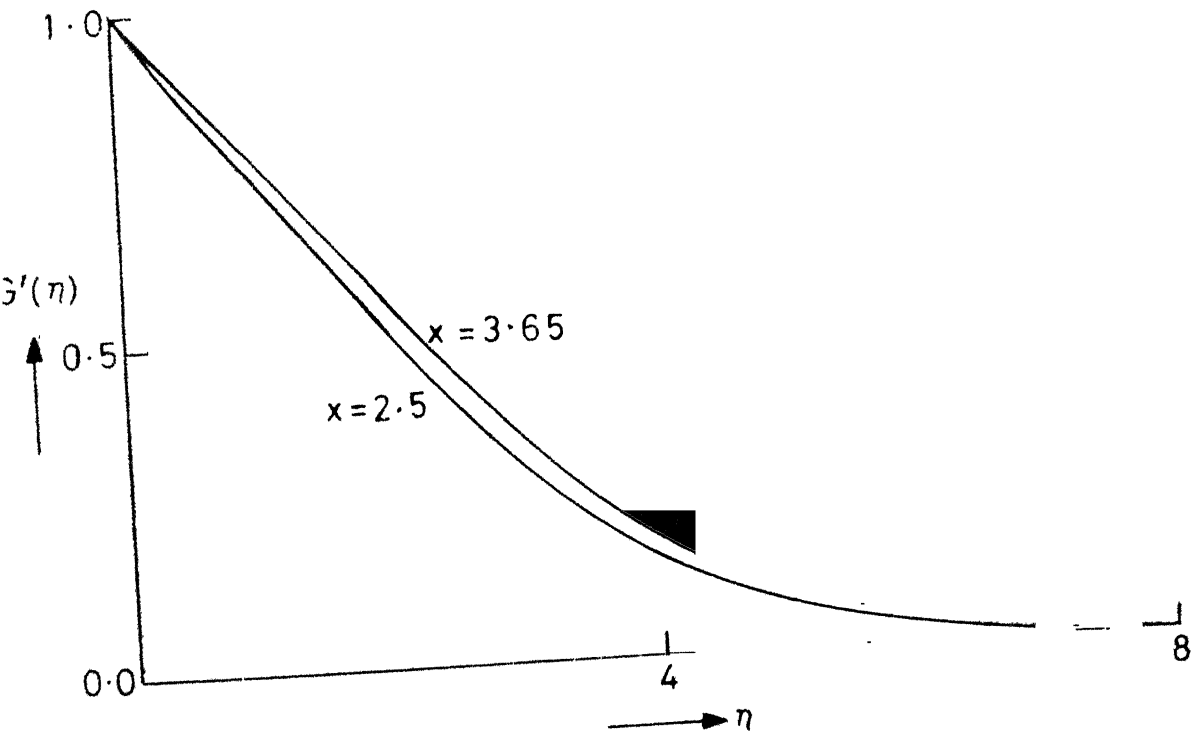

Fig.18 Temperature profiles when $\Lambda = -1{\cdot}0$ and $\sigma = 0{\cdot}72$.

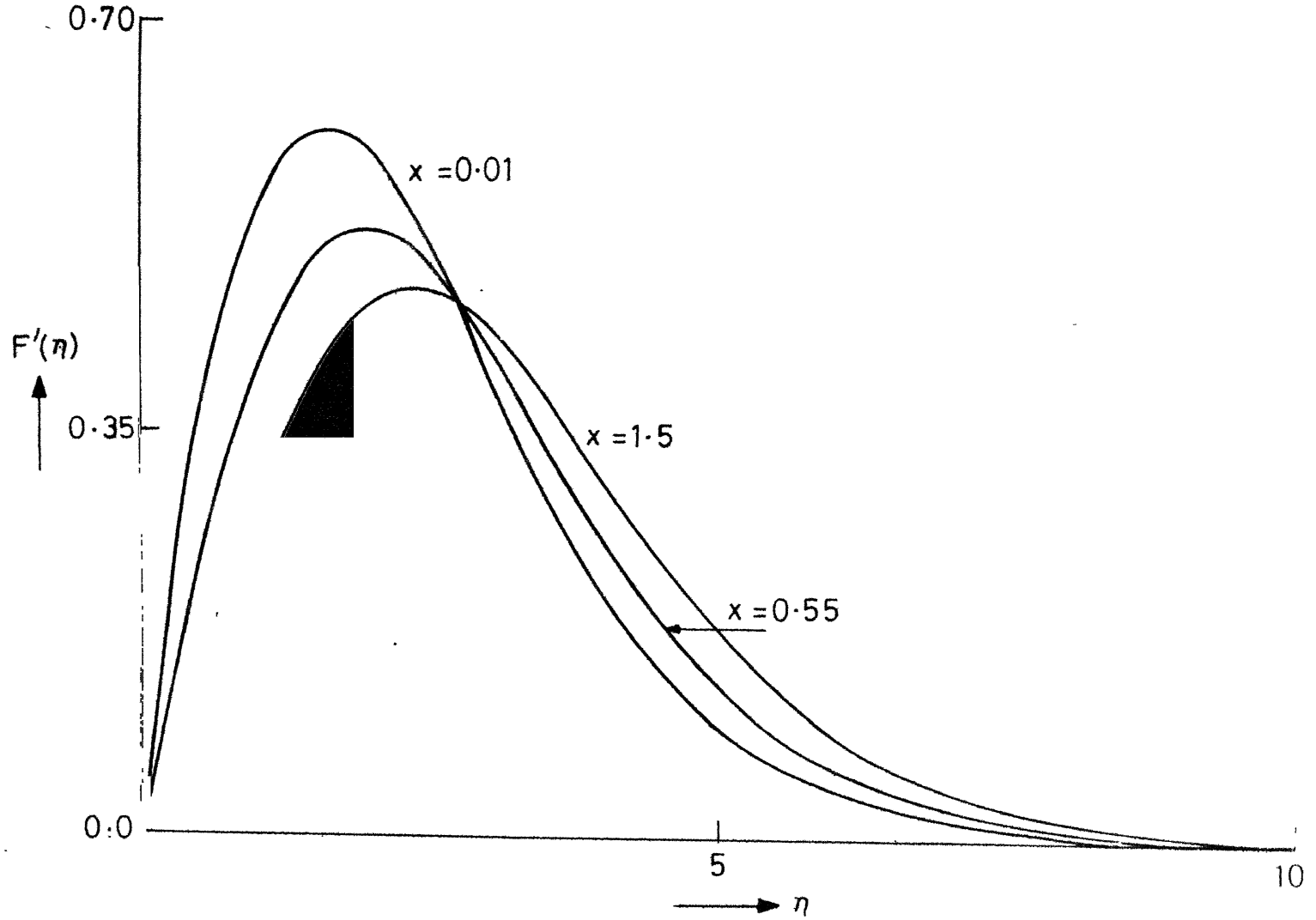

Fig. 19 Velocity profiles when $\Lambda = -1{\cdot}0$ and $\sigma = 1{\cdot}0$.

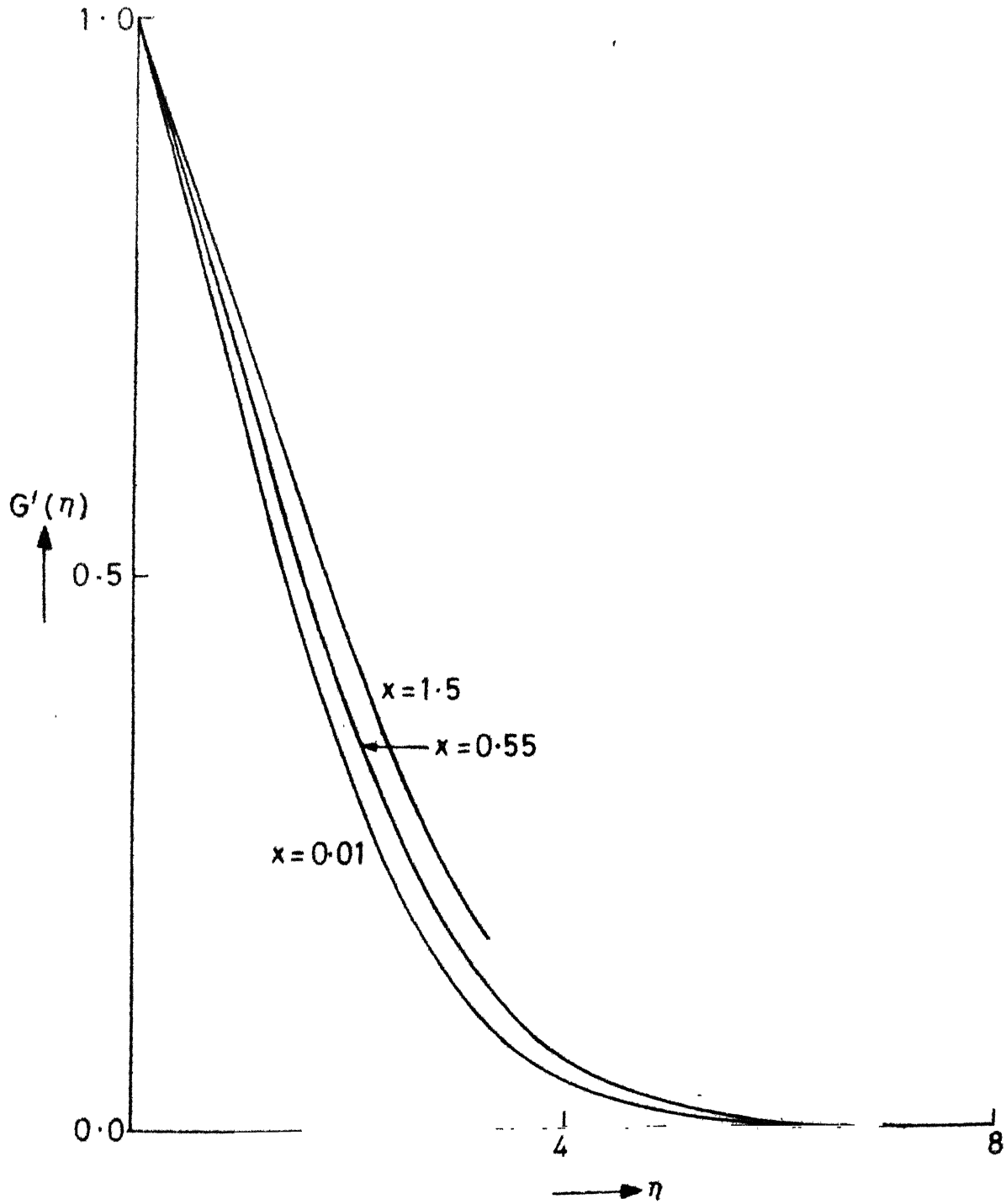

Fig. 20 Temperature profiles when $\Lambda = -1{\cdot}0$ and $\sigma = 1{\cdot}0$.

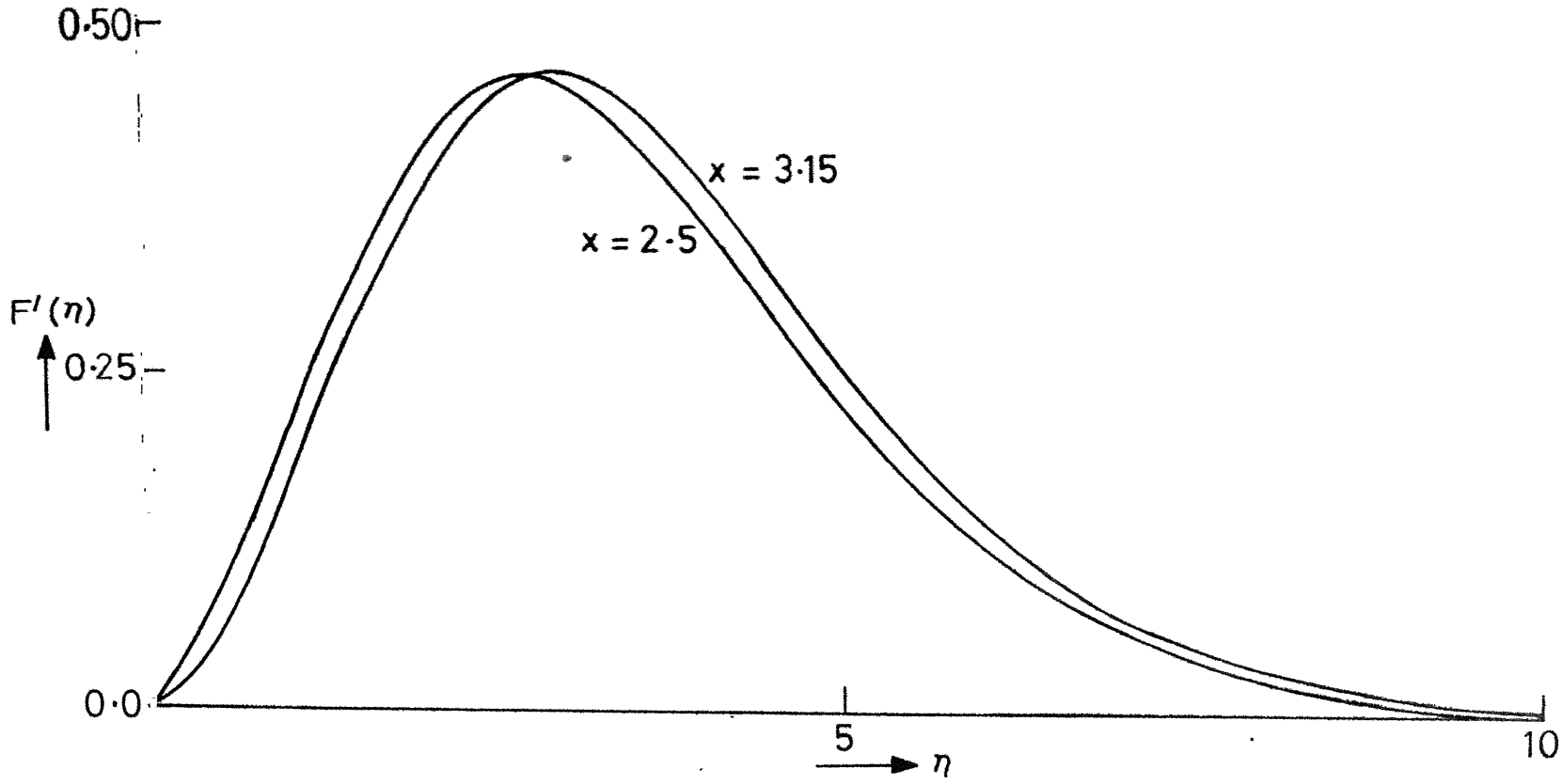

Fig. 21 Velocity profiles when $\Lambda = -1{\cdot}0$ and $\bar{\sigma} = 1{\cdot}0$.

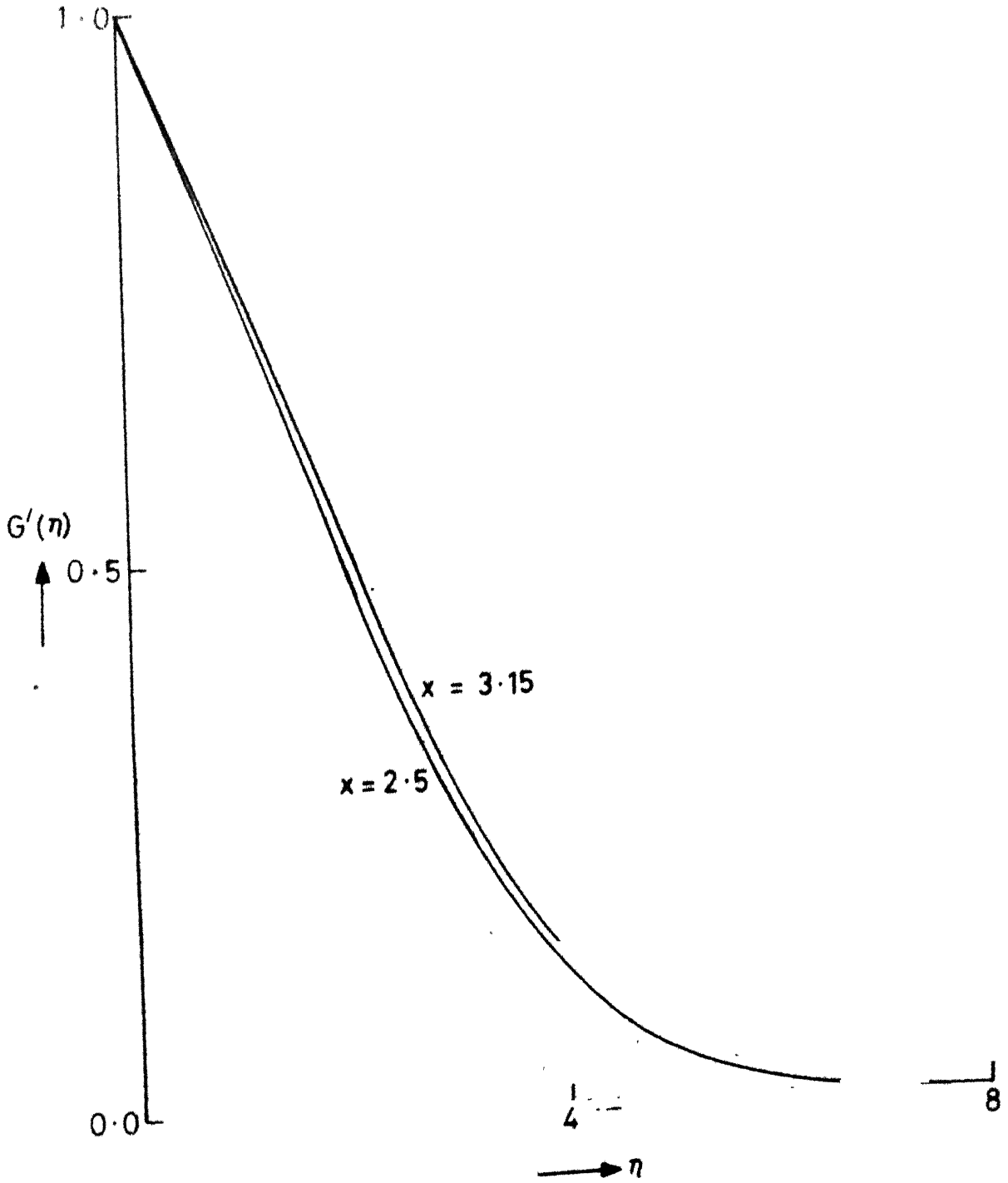

Fig. 22 Temperature profile when $\Lambda = -1{\cdot}0$ and $\bar{\sigma} = 1{\cdot}0$.

CHAPTER IV

POSSIBLE SIMILARITY SOLUTIONS FOR LAMINAR FREE CONVECTION ON HORIZONTAL PLATES

1. INTRODUCTION

Natural convection flow adjacent to horizontal surfaces bounded by an extensive body of fluid above is of considerable importance in micrometerological and industrial applications. Most of the earlier theoretical studies [1,2,3,4,5,6] are devoted to the problem of finding similarity solutions for steady free convection over horizontal surfaces; in all of these analysis, boundary layer approximations are employed and power form variations of wall temperature distribution are assumed. Recently, a few analytical studies dealing with unsteady free convection flow over semi-infinite horizontal plate have appeared [7,8,9] . But they all deal with the cases when the plate temperature oscillates in time about a constant non-zero mean temperature. In view of what has been done so far, it leaves us in doubt as to whether these studies have exhausted all possible similarity solutions or not for free convection over semi-infinite horizontal plate.

In this chapter, we derive in a systematic way all possible similarity solutions for both steady and unsteady free convection boundary layer flow over a semi-infinite horizontal plate. The solutions presented here were obtained not by assuming specific wall temperature distributions, but rather by deriving the solution forms from similarity conditions. This approach not only results in more general

forms than hitherto obtained, but results in all other possible solution forms. These solutions are of importance as they represent test cases for approximate and numerical approaches. Also, they could as well be used for understanding the effects of pressure gradient and heat transfer.

The method employed here is similar to that used by Hansen [10] , Yang [11] and Nanda [12] for certain other laminar boundary layer problems. It consists of defining a new independent variable and three dependent similarity variables in terms of the generalized transformation variables. When these similarity variables are substituted into the boundary layer equations, they are reduced to a set of ordinary differential equations only if the coefficients of the similarity variables and their derivatives can be made constant. These coefficients when made constant are referred to as similarity conditions; they usually contain derivatives of the transformation variables and are thus differential equations themselves. Any solution to the similarity conditions which will result in explicit forms for the transformation variables, will transform the original set of partial differential equations into a set of ordinary differential equations and these are called similarity equations.

We conclude from our investigation that there are in all four possible cases of similarity for free convection boundary layer flow over a heated horizontal plate. While

this analysis has verified that the similarity possibilities for steady cases have essentially been covered in the literature, it also opens a new possibility that somewhat more general wall thermal conditions could also be taken into account. The other two new possible cases deal with unsteady conditions.

2 BASIC EQUATIONS

Let us consider two-dimensional laminar free convection boundary layer flow over a semi-infinite horizontal flat plate, placed in an infinite expanse of Boussinesq fluid. The governing equations to the flow are then given by

$$\frac{\partial \bar{u}}{\partial \bar{x}} + \frac{\partial \bar{v}}{\partial \bar{y}} = 0 , \tag{4.1}$$

$$\frac{\partial \bar{u}}{\partial \bar{t}} + \bar{u}\frac{\partial \bar{u}}{\partial \bar{x}} + \bar{v}\frac{\partial \bar{u}}{\partial \bar{y}} = -\frac{1}{\rho}\frac{\partial \bar{p}}{\partial \bar{x}} + \nu \frac{\partial^2 \bar{u}}{\partial \bar{y}^2} , \tag{4.2}$$

$$\frac{1}{\rho}\frac{\partial \bar{p}}{\partial \bar{y}} = g\beta\,(\bar{T} - \bar{T}_\infty), \tag{4.3}$$

$$\frac{\partial \bar{T}}{\partial \bar{t}} + \bar{u}\frac{\partial \bar{T}}{\partial \bar{x}} + \bar{v}\frac{\partial \bar{T}}{\partial \bar{y}} = \bar{\alpha}\frac{\partial^2 \bar{T}}{\partial \bar{y}^2} \tag{4.4}$$

where $\bar{T}$ and $\bar{T}_\infty$ are the temperatures of the boundary layer and free stream respectively, $\bar{u}$ and $\bar{v}$ are the velocity components along the $\bar{x}$ and $\bar{y}$ directions respectively, $\bar{x}$ being the coordinate along the plate and $\bar{y}$ normal to it, g is the acceleration due to gravity, $\bar{p}$ is the pressure

inside the boundary layer, $\bar{t}$ is time, β is the coefficient of thermal expansion, $\bar{\alpha}$ is the thermal diffusivity, ρ is the density and ν is the kinematic viscosity. In our discussion the heated plate with temperature $\bar{T}_w(\bar{x},\bar{t})$ is taken to be facing upwards and $\bar{T}_w$ is higher than $\bar{T}_\infty$. While the initial conditions generally depend on the particular problem, the boundary conditions are given as

$$\begin{aligned} &\bar{y} = 0: \quad \bar{u} = 0 = \bar{v}\,, \quad \bar{T} = \bar{T}_w(\bar{x},\bar{t}) \text{ or } \frac{\partial \bar{T}}{\partial \bar{y}} = -\frac{\bar{q}(\bar{x},\bar{t})}{k}\,, \\ &\bar{y} = \infty: \quad \bar{u} = 0\,, \quad \bar{p} = 0 \quad \text{and} \quad \bar{T} = \bar{T}_\infty\,. \end{aligned} \tag{4.5}$$

Here $\bar{q}$ is the prescribed surface heat flux and k the thermal conductivity.

We now introduce the following transformation

$$t = \frac{\nu \bar{t}}{L^2}\,, \quad x = \frac{\bar{x}}{L}\,, \quad y = \frac{\bar{y}}{L}\,, \quad u = \frac{\bar{u}L}{\nu}\,, \quad v = \frac{\bar{v}L}{\nu}\,,$$

$$G = \frac{g\beta L^3(\bar{T} - \bar{T}_\infty)}{\nu^2}\,, \quad p = \frac{\bar{p}L^2}{\rho\nu^2} \tag{4.6}$$

to render the equations (4.1) to (4.4) in dimensionless form:

$$\frac{\partial u}{\partial x} + \frac{\partial v}{\partial y} = 0, \tag{4.7}$$

$$\frac{\partial u}{\partial t} + u\frac{\partial u}{\partial x} + v\frac{\partial u}{\partial y} = -\frac{\partial p}{\partial x} + \frac{\partial^2 u}{\partial y^2}\,, \tag{4.8}$$

$$\frac{\partial p}{\partial y} = G\,, \tag{4.9}$$

$$\frac{\partial G}{\partial t} + u\frac{\partial G}{\partial x} + v\frac{\partial G}{\partial y} = \frac{1}{\sigma}\frac{\partial^2 G}{\partial y^2}\,. \tag{4.10}$$

The boundary conditions now are

$$y = 0: \quad u = 0 = v, \quad G = G_w(x,t) \text{ or } \frac{\partial G}{\partial Y} = -q(x;t);$$

$$y = \infty; \quad u = 0, \quad p = 0 \quad \text{and} \quad G = 0. \tag{4.11}$$

We introduce the stream function Ψ, defined as

$$u = \frac{\partial \Psi}{\partial y} \quad \text{and} \quad v = - \frac{\partial \Psi}{\partial x}, \tag{4.12}$$

in equations (4.7) to (4.11) to get

$$\Psi_{yt} + \Psi_y \Psi_{xy} - \Psi_x \Psi_{yy} = -p_x + \Psi_{yyy}, \tag{4.13}$$

$$p_y = G, \tag{4.14}$$

$$G_t + \Psi_y G_x - \Psi_x G_y = \frac{1}{\sigma} G_{yy}, \tag{4.15}$$

with

$$y = 0: \quad \Psi = \Psi_y = 0, \quad G = G_w(x,t) \text{ or } \frac{\partial G}{\partial y} = - q(x,t),$$

$$y = \infty: \Psi_y = p = G = 0. \tag{4.16}$$

3. SIMILARITY CONDITIONS

The first step in the similarity analysis is to introduce a similarity variable η in the form

$$\eta = y\varphi_1(x,t), \tag{4.17}$$

and the stream function Ψ, pressure p and the temperature G are taken as

$$f(\eta) = \frac{\Psi}{\varphi_2(x,t)} , \tag{4.18}$$

$$\pi(\eta) = \frac{p}{\varphi_3(x,t)} , \tag{4.19}$$

$$\theta(\eta) = \frac{G}{G_w(x,t)} . \tag{4.20}$$

The problem now essentially reduces to determining the functions $\varphi_1(x,t)$, $\varphi_2(x,t)$, $\varphi_3(x,t)$ and $G_w(x,t)$ so that the partial differential equations (4.13) to (4.15) are reduced to ordinary differential equations for $f(\eta)$, $\pi(\eta)$ and $\theta(\eta)$ with proper boundary conditions to be obtained from (4.16). Though we will be deriving possible forms of the similar solutions for the case of prescribed surface temperature variation, the corresponding cases for prescribed surface heat flux distribution will also be indicated.

We now pass on to the key step in the analysis by substituting the identities

$$u = \frac{\partial \Psi}{\partial y} = \varphi_1 \varphi_2 f' , \tag{4.21}$$

$$v = -\frac{\partial \Psi}{\partial x} = -\left[\left(\frac{\partial \varphi_2}{\partial x}\right) f + \frac{\varphi_2}{\varphi_1}\left(\frac{\partial \varphi_1}{\partial x}\right) \eta f'\right] , \tag{4.22}$$

$$p = \varphi_3 \pi , \tag{4.23}$$

and

$$G = G_w \theta \tag{4.24}$$

in equations (4.13) to (4.15) so as to reduce them into the form

$$f'''-a_2\eta f''-(a_2+a_3)f'+a_5 ff''-(a_5+a_4)f'^2-a_1\pi-a_8\eta\pi'=0\ , \tag{4.25}$$

$$\pi' = a_9\theta\ , \tag{4.26}$$

$$\frac{1}{\sigma}\theta''-(a_2\eta-a_5 f)\theta'-(a_6+a_7 f')\theta = 0 \tag{4.27}$$

where

$$a_1 = \frac{(\frac{\partial \varphi_3}{\partial x})}{\varphi_1^3\varphi_2}\ , \tag{4.28}$$

$$a_2 = \frac{1}{\varphi_1^3}(\frac{\partial \varphi_1}{\partial t})\ , \tag{4.29}$$

$$a_3 = \frac{1}{\varphi_1^2\varphi_2}(\frac{\partial \varphi_2}{\partial t})\ , \tag{4.30}$$

$$a_4 = \frac{\varphi_2}{\varphi_1^2}(\frac{\partial \varphi_1}{\partial x})\ , \tag{4.31}$$

$$a_5 = \frac{1}{\varphi_1}(\frac{\partial \varphi_2}{\partial x})\ , \tag{4.32}$$

$$a_6 = \frac{1}{\varphi_1^2}\frac{1}{G_w}(\frac{\partial G_w}{\partial t})\ , \tag{4.33}$$

$$a_7 = \frac{-\varphi_2}{\varphi_1 G_w}(\frac{\partial G_w}{\partial x})\ , \tag{4.34}$$

$$a_8 = \frac{\varphi_3}{\varphi_1^4\varphi_2}(\frac{\partial \varphi_1}{\partial x})\ , \tag{4.35}$$

$$a_9 = \frac{G_w}{\varphi_2\varphi_1}\ . \tag{4.36}$$

The boundary conditions with prescribed temperature variation are

$$f(0) = 0 = f'(0),\ \theta(0) = 1,$$

$$f'(\infty) = \pi(\infty) = \theta(\infty) = 0. \tag{4.37}$$

It is clear now that the similarity solutions are possible if and only if a_1 to a_9 are all constants. Thus the equations (4.28) to (4.36) comprise of what is known as similarity conditions for our problem. Since the number of these conditions exceed the number of unknown functions, $\varphi_1, \varphi_2, \varphi_3$ and G_w, to be determined, not all of these constants can be taken arbitrarily. For instance, it can be verified that

$$a_6 = 2a_3 + 3a_2, \tag{4.38}$$

$$a_7 = 2a_5 + 3a_4, \tag{4.39}$$

$$a_7 a_8 = a_4(a_1 + a_8), \tag{4.40}$$

$$a_2 a_5 = (2a_4 + a_5)a_3, \tag{4.41}$$

$$a_7 a_2 = 2a_6 a_4 + a_3 a_7. \tag{4.42}$$

A general method of determining the unknown functions $\varphi_1, \varphi_2, \varphi_3$ and G_w is first to solve for φ_1 and φ_2 from differential equations (4.29) to (4.32). Then equation (4.35) yields φ_3. The surface temperature variation for which a similarity solution is possible can be obtained from (4.36).

4. POSSIBLE FORMS OF SIMILARITY SOLUTIONS

Case 1. Steady Free Convection with Surface Temperature Varying with any Power of a Linear Function of x.

Since we deal with steady cases,

$$a_2 = a_3 = a_6 = 0 .$$

We derive a general solution to (4.31) and (4.32) first by combining them to yield

$$\frac{a_5}{a_4} = \frac{\varphi_1}{\varphi_2} \frac{(\frac{d\varphi_2}{dx})}{(\frac{d\varphi_1}{dx})} .$$

Taking $\varepsilon = \frac{a_5}{a_4}$ and solving the equation we have

$$\varphi_2 = a_{10} \varphi_1^{\varepsilon} , \tag{4.43}$$

a_{10} being a constant of integration. On substituting (4.43) into (4.31), we obtain on solving the resulting equation for $\varepsilon \neq 1$,

$$\varphi_1 = [a_{11} + x \frac{a_4}{a_{10}} (\varepsilon-1)]^{\frac{1}{\varepsilon-1}} \tag{4.44}$$

where a_{11} is another arbitrary constant of integration. Using this in (4.43), we can write

$$\varphi_2 = a_{10} [a_{11} + x \frac{a_4}{a_{10}} (\varepsilon-1)]^{\frac{\varepsilon}{\varepsilon-1}} . \tag{4.45}$$

From (4.35) and (4.36), we obtain

$$G_w = \frac{a_8 a_9 a_{10}^2}{a_4} \left[a_{11} + x \frac{a_4}{a_{10}} (\varepsilon-1)\right]^{\frac{3+2\varepsilon}{\varepsilon-1}} . \qquad (4.46)$$

Here constants $a_8, a_9, a_{10}, a_4, a_{11}$ and ε are all arbitrary. But still it is possible to assign specific values for some of these constants without actually restricting in any way the form of G_w in (4.46). Since characteristic length L is included in x and a_{10} is entirely arbitrary in the sense it does not occur in any of the similarity conditions, a_4, a_8 and a_9 can all be assigned specific values leaving ε, a_{10} and a_{11} as arbitrary constants.

We now introduce a constant n such that

$$n = \frac{3+2\varepsilon}{\varepsilon-1}.$$

From this we get

$$\varepsilon = \frac{n+3}{n-2}. \qquad (4.47)$$

Let us now assume

$$a_4 = \frac{n-2}{5}, \quad a_8 = \frac{n-2}{5} \quad \text{and} \quad a_9 = 1.$$

Thus we have

$$a_5 = \frac{n+3}{5} \quad \text{from (4.47)},$$

$$a_7 = n \quad \text{from (4.39)},$$

and

$$a_1 = \frac{4n+2}{5} \quad \text{from (4.40)}.$$

Now the forms of the functions φ_1, φ_2 and G_w are

$$\varphi_1 = (a_{11} + \frac{x}{a_{10}})^{\frac{n-2}{5}} ,$$

$$\varphi_2 = a_{10}(a_{11} + \frac{x}{a_{10}})^{\frac{n+3}{5}} ,$$

and

$$G_w = a_{10}^2 (a_{11} + \frac{x}{a_{10}})^n . \tag{4.48}$$

Equations (4.25) to (4.27) can now be written as

$$f''' + \frac{n+3}{5} ff'' - \frac{2n+1}{5} f'^2 - \frac{2}{5}(2n+1)\pi + \frac{2-n}{5}\eta\pi' = 0 ,$$

$$\pi' = \theta ,$$

$$\frac{1}{\sigma}\theta'' + \frac{n+3}{5} f\theta' - nf'\theta = 0 \tag{4.49}$$

with boundary conditions (4.37).

The velocity components u, v and the temperature G within the boundary layer may now be written as

$$u = a_{10}(a_{11} + \frac{x}{a_{10}})^{\frac{2n+1}{5}} f' , \tag{4.50}$$

$$v = -(a_{11} + \frac{x}{a_{10}})^{\frac{n-2}{5}} [\frac{n-2}{5}\eta f' + \frac{n+3}{5} f] , \tag{4.51}$$

$$G = a_{10}^2 (a_{11} + \frac{x}{a_{10}})^n \theta \tag{4.52}$$

and the rate of heat transfer at the surface is

$$q = -a_{10}^{2}\,\theta'(0)\,\left(a_{11} + \frac{x}{a_{10}}\right)^{\frac{6n-2}{5}} . \qquad (4.53)$$

For $n = 0$ and $a_{11} = 0$, equations (4.49) together with boundary conditions (4.37) represent the steady free convection flow over an isothermal semi-infinite horizontal plate. Rotem and Claassen [4] have dealt with this case and gave numerical solutions for several Prandtl numbers including large and small values of it. By putting $a_{11} = 0$ and $n = 1/3$ in (4.52) and (4.53), one finds that the surface temperature varies with one third power of the distance away from the leading edge while the resulting heat-flux at the surface is uniform. Numerical solutions for this case have been given by Pera and Gebhart [6] for a range of values of Prandtl number $\frac{1}{10}$ to 100. Previous similarity solutions given by Rotem and Claassen can be obtained by taking $a_{11} = 0$ and n arbitrary. The present analysis shows that the numerical results discussed previously can be directly applied to cases where $a_{11} \neq 0$ and $a_{11} > 0$. The physical implication of $a_{11} \neq 0$ is that the surface temperature at the leading edge of the plate is different from that of the ambient fluid, a feature which is certainly more realistic, since it is difficult physically to heat the plate without raising the temperature of its leading edge. However, it is to be noted that for such a case of non-zero a_{11} the velocity component u is not identically zero along

$x = 0$, but is only zero at $\bar{y} = 0$ and $\bar{y} = \infty$ and thus we observe some plate length and temperature difference must precede $x = 0$ in order for the boundary layer thickness to build up. Thus the effect of a_{11} is merely to allow a shift in the x coordinate. If we assume that $x = 0$ corresponds to the leading edge of the plate, we have $a_{11} = 0$ and a simplified general form for $\varphi_1, \varphi_2, G_w$ is given by

$$\varphi_1 = D_1 x^{\frac{n-2}{5}} , \quad \varphi_2 = D_1 x^{\frac{n+3}{5}} , \quad G_w = D_2 x^n$$

where $D_2 = 5D_1$ and D_1, D_2 are constants.

For $\varepsilon \neq 1$, the boundary layer thickness is constant or increasing with x if $n < 2$ and that the same is true for n if $n \geq -1/2$. When $n = -1/2$, the thermal energy that is convected at any location is constant and hence the surface is adiabatic and all the convected energy is released by a line source at the leading edge which means, physically, that there is no boundary layer flow. Thus the restriction on n, namely $-\frac{1}{2} < n < 2$, becomes necessary to retain the boundary layer approximations.

In view of equation (4.53), it can be easily seen that the present similarity solution is equally possible when the surface heat flux is prescribed. The condition is that the surface heat flux q must be of the form

$$q = (a_{11} + \frac{x}{a_{10}})^{\beta} \tag{4.54}$$

where β is another constant parameter. If we let $\beta = \frac{6n-2}{5}$ or $n = \frac{5\beta+2}{6}$, these two problems then become identical.

Case 2. Steady Free convection with Surface Temperature Varying with an Exponential Function of x.

We deal again with steady laminar free convection flow, hence

$$a_2 = a_3 = a_6 = 0.$$

Now taking $\varepsilon = 1$, equation (4.43) becomes

$$\varphi_2 = a_{10}\varphi_1 . \tag{4.55}$$

The equation (4.31) yields:

$$\varphi_1 = a_{12} e^{\frac{a_4}{a_{10}}x} , \tag{4.56}$$

which on substituting in (4.55) gives

$$\varphi_2 = a_{10}a_{12} e^{\frac{a_4}{a_{10}}x} . \tag{4.57}$$

From (4.35) and (4.36), we obtain

$$G_w = \frac{a_8 a_9}{a_4} \varphi_1^3 \varphi_2^2$$

$$= \frac{a_8 a_9}{a_4} a_{12}^5 a_{10}^2 e^{5\frac{a_4}{a_{10}}x} . \tag{4.58}$$

Since the integration constants are entirely arbitrary and a characteristic length is included in x, we assign $a_9 = 1$, $a_4 = 1$ and $a_8 = \frac{1}{5}$. We then have $a_7 = 5$ from (4.39) and $a_1 = \frac{4}{5}$ from (4.40). Finally equations (4.25) to (4.27) are

$$f''' + ff'' - 2f'^2 - \frac{4}{5}\pi - \frac{1}{5}\eta\pi' = 0,$$

$$\pi' = \theta ,$$

$$\frac{1}{\sigma}\theta'' + f\theta' - 5f'\theta = 0 , \qquad (4.59)$$

with the boundary conditions given by (4.37).

Putting $m = \frac{5a_4}{a_{10}} = \frac{5}{a_{10}}$ and using (4.56), (4.57) and (4.58) we have

$$\varphi_1 = a_{12} e^{\frac{mx}{5}} , \qquad (4.60)$$

$$\varphi_2 = \frac{5}{m} a_{12} e^{\frac{mx}{5}} , \qquad (4.61)$$

$$G_w = \frac{5}{m^2} a_{12}^5 e^{mx} . \qquad (4.62)$$

Also from (4.21), (4.22) and (4.24), we obtain

$$u = \frac{5}{m} a_{12}^2 e^{\frac{2mx}{5}} , \qquad (4.63)$$

$$v = -a_{12} e^{\frac{mx}{5}} (f + \eta f') , \qquad (4.64)$$

$$G = \frac{5}{m^2} a_{12}^5 e^{mx} \theta \qquad (4.65)$$

and the rate of heat transfer at the surface is given by

$$q = -\frac{5}{m^2}\, a_{12}^6\, e^{\frac{6mx}{5}}\, \theta'(0). \qquad (4.66)$$

By assuming the distribution of wall temperature to be exponential, Jaluria [13] has arrived at the same equations as (4.59). We note here that the parameter m is absent in the resulting similarity equations and this will be so, since the value of the parameter ε is taken unity at the outset. According to equation (4.66), the present similarity solution is again seen to be identical to that of prescribed plate-surface heat flux

$$q = \frac{36}{5\gamma^2}\, a_{12}^6\, e^{\gamma x},$$

where $\gamma = \frac{6m}{5}$.

Case 3. Unsteady Free Convection with Surface Temperature Varying Inversely as Square Root of a Linear Combination of x and t:

To our knowledge, no similarity solution for free convection boundary layer equations over horizontal plate under unsteady surface thermal conditions exists in the literature. But recently a few analytical studies on free convection over horizontal surfaces with fluctuating surface temperature about a non-zero mean have been published [7,8,9]. The similarity conditions already derived can now be used to

explore the forms of the possible similarity solutions under unsteady conditions.

An integral of (4.29) is of the form

$$\varphi_1 = (A(x) - 2a_2 t)^{-1/2} \tag{4.67}$$

where $A(x)$ is to be determined. Also from (4.29) and (4.30), we get

$$\varphi_2 = B(x)\ (A(x) - 2a_2 t)^{-\omega/2} \tag{4.68}$$

where $$\omega = \frac{a_3}{a_2}, \quad a_2 \neq 0.$$

Again, from equations (4.31) and (4.32), we have

$$\varphi_2 = C(t)\ \varphi_1^{\varepsilon} \tag{4.69}$$

where $$\varepsilon = \frac{a_5}{a_4}, \quad a_4 \neq 0.$$

Solving (4.31) using (4.69), we obtain

$$\varphi_1 = \left[\frac{a_4(\varepsilon - 1)}{C(t)}\, x + D(t)\right]^{\frac{1}{\varepsilon - 1}} \tag{4.70}$$

and hence from (4.69) we get

$$\varphi_2 = C(t)\left[\frac{a_4(\varepsilon-1)}{C(t)}\, x + D(t)\right]^{\frac{\varepsilon}{\varepsilon-1}}. \tag{4.71}$$

On comparing the equations (4.67) to (4.70), a suitable solution is obtainable if the following identities hold

$$\varepsilon = \omega = -1, \quad B(x) = C(t) = a_{13},$$

$$A(x) = -\frac{2a_4}{a_{13}} x \quad \text{and} \quad D(t) = -2a_2 t. \tag{4.72}$$

From (4.35) and (4.36), G_w is obtained as

$$G_w = \frac{a_8 a_9}{a_4} a_{13}^2 \frac{1}{(-\frac{2a_4}{a_{13}} x - 2 a_2 t)^{1/2}}. \tag{4.73}$$

Though arbitrary values may be assigned to a_8, a_9, a_4, we have to keep a_2 as parameter in the reduced similarity equations for this case. We now have

$$a_3 = -a_2, \; a_5 = -a_4 .$$

From (4.38) and (4.39) it follows that

$$a_6 = a_2, \; a_7 = a_4.$$

From (4.40), we get $a_1 = 0$. Taking $a_4 = -1$, $a_8 = -1$ and $a_9 = 1$, the similarity equations for the flow may now be written as

$$f''' - a_2 \eta f'' + f f'' + \eta \pi' = 0,$$

$$\pi' = \theta,$$

$$\frac{1}{\sigma} \theta'' - (a_2 \eta - f) \theta' - (a_2 - f') \theta = 0 \tag{4.74}$$

and the boundary conditions (4.37) are retained as such. Final forms of the unknown functions $\varphi_1, \varphi_2, G_w$ in the similarity transformation are:

$$\varphi_1 = \left(\frac{2x}{a_{13}} - 2a_2 t\right)^{-1/2} , \tag{4.75}$$

$$\varphi_2 = a_{13}\left(\frac{2x}{a_{13}} - 2a_2 t\right)^{1/2} , \tag{4.76}$$

$$G_w = a_{13}^2 \frac{1}{\left(\frac{2x}{a_{13}} - 2a_2 t\right)^{1/2}} . \tag{4.77}$$

The boundary layer characteristics can now, be written as:

$$u = a_{13} f' ,$$

$$v = -\left(\frac{2x}{a_{13}} - 2a_2 t\right)^{-1/2} (f - \eta f') ,$$

$$G = a_{13}^2 \frac{1}{\left(\frac{2x}{a_{13}} - 2a_2 t\right)^{1/2}} \theta . \tag{4.78}$$

The rate of heat transfer at the surface is

$$q = -\frac{a_{13}^2}{\left(\frac{2x}{a_{13}} - 2a_2 t\right)} \theta'(0) . \tag{4.79}$$

It is evident that the similarity solution breaks down if the quantity $\left(\frac{2x}{a_{13}} - 2a_2 t\right)$ is non-positive. Thus it is important to choose a_2 carefully for numerical calculations and also the range of validity of the solution for x and t is to be prescribed beforehand. This restriction is necessary to keep the surface temperature and surface heat flux within bounds. Obviously, the leading edge is to be discarded from

consideration in respect of this similarty solution. Otherwise, at any finite $x \neq 0$, the surface temperature decreases monotonically with time for $a_2 \leq 0$ and increases with time for $a_2 > 0$ and $t < \left(\frac{x}{a_2\, a_{13}}\right)$. As a_2 and a_{13} are arbitrary constants, this time limit is not very restrictive. Since, physically, the parameter a_2 is an indication of the unsteadiness of surface temperature variation, this similarity solution could prove useful in determining the validity of quasi-steady solutions. By taking prescribed surface heat flux as

$$q = a_{13}^2 \left(\frac{2x}{a_{13}} - 2a_2 t\right) ,$$

we arrive at the same similarity solution as given above.

Case 4. Unsteady Free Convection with Surface Temperature Varying Directly as Square of a Linear Function of x and Inversely as $\frac{5}{2}^{th}$ Power of a Linear Function of t.

We shall consider here $a_4 = 0$. Now from equation (4.29), we have

$$\varphi_1 = (a_{14} - 2a_2 t)^{-1/2} , \qquad (4.80)$$

where a_{14} is a constant of integration.

From (4.30), we obtain

$$\varphi_2 = E(x)\ (a_{14} - 2a_2 t)^{-\omega/2} ,$$

where $E(x)$ is to be determined from (4.32) using (4.80).

The equation for $E(x)$ is

$$a_5(a_{14} - 2a_2 t)^{-1/2} = \frac{dE}{dx}(a_{14} - 2a_2 t)^{-\omega/2}.$$

With $\omega = 1$, $E(x) = a_5 x + a_{14}$; φ_2 becomes

$$\varphi_2 = \frac{a_5 x + a_{15}}{(a_{14} - 2a_2 t)^{1/2}} . \qquad (4.81)$$

From (4.40), we have $a_8 = 0$ since $a_7 \neq 0$. If $a_7 = 0$, then $a_5 = 0$ which in turn gives $G_w, \varphi_1, \varphi_2$ as functions of time alone and thus $a_8 = 0$ and $a_1 = 0$. But then, it implies that the flow is not driven by the ''indirect'' mechanism. Thus $a_7 = 0$ will lead to, physically, unacceptable solution for free convection flow over a semi-infinite horizontal plate. Hence $a_7 \neq 0$. Now we obtain G_w by combining (4.36), (4.28) and (4.34), as

$$G_w = \frac{a_1 a_9}{2a_5} \frac{(a_5 x + a_{15})^2}{(a_{14} - 2a_2 t)^{5/2}} . \qquad (4.82)$$

In this case, we have $a_3 = a_2$ and $a_6 = 5a_2$. The parameters a_2, a_5, a_1, a_9 all have to remain in the similarity equations which are now

$$f''' - a_2 \eta f'' + 2a_2 f' + a_5 f f'' - a_5 f'^2 - a_1 \pi = 0,$$

$$\pi' = a_9 \theta,$$

$$\frac{1}{\sigma}\theta'' - (a_2 \eta - a_5 f)\theta' - (5a_2 + 2a_5 f')\theta = 0. \qquad (4.83)$$

The boundary conditions are the same as given by (4.37). Also we have

$$u = \frac{a_5 x + a_{15}}{a_{14} - 2a_2 t} f' ,$$

$$v = - \frac{a_5 f}{(a_{14}-2a_2 t)^{1/2}} ,$$

$$G = \frac{a_1 a_9}{2a_5} \frac{(a_5 x + a_{15})^2}{(a_{14}-2a_2 t)^{5/2}} \theta \qquad (4.84)$$

and the rate of heat rransfer at the plate is given by

$$q = - \frac{a_1 a_9}{2a_5} \frac{(a_5 x + a_{15})^2}{(a_{14} - 2a_2 t)^3} \theta'(0). \qquad (4.85)$$

Similar to previous case, constants a_{14} and a_2 should be so chosen that the quantity $(a_{14} - 2a_2 t)$ remains always positive. It is to be noted that for $a_2 < 0$, the surface temperature (4.82) at any x changes directly with time while this trend is reversed for $a_2 > 0$. For this latter case, a limit on time t is not necessary since the arbitrary constant a_{14} can be assigned large values. Similar to the previous case, this similarity solution is also applicable to the problem with surface heat flux prescribed by

$$q = \frac{a_1 a_9}{2a_5} \frac{(a_5 x + a_{15})^2}{(a_{14} - 2a_2 t)^3} .$$

In view of the generality of the present analysis, it may be concluded that the four cases discussed here represent possible similarity solutions for laminar free convection boundary layer flow and heat transfer over a two dimensional heated semi-infinite horizontal plate.

REFERENCES

[1] Stewartson, K., Z.A.M.P., 9a 276-282 (1958).

[2] Gill, W.N., Zeh, D.W. and del-Casal, E., ibid 16, 539-541 (1965).

[3] Rotem, Z., First Canadian National Congress of Applied Mech., Proceedings, 2b, 309-310 (1967).

[4] Rotem, Z. and Claassen, L. , J. Fluid Mech, 39, 173-192 (1969).

[5] Rotem, Z. and Claassen, L. , The Canadian Journal of Chemical Engineering, 47, 461-468 (1969).

[6] Pera, L. and Gebhart, B., Int. J. Heat Mass Transfer, 16, 1131-1146 (1973).

[7] Singh, P., Ph.D. Thesis, I.I.T., Kharagpur, India (1967).

[8] Verma, R.L. and Singh, P., Aust. J. Phys., 30, 335-345, (1977).

[9] Verma, A.R., Int. Jl. Engng. Sci. 21, 35-43 (1983).

[10] Hansen, A.G., Trans. ASME 80, 1553-1559 (1958).

[11] Yang, K.T., Trans. ASME Jl. of Applied Mechanics, 27, 230-236 (1960).

[12] Nanda, R.S., Proc. Symposium on Magnetohydrodynamics, I.I.Sc., Bangalore, India (1965).

[13] Jaluria, Y., Natural Convection Heat and Mass Transfer, Pergamon Press, Oxford, 79-84 (1980).

CHAPTER V

LAMINAR FREE CONVECTION OVER NON-ISOTHERMAL SEMI-INFINITE HORIZONTAL PLATE

1. INTRODUCTION

In this chapter we study the laminar free convection flow and heat transfer over a non-isothermal semi-infinite horizontal plate with an arbitrarily prescribed surface temperature distributions. In free convection over horizontal surfaces, most of the previous studies deal with either uniform surface temperature distribution or the surface temperature varying according to power-law in streamwise distance from the leading edge. These cases are easily amenable mathematically because they yield to similarity solutions [1,2,3,4,5,6,7] . Though these conditions are readily realizable in the laboratory, however arbitrary non-isothermal surface conditions are expected to exist in most physically realistic situations. For the arbitrarily prescribed non-uniform surface temperature distribution for a semi-infinite vertical plate, the free convection flow and heat transfer has been studied by many authors [8,9,10, 11,12,13,14] . Unlike the vertical plate problem where the surface characteristics to be determined relate to shear-stress and heat-flux, the horizontal plate problem includes also of determining the induced pressure at the wall. For vertical problem, methods ranging from Karman-Pohlausen technique with relatively crude profiles to full scale numerical computation procedures have been developed. On the other hand, to our knowledge, no single study either

analytical or experimental has been attempted so far for the corresponding case of a horizontal plate. Therefore, we initiate here this study and give some exact solutions of the governing boundary layer equations when the surface thermal condition is non-uniform, with the exception of the cases that allow similarity solutions.

In what follows, a Görtler-type transformation is introduced to treat the problem of non-isothermal free convection with general wall temperature distribution. A new parameter characterizing the non-isothermal conditions of the wall is introduced. The resulting transformed non-similar form of the boundary layer equations are solved by the Görtler series expansion [15] and the local non-similarity method [16]. The series expansion is valid for an arbitrary surface temperature variations given by

$$G_w = x^n \sum_{k=o}^{\infty} G_k \, x^{(n+1)pk} \qquad (5.1)$$

where n, p, G_k are constants, $G_o \neq 0$ and x is a suitably normalized streamwise coordinate. Such wall temperature variations are generally encountered in experiments. In the expansion of flow variables as a series, the zeroth-order term in the expansion satisfies all the boundary conditions in the complete problem and hence already represents a solution to the full problem. Succeeding terms in the series only serve to improve the accuracy

of the solution inside the boundary layers. Also, since equations governing higher order terms are linear, they are integrated independent of the coefficients G_k of wall temperature data (5.1) for a particular problem by splitting the higher order terms into universal functions. Universal functions associated with the first four terms of the series expansion for flow variables are determined for air when $p = 1.0,\ 0.5,\ 0.25$. With the help of these functions, we can investigate the boundary layer flows by simple algebraic process. An application of the series solution method is illustrated for a class of wall temperature distributions given by

$$G_w = G_o\ (1 + \varepsilon\ x^p) \qquad (5.2)$$

for some constants G_o and ε. On the other hand, the local non-similarity method at the second level of truncation, namely the two-equation model, is applied for this special case to predict local heat-transfer coefficient at the wall for $Pr = 0.1,\ 0.72,\ 5.0$ when $p = 1,\ 0.5,\ 0.25$. A comparison of results for local heat-transfer at the surface for air indicates that the local non-similarity method gives accurate results for a larger region in the downstream flow covered here than the four-term sum of the series expansion can give. The effect of non-isothermal wall is significant on heat-transfer at the surface and the variations in heat-

transfer at the surface is greatly influenced by Prandtl number and the shape of variation of wall temperature distribution as given by values of p.

2. BASIC EQUATIONS

We consider the steady two-dimensional boundary layer flow on a semi-infinite horizontal plate placed in an infinite expanse of Boussinesq fluid. The leading edge of the plate is taken as the origin of coordinates, $\bar{x}$ is along the plate and $\bar{y}$ normal to the plate. The governing continuity, momentum and energy equations are

$$\frac{\partial \bar{u}}{\partial \bar{x}} + \frac{\partial \bar{v}}{\partial \bar{y}} = 0 , \tag{5.3}$$

$$\bar{u} \frac{\partial \bar{u}}{\partial \bar{x}} + \bar{v} \frac{\partial \bar{u}}{\partial \bar{y}} = - \frac{1}{\rho} \frac{\partial \bar{p}}{\partial \bar{x}} + \nu \frac{\partial^2 \bar{u}}{\partial \bar{y}^2} , \tag{5.4}$$

$$\frac{1}{\rho} \frac{\partial \bar{p}}{\partial \bar{y}} = g\bar{\beta} (\bar{T} - \bar{T}_\infty), \tag{5.5}$$

$$\bar{u} \frac{\partial \bar{T}}{\partial \bar{x}} + \bar{v} \frac{\partial \bar{T}}{\partial \bar{y}} = \alpha \frac{\partial^2 \bar{T}}{\partial \bar{y}^2} \tag{5.6}$$

where $\bar{u}, \bar{v}$ are the velocity components along $\bar{x}$ and $\bar{y}$ directions respectively, $\bar{p}$ is the dynamic pressure, $\bar{T}$ is the temperature, $\bar{T}_\infty$ is the temperature of the ambient fluid, ν, ρ, α, $\bar{\beta}$ and g are respectively the kinematic viscosity, density, thermal diffusivity, the coefficient of thermal expansion and gravitational acceleration.

The boundary conditions of the problem are

$$\bar{y} = 0 : \quad \bar{u} = \bar{v} = 0, \quad \bar{T} = \bar{T}_w(\bar{x}) ,$$
$$\bar{y} \to \infty : \quad \bar{u} \to 0, \ \bar{p} \to 0, \ \bar{T} \to \bar{T}_\infty \tag{5.7}$$

where $\bar{T}_w(\bar{x})$ is the temperature of the plate.

By introducing the following non-dimensional variables

$$x = \frac{\bar{x}}{L} , \ y = \frac{\bar{y}}{L} , \ u = \frac{\bar{u}L}{\nu} , \ v = \frac{\bar{v}L}{\nu} ,$$
$$p = \frac{\bar{p}L^2}{\rho\nu^2} , \quad T = \frac{\bar{T} - \bar{T}_\infty}{\bar{T}_w(\bar{x}) - \bar{T}_\infty} , \tag{5.8}$$

we transform the equations (5.3 to 5.6) in dimensionless form

$$\frac{\partial u}{\partial x} + \frac{\partial v}{\partial y} = 0 , \tag{5.9}$$

$$u \frac{\partial u}{\partial x} + v \frac{\partial u}{\partial y} = - \frac{\partial p}{\partial x} + \frac{\partial^2 u}{\partial y^2} , \tag{5.10}$$

$$\frac{\partial p}{\partial y} = G_w T , \tag{5.11}$$

$$u \frac{\partial T}{\partial x} + v \frac{\partial T}{\partial y} + \frac{1}{G_w} \frac{dG_w}{dx} uT = \frac{1}{\sigma} \frac{\partial^2 T}{\partial y^2} \tag{5.12}$$

where G_w is a variable Grashof number defined by

$$G_w = \frac{g\bar{\beta}L^3 \ (\bar{T}_w(\bar{x}) - \bar{T}_\infty)}{\nu^2} ,$$

L denotes a characteristic length and σ is the Prandtl number of the fluid.

The boundary conditions reduce to

$$\begin{aligned} y = 0 &: \quad u = v = 0, \quad T = 1 , \\ y \to \infty &: \quad u \to 0, \; p \to 0, \; T \to 0 \end{aligned} \tag{5.13}$$

3. TRANSFORMATION OF BOUNDARY LAYER EQUATIONS

The non-isothermal condition in terms of the function G_w still remains in the boundary layer equations (5.9 - 5.12). In order to achieve a description in which the function G_w no longer appears explicitly, we introduce in the equations the following transformations

$$\xi = \int_0^x G_w \, dx ,$$

$$\eta = y \frac{G_w^{3/5}}{(n+1)^{2/5} \, \xi^{2/5}} ,$$

$$\Psi = \frac{(n+1)^{3/5} \, \xi^{3/5}}{G_w^{2/5}} \, f(\xi,\eta) ,$$

$$p = [\xi G_w (n+1)]^{2/5} \, g(\xi,\eta)$$

and

$$T = \theta(\xi,\eta) \tag{5.14}$$

where Ψ is the stream function and satisfies the continuity equation (5.9).

The boundary layer equations (5.10 - 5.12) now become

$$f''' + \frac{(n+1)}{5}\left[(3-2\beta)\, ff'' - (1+\beta)\, f'^2 + (2-3\beta)\,\eta g' - 2(1+\beta) g\right]$$

$$= (n+1)\,\xi\left[f' \frac{\partial f'}{\partial \xi} - f'' \frac{\partial f}{\partial \xi} + \frac{\partial g}{\partial \xi}\right], \qquad (5.15)$$

$$g' = \theta\,, \qquad (5.16)$$

$$\frac{1}{\sigma}\theta'' + \frac{(n+1)}{5}(3-2\beta) f\theta' - (n+1)\beta\theta f' = (n+1)\xi\left[f' \frac{\partial \theta}{\partial \xi} - \theta' \frac{\partial f}{\partial \xi}\right]. \qquad (5.17)$$

In the foregoing equations, the primes denote partial differentiation with respect to η and $\beta(\xi)$ is the GÖRTLER'S Principal Function of the problem which characterizes the non-isothermal surface condition and is given by

$$\beta(\xi) = \frac{\xi}{G_w^2} \frac{dG_w}{dx}\,. \qquad (5.18)$$

The boundary conditions for the transformed equations are:

$$f(\xi,0) = f'(\xi,0) = 0,\ \theta(\xi,0) = 1\,,$$
$$f'(\xi,\infty) = g(\xi,\infty) = \theta(\xi,\infty) = 0\,. \qquad (5.19)$$

In the case of power-law distribution of wall-temperature, the equations (5.15 - 5.17) reduce essentially to those of the similarity equations dealt with by Rotem and Claassen [4]. To solve the partial differential equations (5.15 - 5.17), we employ first Görtler series expansion technique and then local non-similarity method.

4. GÖRTLER SERIES EXPANSION METHOD

To solve the flow problem by Görtler series method we first invert the transformation

$$\xi = \int_0^x G_w \, dx \,, \tag{5.20}$$

with G_w given by (5.1), by using Lagrange's theorem for reversion of power series. This inversion process gives x as a power series in ξ which we substitute in (5.18) to get the following series for β:

$$\beta(\xi) = \beta_0 + \beta_1 \xi^p + \beta_2 \xi^{2p} + \beta_3 \xi^{3p} + \cdots \tag{5.21}$$

where β_i's are to be fixed by knowing the coefficients $G_0, G_1, G_2 \ldots$ in (5.1) for a given surface temperature distribution. The procedure to obtain $\beta(\xi)$ as a power series in ξ follows the same way as shown in the appendix of Chapter IIA.

To solve the equations (5.15 - 5.17) we assume the following series for the functions $f(\xi,\eta)$, $g(\xi,\eta)$ and $\theta(\xi,\eta)$:

$$f(\xi,\eta) = \sum_{k=0}^{\infty} f_k(\eta) \; \xi^{pk} \,,$$

$$g(\xi,\eta) = \sum_{k=0}^{\infty} g_k(\eta) \; \xi^{pk} \,,$$

$$\theta(\xi,\eta) = \sum_{k=0}^{\infty} \theta_k(\eta) \; \xi^{pk} \,. \tag{5.22}$$

Substituting equations (5.21) and (5.22) in equations (5.15 to 5.17) and collecting the coefficients of like powers of ξ, we obtain the following set of ordinary differential equations in $f_k(\eta)$, $g_k(\eta)$ and $\theta_k(\eta)$:

$$f_o''' + \frac{(n+3)}{5} f_o f_o'' - \frac{(2n+1)}{5} f_o'^2 + \frac{(2-n)}{5} \eta g_o' - \frac{2}{5}(2n+1) g_o = 0,$$

$$g_o' = \theta_o ,$$

$$\frac{1}{\sigma} \theta_o'' + \frac{(n+3)}{5} f_o \theta_o' - n f_o' \theta_o = 0 , \qquad (5.23)$$

and

$$f_k''' + \frac{(n+3)}{5} f_o f_k'' - \left[2 \frac{(2n+1)}{5} + pk(n+1) \right] f_o' f_k' + \left[\frac{(n+3)}{5} + pk(n+1) \right] f_o'' f_k + \frac{(2-n)}{5} \eta g_k' - \frac{(2n+1)}{5} g_k$$

$$= \frac{(n+1)}{5} \beta_k (2 f_o f_o'' + f_o'^2 + 3\eta g_o' + 2 g_o)$$

$$+ \sum_{j=1}^{k-1} \left[\{ pj(n+1) + \frac{(2n+1)}{5} \} f_j' f_{k-j}' - \{ pj(n+1) + \frac{n+3}{5} \} f_j f_{k-j}'' \right.$$

$$\left. + \beta_{k-j} \frac{(n+1)}{5} \{ 3\eta g_j' + 2 g_j + \sum_{i=0}^{j} (2 f_i f_{j-i}'' + f_i' f_{j-i}') \} \right] ,$$

$$g_k' = \theta_k ,$$

$$\frac{1}{\sigma} \theta_k'' + \frac{(n+3)}{5} f_o \theta_k' - \left[n + (n+1)pk \right] f_o' \theta_k + \left[\frac{(n+3)}{5} + (n+1)pk \right] \theta_o' f_k - n \theta_o f_k'$$

$$= \frac{(n+1)}{5} \beta_k (2 f_o \theta_o' + 5 f_o' \theta_o)$$

$$+ \sum_{j=1}^{k-1} \left[\{ (n+1)p + n \} f_j' \theta_{k-j} - \{ \frac{(n+3)}{5} + (n+1)p \} f_j \theta_{k-j}' \right.$$

$$\left. + \frac{(n+1)}{5} \beta_{k-j} \sum_{i=0}^{j} (5 f_i' \theta_{j-i} + 2 f_i \theta_{j-i}') \right]$$

$$\text{for } k = 1, 2, 3, \cdots \qquad (5.24)$$

The boundary conditions are:

$$f_o(0) = f_o'(0) = 0\,, \quad \theta_o(0) = 1,$$

$$f_o'(\infty) \to 0,\ g_o(\infty) \to 0,\ \theta_o(\infty) \to 0 \qquad (5.25)$$

and

$$f_k(0) = f_k'(0) = \theta_k(0) = 0,$$

$$f_k'(\infty) \to 0,\ g_k(\infty) \to 0,\ \theta_k(\infty) \to 0 \qquad (5.26)$$

$$\text{for } k = 1,2,3, \ldots$$

It may be noted that the zero-order equations (5.23) are the similarity equations for G_w varying as x^n, where the constant exponent n is to be determined by the actual behaviour of G_w as x approaches 0. In physically realistic situations the plate temperature remains finite and hence the leading edge behaviour of G_w can be very adequately described by x^n with $n \geq 0$. The rest of the equations are linear and form a recursive set of equations. These linear equations depend upon the prescribed surface thermal conditions through the appearance of β_j. To eliminate this dependence, we write functions f_k, g_k, θ_k, $k \geq 1$ as linear combination of certain other functions:

$$f_1 = \beta_1 Y_{11}(\eta)\ ;\ g_1 = \beta_1 Z_{11}(\eta)\ ;\ \theta_1 = \beta_1 W_{11}(\eta),$$

$$f_2 = \beta_2 Y_{22}(\eta) + \beta_1^2 Y_{21}(\eta)\ ;\ g_2 = \beta_2 Z_{22}(\eta) + \beta_1^2 Z_{21}(\eta)\ ;$$

$$\theta_2 = \beta_2 W_{22}(\eta) + \beta_1^2 W_{21}(\eta)\,,$$

$$f_3 = \beta_3 Y_{33}(\eta) + \beta_1^3 Y_{31}(\eta) + \beta_1\beta_2 Y_{32}(\eta);\ g_3 = \beta_3 Z_{33}(\eta) +$$

$$+ \beta_1^3 Z_{31}(\eta) + \beta_1\beta_2 Z_{32}(\eta);\ \theta_3 = \beta_3 W_{33}(\eta) +$$

$$+ \beta_1^3 W_{31}(\eta) + \beta_1\beta_2 W_{32}(\eta) \qquad (5.27)$$

and so on. The functions Y, Z and W are universal functions of η with parameters n, p and σ. These universal functions satisfy the following set of equations:

$$L_1(Y_{11}, Z_{11}, W_{11}) = \frac{(n+1)}{5}\,(2f_o f_o'' + 3\eta\, g_o' + 2g_o + f_o'^{\,2}),$$

$$Z_{11}''' = W_{11}, \qquad (5.28)$$

$$L_2(Y_{11}, Z_{11}, W_{11}) = \frac{(n+1)}{5}\,(2f_o\theta_o' + 5f_o'\theta_o);$$

$$L_1(Y_{22}, Z_{22}, W_{22}) = \frac{(n+1)}{5}\,(2f_o f_o''' + f_o'^{\,2} + 3\eta\, g_o' + 2g_o),$$

$$Z_{22}' = W_{22}, \qquad (5.29)$$

$$L_2(Y_{22}, Z_{22}, W_{22}) = \frac{(n+1)}{5}\,(2f_o\theta_o' + 5f_o'\theta_o);$$

$$L_1(Y_{21}, Z_{21}, W_{21}) = \left[p(n+1) + \frac{(2n+1)}{5}\right]Y_{11}'^{\,2} - \left[\frac{(n+3)}{5} + p(n+1)\right]Y_{11}Y_{11}'' \cdot$$

$$+ \frac{2}{5}(n+1)(Y_{11}f_o'' + f_o Y_{11}''') + \frac{2}{5}(n+1)Z_{11} + \frac{3}{5}(n+1)Z_{11}',$$

$$Z_{21}' = W_{21},$$

$$L_2(Y_{21}, Z_{21}, W_{21}) = \left[p(n+1) - \frac{(n+3)}{5}\right]Y_{11}W_{11}' + \left[n + p(n+1)\right]Y_{11}'W_{11}$$

$$+ \frac{2}{5}(n+1)Y_{11}\theta_o' + (n+1)Y_{11}'\theta_o + \frac{2}{5}(n+1)f_o\theta_{11}'$$

$$L_1(Y_{33}, Z_{33}, W_{33}) = \frac{(n+1)}{5}\,(2f_o f_o'' + f_o'^2 + 3\eta\, g_o' + 2g_o)\,,$$

$$Z_{33}' = W_{33}\,,$$

$$L_2(Y_{33}, Z_{33}, W_{33}) = \frac{(n+1)}{5}\,(2f_o\theta_o' + 5f_o'\theta_o)\,; \qquad (5.31)$$

$$L_1(Y_{31}, Z_{31}, W_{31}) = -\left[p(n+1) + \frac{n+3}{5}\right] Y_{11} Y_{21}'' + \left[3p(n+1) + \frac{2}{5}(2n+1)\right] Y_{11}' Y_{21}' -$$

$$-\left[2p(n+1) + \frac{(n+3)}{5}\right] Y_{11}'' Y_{21} + \frac{(n+1)}{5}\left(Y_{11}'^2 + 2Y_{11} Y_{11}''\right) +$$

$$+ \frac{(n+1)}{5}\,(2f_o Y_{21}'' + 2f_o' Y_{21} + 2f_o'' Y_{21}' + 3\eta\, Z_{21}' + 2Z_{21})\,,$$

$$Z_{31}' = W_{31}\,,$$

$$L_2(Y_{31}, Z_{31}, W_{31}) = -\left[\frac{(n+3)}{5} + p(n+1)\right] Y_{11} Z_{21}'' + \left[n + 2p(n+1)\right] Y_{11}' Z_{21}' -$$

$$-\left[\frac{(n+3)}{5} + 2p(n+1)\right] Y_{21} Z_{11}'' + \left[n + p(n+1)\right] Y_{21}' Z_{11}' +$$

$$+ \frac{2}{5}(n+1) Y_{11} Z_{11}'' + (n+1) Y_{11}' Z_{11}' + \frac{2}{5}(n+1) f_o Z_{21}'' +$$

$$+ (n+1) f_o' Z_{21}' + \frac{2}{5}(n+1) g_o'' Y_{21} + (n+1) g_o' Y_{21}\,; \qquad (5.32)$$

$$L_1(Y_{32}, Z_{32}, W_{32}) = -\left[p(n+1) + \frac{(n+3)}{5}\right] Y_{11} Y_{22}'' + \left[2\,\frac{(2n+1)}{5} + 3p(n+1)\right] Y_{11}' Y_{22}' -$$

$$-\left[2p(n+1) + \frac{(n+3)}{5}\right] Y_{11}'' Y_{22} + \frac{3}{5}(n+1)\,\eta\, Z_{22}' +$$

$$+ \frac{2}{5}(n+1) Z_{22} + \frac{2}{5}(n+1)(f_o'' Y_{22} + f_o' Y_{22}' + f_o Y_{22}'')\,,$$

$$Z_{32}' = W_{32}\,,$$

$$L_2(Y_{32}, Z_{32}, W_{32}) = -\left[\frac{(n+3)}{5} + p(n+1)\right]Y_1 Z_{22}'' + \left[n+2p(n+1)\right]Y_1' Z_{22}' -$$

$$-\left[\frac{(n+3)}{5} + 2p(n+1)\right]Y_{22} Z_{11}'' + \left[n+p(n+1)\right]Y_{22}' Z_{11}'$$

$$+ \frac{2}{5}(n+1)\, g_o'' Y_{22} + (n+1) f_o' Z_{22}' + \frac{2}{5}(n+1) f_o Z_{22}''$$

$$+ (n+1) g_o' Y_{22}' + \frac{2}{5}(n+1) f_o Z_{11}'' + (n+1) f_o' Z_{11}' +$$

$$+ \frac{2}{5}(n+1)\, Y_1 g_o'' + (n+1) g_o' Y_{11}' \qquad (5.33)$$

where

$$L_1(Y_{kr}, Z_{kr}, W_{kr}) = Y_{kr}''' + \frac{(n+3)}{5} f_o Y_{kr}'' - \left[2\cdot\frac{(2n+1)}{5} + kp(n+1)\right] f_o' Y_{kr}' +$$

$$+ \left[\frac{(n+3)}{5} + kp(n+1)\right] f_o'' Y_{kr} + \frac{(2-n)}{5}\eta Z_{kr}' - \frac{(2n+1)}{5} Z_{kr}'$$

$$L_2(Y_{kr}, Z_{kr}, W_{kr}) = \frac{1}{\sigma} W_{kr}'' + \frac{(n+3)}{5} f_o W_{kr}' - \left[n+(n+1)pk\right] f_o' W_{kr} +$$

$$+ \left[\frac{(n+3)}{5} + (n+1)pk\right] \theta_o' Y_{kr} - n\, \theta_o\, Y_{kr}' \qquad (5.34)$$

for $k \geq 1$ and $r = 1, 2, 3, \ldots, k$.

The boundary conditions are:

$$Y_{kr}(0) = Y_{kr}'(0) = W_{kr}(0) = 0$$

and

$$Y_{kr}'(\infty) \to 0, \quad W_{kr}(\infty) \to 0, \quad Z_{kr}(\infty) \to 0 \qquad (5.35)$$

for $k \geq 1$ and $r = 1, 2, 3, \ldots, k$.

The above system of equations for determining universal functions can now be easily solved for the various set of values of parameters n,p and σ. Hence the calculation of flow and heat transfer characteristics of the free convection boundary layer over a non-isothermal horizontal plate becomes a simple matter.

A standard shooting technique as described by Nachtsheim and Swigert [17] has been employed to solve the zero-order equations for $n = 0$ and $\sigma = 0.72$. The solutions $f_o''(0)$, $g_o(0)$, $\theta_o(0)$ are calculated to an accuracy upto six decimal places. The linear equations (5.28 to 5.33) are solved recursively upto third-order terms in the series expansion (5.22) for $p = 1.0, 0.5, 0.25$ with $n = 0$ and $\sigma = 0.72$. The method of solution adopted here is the same as given in ChapterII except for the fact that here we have to consider evaluations of complementary functions thrice with three sets of initial conditions at the surface instead of two for the problem in ChapterII. The equations were integrated by Runge-Kutta integration scheme with step-size $H = 1/64$ and the edge of the boundary layer fixed at $\eta_\infty = 15$. This yields

$$|Y'_{kr}(\eta_\infty)|, \ |Z_{kr}(\eta_\infty)|, \ |W_{kr}(\eta_\infty)| \quad \text{all less than } 10^{-6}.$$

Throughout the computation, calculations were carried out

upto eight decimal places. For the Prandtl number, $\sigma = 0.72$ and $n = 0$ the universal functions are determined upto and including the third order terms for values of $p = 1.0, 0.5, 0.25$ The missing wall values for the functions f_o, g_o; θ_o and the universal functions Y, Z, W are shown in Table 1.

The rate of heat transfer from the plate to the fluid is the most important characteristic of the free convection boundary layer problem, which is calculated by using Fourier law:

$$q = - \lambda \left(\frac{\partial \bar{T}}{\partial \bar{y}}\right)_{\bar{y}=0} .$$

Introducing the dimensionless variables, the expression for q becomes

$$q = - \frac{\lambda}{L} (\bar{T}_w(\bar{x}) - \bar{T}_\infty) \frac{G_w^{3/5}}{[(n+1)\xi]^{2/5}} \frac{\partial \theta(\xi, 0)}{\partial \eta}$$

$$= - \frac{\lambda}{L} (\bar{T}_w(\bar{x}) - \bar{T}_\infty) \frac{G_w^{3/5}}{[(n+1)\xi]^{2/5}} \left[\sum_{k=0}^{\infty} \xi^{pk} \frac{d\theta_k(0)}{d\eta} \right] \tag{5.36}$$

Now introducing the local heat transfer coefficient, local Nusselt-number, and local Grashof number as

$$h = \frac{q}{\bar{T}_w - \bar{T}_\infty}, \quad Nu_{\bar{x}} = \frac{h\bar{x}}{\lambda}, \quad Gr_{\bar{x}} = \frac{g\beta \bar{x}^3 (\bar{T}_w(\bar{x}) - \bar{T}_\infty)}{\nu^2},$$

the dimensionless representation of the local heat transfer becomes

$$\frac{Nu_{\bar{x}}}{Gr_{\bar{x}}^{1/5}} = -\left[\frac{x\, G_w}{(n+1)\xi}\right]^{2/5} \frac{\partial \theta(\xi,0)}{\partial \eta}$$

$$= -\left[\frac{x\, G_w}{(n+1)\xi}\right]^{2/5} \left[\sum_{k=0}^{\infty} \xi^{pk} \frac{d\theta_k(0)}{d\eta}\right]. \qquad (5.37)$$

5. LOCAL NON-SIMILARITY METHOD

We apply this method of solution for the wall-temperature distribution given by (5.2). Before proceeding with the formulation of the system of equations for local non-similarity method, we shall obtain first ξ, $\beta(\xi)$ in terms of p and s, where

$$s = 1+\varepsilon x^p . \qquad (5.38)$$

Using equations (5.2) and (5.38) in the definitions of ξ and $\beta(\xi)$ given respectively in (5.14) and (5.18), we obtain

$$\xi = (s-1)^{1/p} \frac{(p+s)}{(p+1)} \frac{1}{\varepsilon^{1/p}} G_o \qquad (5.39)$$

and

$$\beta(\xi) = \frac{p(p+s)(s-1)}{(p+1)\, s^2} . \qquad (5.40)$$

Also it can be shown that

$$\xi \frac{ds}{d\xi} = s\beta(s). \qquad (5.41)$$

In order to describe our results for heat transfer coefficient as a function of $\frac{G_w}{G_o}$ (=s), we transform the non-similar form of the boundary layer equations (5.15 to 5.17) in terms of s and η instead of ξ and η using (5.41). Then equations (5.15 to 5.17) become

$$f''' + \frac{1}{5}\left[(3-2\beta)ff'' - (1+\beta)f'^2 + (2-3\beta)\eta g' - 2(1+\beta)g\right]$$

$$= s\beta(s)\left[f'\bar{f}' - f''\bar{f} + \bar{g}\right], \qquad (5.42)$$

$$g' = \theta, \qquad (5.43)$$

$$\frac{1}{\sigma}\theta'' + \frac{1}{5}(3-2\beta)f\theta' - \beta\theta f' = s\beta(s)\left[\bar{\theta}\, f' - \bar{f}\,\theta'\right] \qquad (5.44)$$

where

$$\bar{f} = \frac{\partial f}{\partial s}, \quad \bar{g} = \frac{\partial g}{\partial s}, \quad \bar{\theta} = \frac{\partial \theta}{\partial s}. \qquad (5.45)$$

The boundary conditions (5.19) now take the form

$$f(s,0) = f'(s,0) = 0, \quad \theta(s,0) = 1,$$
$$f'(s,\infty) = g(s,\infty) = \theta(s,\infty) = 0. \qquad (5.46)$$

Now we proceed with the formulation of the two-Equation model in the local non-similarity method of solution. The derivation of this model follows in the same manner as described in Chapter III for free convection boundary layer flow over a non-isothermal plate inclined at

a small angle to the horizontal and hence the details of the method are omitted here.

The system of equations for the two-equation model can then be summarized as:

(a) Equations (5.42 - 5.44)

(b) the truncated equations for $\bar{f}, \bar{g}$ and $\bar{\theta}$

$$\bar{f}''' + \frac{(3-2\beta)}{5} f\bar{f}'' - \left[s\frac{d\beta}{ds} + \frac{(2+7\beta)}{5} \right] f' \bar{f}' + \left[s\frac{d\beta}{ds} + \frac{3}{5}(1+\beta) \right] f'' \bar{f}$$

$$+ \frac{1}{5}(2-3\beta)\eta \bar{g}' - \left[s\frac{d\beta}{ds} + \frac{1}{5}(2+7\beta) \right] \bar{g} = \frac{1}{5}\frac{d\beta}{ds}(2ff''+f'^2+3\eta g'+2g), \tag{5.47}$$

$$\bar{g}' = \bar{\theta}, \tag{5.48}$$

$$\frac{1}{\sigma}\bar{\theta}'' + \frac{1}{5}(3-2\beta) f\bar{\theta}' + \left[s\frac{d\beta}{ds} + \frac{3}{5}(1+\beta) \right] \theta' \bar{f} - \left[s\frac{d\beta}{ds} + 2\beta \right] f'\bar{C} - \beta\bar{f}'\theta$$

$$= \frac{1}{5}\frac{d\beta}{ds}(2f\theta' + f'\theta) . \tag{5.49}$$

(c) The boundary conditions

$$f(s,0) = f'(s,0) = \bar{f}(s,0) = \bar{f}'(s,0) = \bar{\theta}(s,0) = 0 ,$$

$$\theta(s,0) = 1 ,$$

$$f'(s,\infty) = g(s,\infty) = \theta(s,\infty) = \bar{f}'(s,\infty) = \bar{g}(s,\infty) = \bar{\theta}(s,\infty) = 0 . \tag{5.50}$$

It can be seen that the equations (5.42 - 5.44) and (5.47 - 5.49) are coupled and they must be solved for the six unknown functions $f, g, \theta, \bar{f}, \bar{g}$, and $\bar{\theta}$. With s regarded as known, β and $\frac{d\beta}{ds}$ can then be determined and therefore these equations may be treated as a system of coupled ordinary differential equations of the similarity type.

The system of equations for the second level local non-similarity model was solved by employing the initial value technique as modified by Nachtsheim and Swigert. A solution was considered to be convergent when the magnitudes of the boundary conditions at the edge of the boundary layer $f'(s,\infty)$, $g(s,\infty)$, $\theta(s,\infty)$ and $\bar{f}'(s,\infty)$, $\bar{g}(s,\infty)$, $\bar{\theta}(s,\infty)$ for a fixed s became less than 5×10^{-4} and 5×10^{-3} respectively. In table 2, we give the values for $(\frac{\partial\theta(s,0)}{\partial\eta})$ which describes the dimensionless characteristic of surface heat-flux for $\sigma = 0.72, 0.1, 5.0$ and $p = 1, 0.5, 0.25$.

6. RESULTS AND DISCUSSION

We shall consider the application of Gortler series method of solution to the class of wall temperature variation $G_w = G_o(1+ \varepsilon x^p)$ as already given in (5.2). The exponent p, which gives the shape of the variation, is required to be a positive number, integral or non-integral. Also we note that when the characteristic length is taken as the length of the plate ℓ, then ε represents the maximum deviation of

G_w from G_o in the region $\bar{x} = 0$ to $\bar{x} = \ell$. Here we have considered the wall temperature relative to the ambient to be a finite non-zero value at $\bar{x} = 0$ and this increases steadily from $\bar{x} = 0$ to $\bar{x} = \ell$.

Now comparing the class of surface temperature variation (5.2) with (5.1) we get

$$n = 0, \; G_1 = \varepsilon \, G_o, \; G_2 = G_3 = \cdots = 0.$$

Using these values and the procedure as followed in Chapter II we obtain the coefficients β_j of the Principal function $\beta(\xi)$ as follows:

$$\beta_o = \frac{n}{n+1} = 0 \;,$$

$$\beta_1 = \frac{p\varepsilon}{G_o^p} \;,$$

$$\beta_2 = -\left[2p - \frac{p(1-p)}{(1+p)}\right] \frac{\varepsilon^2}{G_o^{2p}} \;,$$

$$\beta_3 = \left[(2+5p)\,\frac{p}{p+1} + (1+4p)\right] \frac{p}{(p+1)} \; \frac{\varepsilon^3}{G_o^{3p}} \;,$$

$$\beta_4 = -\left[(3+7p)\left(\frac{p}{p+1}\right)^2 + \frac{4}{3}(4+11p)\,\frac{p}{p+1} + (1+4p)\right] \frac{p}{(p+1)} \; \frac{\varepsilon^4}{G_o^{4p}} \;. \tag{5.51}$$

From the definition of ξ as given in equation (5.14), after simplification, we get

$$\xi = \left(\frac{G_w}{G_o} - 1\right)^{1/p} \left[1 + \frac{1}{(p+1)} \left(\frac{G_w}{G_o} - 1\right)\right] \frac{G_o}{\varepsilon^{1/p}} \tag{5.52}$$

Using (5.52) and (5.51), the dimensionless representation of the local heat flux given by equation (5.37) can be written in terms of s for a given p as follows:

$$\frac{Nu_x}{Gr_x^{1/5}} = -\left[\frac{(p+1)s}{p+s}\right]^{2/5} \frac{\partial\theta(\xi,0)}{\partial\eta}, \qquad (5.53)$$

$$= -\left[\frac{(p+1)s}{(p+s)}\right]^{2/5} \left[\theta_o'(0)+\beta_1 W_{11}'(0)\xi^p+\{\beta_1^2 W_{21}'(0)+\beta_2 W_{22}'(0)\}\xi^{2p}\right.$$

$$\left. + \{\beta_1^3 W_{31}'(0)+\beta_1\beta_2 W_{32}'(0)+\beta_3 W_{33}'(0)\}\xi^{3p}+\ldots\right]. \qquad (5.54)$$

The Nusselt-Grashof relation as obtained from (5.53) and (5.54) for the local non-similarity method and Görtler series expansion respectively is shown in figure 1 over the range $1 \leq s \leq 1.4$ for $\sigma = 0.72$ and $p = 1.0, 0.5, 0.25$. A comparison of local heat transfer at the surface shows that the agreement between the two methods of solution for a fixed s depend both on the number of terms used in the series solution and values of p. For a fixed p we find the region of agreement between results for heat-transfer from the two methods of solution improve if 4- term sum instead of 3-term sum is used in Görtler series solution. In the region R where the results from the two methods

deviate there is a significant trend observed for all values of p in using a 4-term sum and 3-term sum from the series solution for comparison purposes. The trend of results from 3-term sum for local heat transfer in R is to underestimate it while, the 4-term sum overestimates even as the region R shrink now a little. Also this alternating behaviour of Görtler series in relation to inclusion of additional terms for obtaining solution in downstream flow is to continue, judging by the trend of the results for universal functions and the value of β_j coefficients. However, the evaluation of further universal functions is hindered by considerable difficulties. These are due not only to the fact that for every additional term in the series the number of differential equations to be solved increases but also and even more forcibly the difficulties are due to the need to evaluate the functions for lower power term with ever increasing accuracy, if the functions for higher power terms are to be sufficiently accurate. Also the chances of carrying out an extension of this method is limited by the fact that a corresponding demand on the need to do increasing algebraic manipulations for finding β_j emerges. On the other hand, in the two-Equation model of local non-similarity method solving of six coupled equations simultaneously by initial value techniques may show divergent behaviour unless good estimates of the missing wall values are known. Fortunately,

in the cases treated here such couplings have mostly insignificant influence on the convergence of the solution. We mention here that quasilinearization technique can be of value to predict good estimates of the missing conditions at the wall as it has already been demonstrated in Chapter III.

The results from local non-similarity method for the Nusselt-Grashof relation as obtained from (5.53) are presented in figure 2(a), (b) as a function of s for $\sigma = 0.1,\ 5.0$ and for $p = 1.0, 0.5, 0.25$. For a fixed σ we see from figures (1) and (2a,b) that the effect of increase in value of p at a fixed s isto increase the local Nusselt number.

The effect of a non-isothermal wall on heat transfer at the surface is computed from the following equation

$$q^{*} = \frac{\left[q/(\bar{T}_w - \bar{T}_\infty)\ Gr_x^{1/5}\right]}{\left[q/(\bar{T}_w - \bar{T}_\infty)\ Gr_x^{1/5}\right]_{iso}} = \frac{(Nu_x/Gr_x^{1/5})}{(Nu_x/Gr_x^{1/5})_{iso}}$$

where the subscript, iso, denotes a quantity corresponding to an isothermal wall. For our special case (5.2) we can write

$$q = \left[\frac{(p+s)s}{(p+1)}\right]^{2/5} \left[\frac{\partial\theta(s,0)}{\partial\eta} \Big/ \theta_0'(0)\right]$$

where $\theta_o'(0)$ is the characteristic dimensionless surface heat flux for isothermal wall. The values of q^* against s for $\sigma = 0.1, 0.72, 5.0$ as obtained by using the two-equation model of the local non-similarity method are shown in figures (3 a),b),c)) for $p = 1.0, 0.5, 0.25$ respectively. For a fixed p, the percentage increase in heat transfer coefficient at the surface over an isothermal wall for a fixed s decreases as the Prandtl number increases.

Table 1

Missing wall values for universal functions for $\sigma = 0.72$, $n = 0$ and $p = 1, 0.5, 0.25$

p	1.0	0.5	0.25
$f_o''(0)$	0.978404	0.978404	0.978404
$g_o(0)$	-1.734925	-1.734925	-1.734925
$\theta_o'(0)$	-0.357409	-0.357409	-0.357409
$Y_{11}''(0)$	0.084434	0.052887	0.027968
$Z_{11}(0)$	0.093690	0.127810	0.154982
$W_{11}'(0)$	-0.181933	-0.201790	-0.215486
$Y_{22}''(0)$	-0.074718	-0.105569	-0.132497
$Z_{22}(0)$	0.121104	0.174429	0.222341
$W_{22}'(0)$	-0.154230	-0.184974	-0.209491
$Y_{21}''(0)$	0.013412	0.014560	0.017082
$Z_{21}(0)$	-0.001766	-0.014304	-0.029020
$W_{21}'(0)$	0.025947	0.042405	0.057273
$Y_{33}''(0)$	0.134195	0.103918	0.070809
$Z_{33}(0)$	0.045798	0.073588	0.108291
$W_{33}'(0)$	-0.141510	-0.167873	-0.190900
$Y_{32}''(0)$	0.009101	0.010961	0.014678
$Z_{32}(0)$	-0.011420	-0.028079	-0.049559
$W_{32}'(0)$	0.037064	0.064116	0.091688
$Y_{31}''(0)$	-0.002411	-0.001616	-0.001687
$Z_{31}(0)$	0.002999	0.005201	0.009876
$W_{31}'(0)$	-0.004009	-0.007265	-0.011573

Table 2

Values of $(-\frac{\partial \theta(s,0)}{\partial \eta})$ obtained from the Two-Equation model for $\sigma = 0.72$, 0.1 and 5.0 for p = 1.0, 0.5, 0.25

	$\sigma = 0.72$			$\sigma = 0.1$			$\sigma = 5.0$		
p	1.0	0.5	0.25	1.0	0.5	0.25	1.0	0.5	0.25
1.0	0.3574	0.3574	0.3574	0.1936	0.1936	0.1936	0.5828	0.5828	0.5828
1.05	0.3659	0.3621	0.3600	0.2022	0.1996	0.1980	0.5946	0.5931	0.5863
1.10	0.3735	0.3664	0.3622	0.2074	0.2024	0.1996	0.6050	0.5951	0.5894
1.15	0.3803	0.3701	0.3643	0.2121	0.2050	0.2010	0.6143	0.6003	0.5923
1.20	0.3863	0.3736	0.3661	0.2162	0.2074	0.2022	0.6225	0.6049	0.5948
1.25	0.3917	0.3766	0.3678	0.2199	0.2094	0.2033	0.6299	0.6091	0.5971
1.30	0.3965	0.3794	0.3694	0.2233	0.2113	0.2044	0.6364	0.6129	0.5992
1.35	0.4009	0.3819	0.3708	0.2263	0.2131	0.2053	0.6423	0.6163	0.6011
1.40	0.4048	0.3842	0.3721	0.2290	0.2146	0.2062	0.6475	0.6194	0.6029

REFERENCES

[1] Stewartson, K., Z.A.M.P. 9a, 276-282 (1958).

[2] Gill, W.N., Zeh, D.W. and del-Casal, E., ibid. 16, 539-541 (1965).

[3] Rotem, Z., First Canadian National Congress of Applied Mechanics, Proceedings, 2b, 309-310 (1967).

[4] Rotem, Z. and Claassen, L., Jl. Fluid Mechanics, 39, 173-192 (1969).

[5] Pera, L. and Gebhart, B., Int. Jl. Heat Mass Transfer, 16, 1131-1146 (1973).

[6] P. Singh, V.P. Sharma and V.N. Mishra, Acta Mechanica 30, 111-128 (1978).

[7] A.R. Verma, Ph.D. Thesis, I.I.T. Kharagpur (1983).

[8] Sparrow, E.M., NACA Tech. Note, No. 3508, 1955.

[9] Kuiken, H.K., Applied Scientific Research, 20, 205-214 (1969).

[10] Kelleher, M. and Yang, K.T., Qtly. Jl. of Mech. and Appl. Math., 25, 447-457 (1972).

[11] G.Nath, Proceedings of Indian Academy of Science, 84-A, 114-123 (1976).

[12] Kao, T.T., Domoto, G.A. and Elrod, H.G., Transactions of ASME Jl of Heat Transfer, 99, 72-79 (1977).

[13] G. Nath, ibid. 100, 163-165 (1978).

[14] Na, T.Y., Applied Scientic Research, 33, 519-543, (1978).

[15] Göertler, H., Jl. of Mathematics and Mechanics, 6, 1-66 (1957).

[16] Sparrow, E.M., Quack, H., and Boerner, C.J., AIAA Jl. 8, 1936-1942 (1970).

[17] Nachtsheim, P.R., Swigert, P., Development of Mechanics, 1, 361-367 (1965).

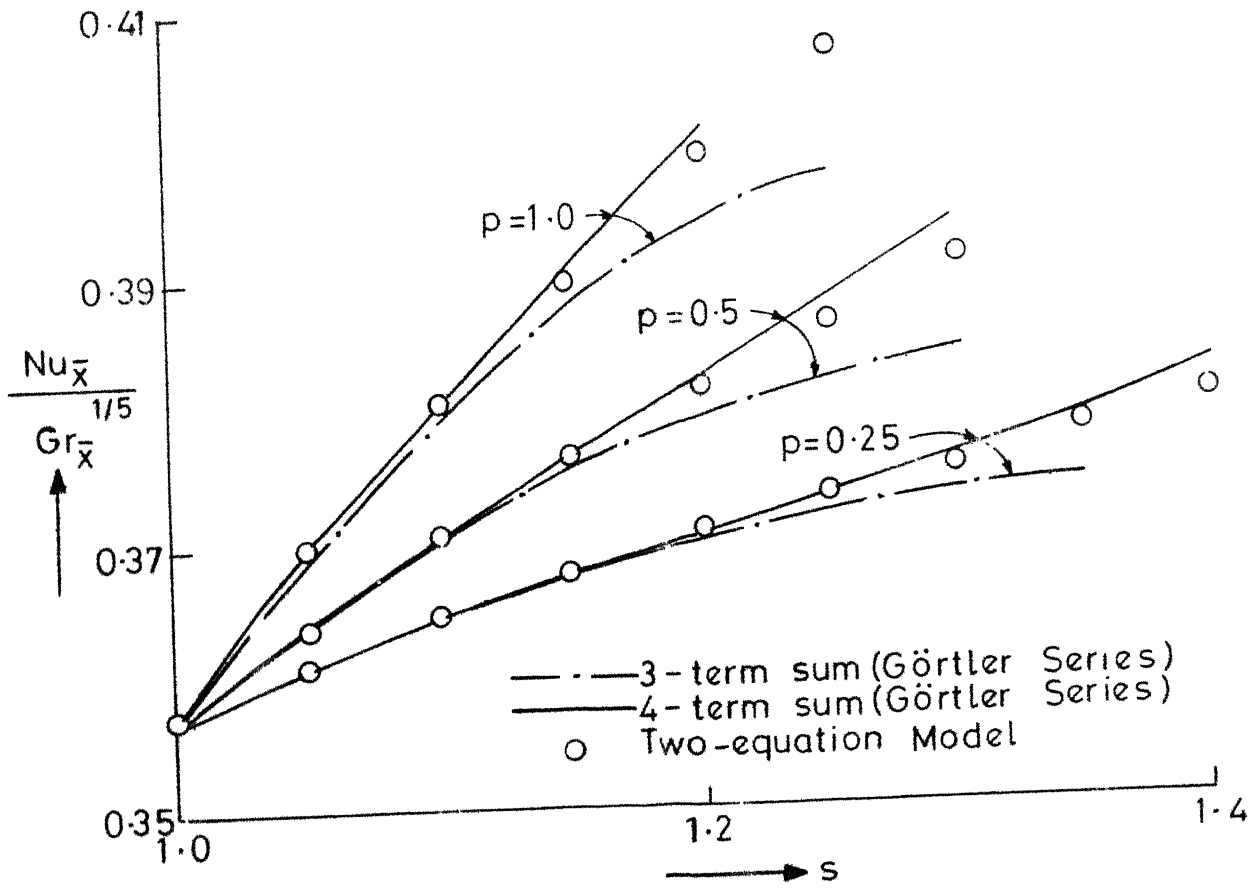

Fig. 1 Comparison of heat transfer variation; $\sigma = 0.72$.

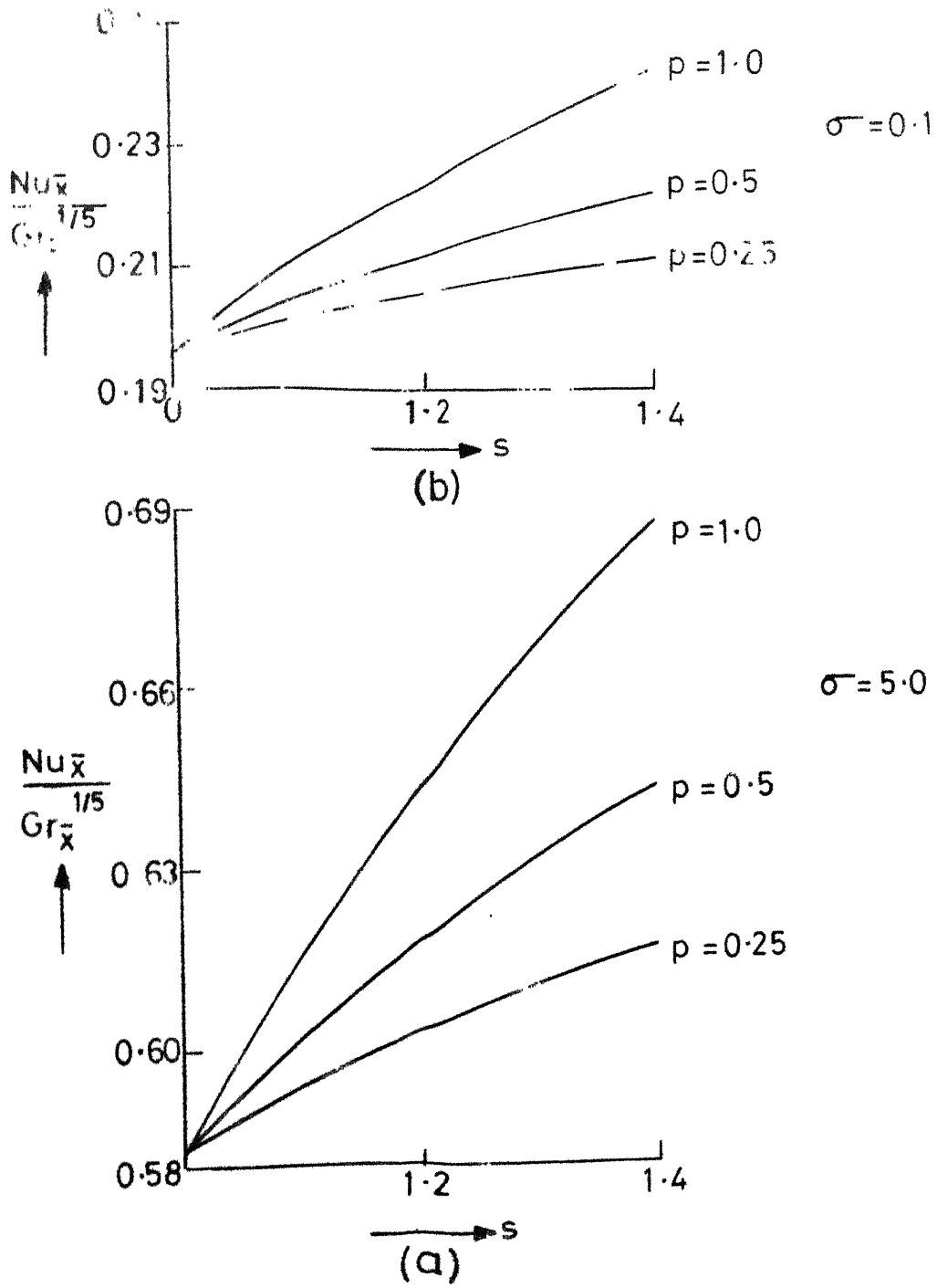

Fig. 2 Heat transfer variation (Local non-similarity method).

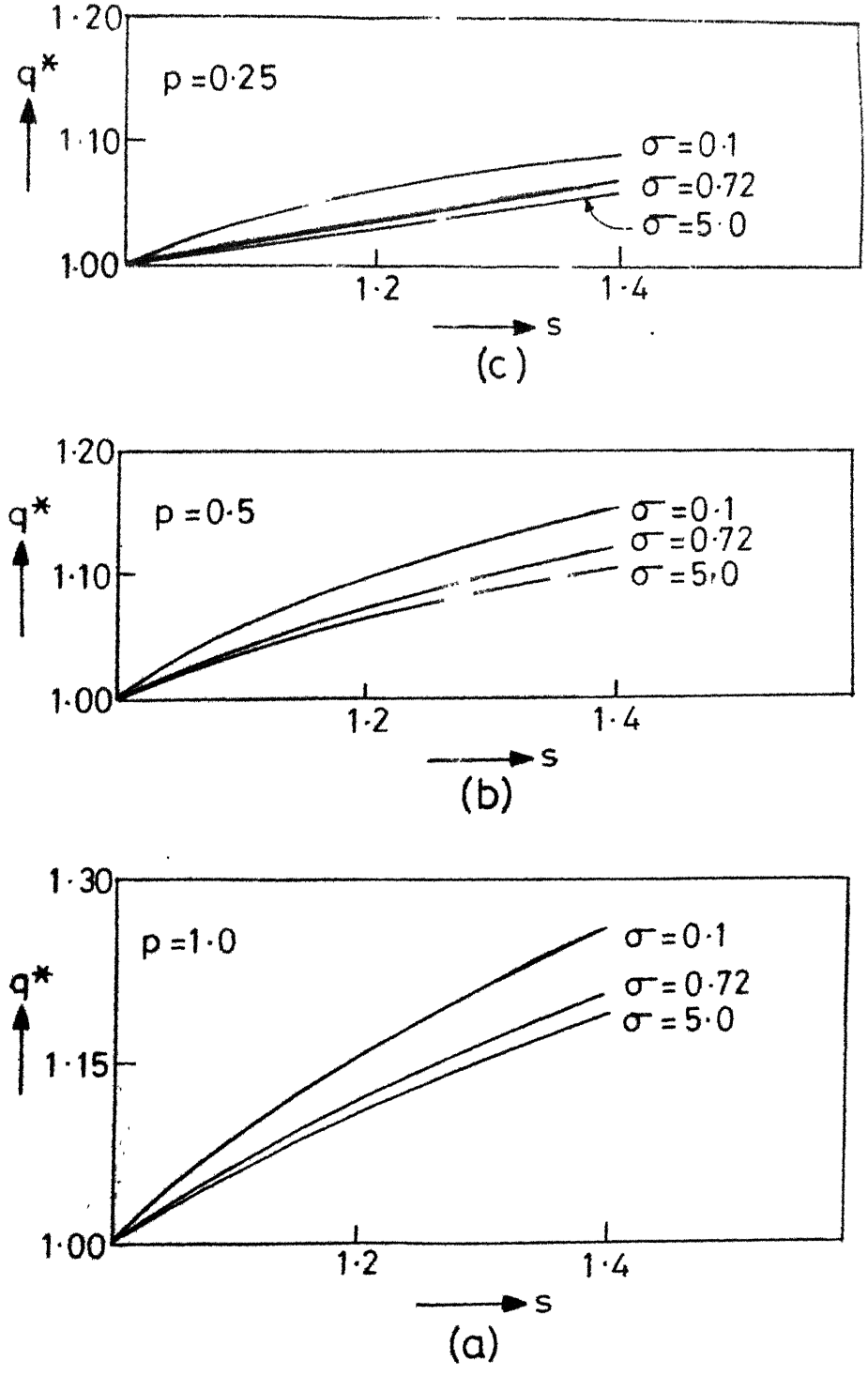

Fig. 3 Effect of non-isothermal wall condition on heat transfer (local non-similarity method).